UNIVERSITE DE LIEGE
FACULTE DE MEDECINE
GIGA-Cancer

Laboratoire de Recherche sur les Métastases
Professeur Vincent CASTRONOVO

Les effets anti-tumoraux des inhibiteurs d'HDAC dans un modèle *in ovo* de cancer pancréatique humain sont significativement améliorés par l'inhibition simultanée de la cyclooxygénase 2.

Gonzalez Arnaud

Maitre en biochimie et biologie cellulaire et moléculaire

Thèse présentée en vue de l'obtention du grade de

Docteur en Sciences Biomédicales et Pharmaceutiques

Promoteurs : Olivier Peulen et Vincent Castronovo.

Année académique 2013-2014

Table des Matières

VI. REFERENCES BIBLIOGRAPHIQUES

Références bibliographiques

Abraham, N. S., H. B. El-Serag, C. Hartman, P. Richardson and A. Deswal, 2007: Cyclooxygenase-2 selectivity of non-steroidal anti-inflammatory drugs and the risk of myocardial infarction and cerebrovascular accident. *Aliment Pharmacol Ther,* **25,** 913-924.

Abrahao, A. C., F. S. Giudice, F. F. Sperandio and D. D. Pinto Junior, 2013: Effects of celecoxib treatment over the AKT pathway in head and neck squamous cell carcinoma. *Journal of oral pathology & medicine : official publication of the International Association of Oral Pathologists and the American Academy of Oral Pathology.*

Aguirre, A. J., N. Bardeesy, M. Sinha, L. Lopez, D. A. Tuveson, J. Horner, M. S. Redston and R. A. DePinho, 2003: Activated Kras and Ink4a/Arf deficiency cooperate to produce metastatic pancreatic ductal adenocarcinoma. *Genes & development,* **17,** 3112-3126.

Ahlgren, J. D., 1996: Chemotherapy for pancreatic carcinoma. *Cancer,* **78,** 654-663.

Aichler, M., C. Seiler, M. Tost, J. Siveke, P. K. Mazur, P. Da Silva-Buttkus, D. K. Bartsch, P. Langer, S. Chiblak, A. Durr, H. Hofler, G. Kloppel, K. Muller-Decker, M. Brielmeier and I. Esposito, 2012: Origin of pancreatic ductal adenocarcinoma from atypical flat lesions: a comparative study in transgenic mice and human tissues. *The Journal of pathology,* **226,** 723-734.

Al-Haddad, M., J. K. Martin, J. Nguyen, S. Pungpapong, M. Raimondo, T. Woodward, G. Kim, K. Noh and M. B. Wallace, 2007: Vascular resection and reconstruction for pancreatic malignancy: a single center survival study. *J Gastrointest Surg,* **11,** 1168-1174.

Albazaz, R., C. S. Verbeke, S. H. Rahman and M. J. McMahon, 2005: Cyclooxygenase-2 expression associated with severity of PanIN lesions: a possible link between chronic pancreatitis and pancreatic cancer. *Pancreatology,* 2005;2005(2004-2005):2361-2009.

Algul, H., M. Treiber, M. Lesina and R. M. Schmid, 2007: Mechanisms of disease: chronic inflammation and cancer in the pancreas--a potential role for pancreatic stellate cells? *Nature clinical practice. Gastroenterology & hepatology,* **4,** 454-462.

Allfrey, V. G., R. Faulkner and A. E. Mirsky, 1964: ACETYLATION AND METHYLATION OF HISTONES AND THEIR POSSIBLE ROLE IN THE REGULATION OF RNA SYNTHESIS. *Proc Natl Acad Sci U S A,* **51,** 786-794.

Allum, W. H., H. J. Stokes, F. Macdonald and J. W. Fielding, 1986: Demonstration of carcinoembryonic antigen (CEA) expression in normal, chronically inflamed, and malignant pancreatic tissue by immunohistochemistry. *Journal of clinical pathology,* **39,** 610-614.

Ammerpohl, O., A. Trauzold, B. Schniewind, U. Griep, C. Pilarsky, R. Grutzmann, H. D. Saeger, O. Janssen, B. Sipos, G. Kloppel and H. Kalthoff, 2007: Complementary effects of HDAC inhibitor 4-PB on gap junction communication and cellular export mechanisms support restoration of chemosensitivity of PDAC cells. *Br J Cancer,* **96,** 73-81.

Aoki, T., Y. Nagakawa, A. Tsuchida, K. Kasuya, K. Kitamura, K. Inoue, T. Ozawa, Y. Koyanagi and T. Itoi, 2002: Expression of cyclooxygenase-2 and vascular endothelial growth factor in pancreatic tumors. *Oncol Rep,* **9,** 761-765.

Appleby, S. B., A. Ristimaki, K. Neilson, K. Narko and T. Hla, 1994: Structure of the human cyclo-oxygenase-2 gene. *Biochem J,* **302 (Pt 3),** 723-727.

Arakawa, T., O. Laneuville, C. A. Miller, K. M. Lakkides, B. A. Wingerd, D. L. DeWitt and W. L. Smith, 1996: Prostanoid receptors of murine NIH 3T3 and RAW 264.7 cells. Structure and expression of the murine prostaglandin EP4 receptor gene. *J Biol Chem,* **271,** 29569-29575.

Arnold, N. B., N. Arkus, J. Gunn and M. Korc, 2007: The histone deacetylase inhibitor suberoylanilide hydroxamic acid induces growth inhibition and enhances gemcitabine-induced cell death in pancreatic cancer. *Clin Cancer Res,* **13,** 18-26.

Ashburner, B. P., S. D. Westerheide and A. S. Baldwin, Jr., 2001: The p65 (RelA) subunit of NF-kappaB interacts with the histone deacetylase (HDAC) corepressors HDAC1 and HDAC2 to negatively regulate gene expression. *Molecular and Cellular Biology,* **21,** 7065-7077.

Bardeesy, N., A. J. Aguirre, G. C. Chu, K. H. Cheng, L. V. Lopez, A. F. Hezel, B. Feng, C. Brennan, R. Weissleder, U. Mahmood, D. Hanahan, M. S. Redston, L. Chin and R. A. Depinho, 2006a: Both p16(Ink4a) and the p19(Arf)-p53 pathway constrain progression of pancreatic adenocarcinoma in the mouse. *Proc Natl Acad Sci U S A,* **103,** 5947-5952.

Bardeesy, N., K. H. Cheng, J. H. Berger, G. C. Chu, J. Pahler, P. Olson, A. F. Hezel, J. Horner, G. Y. Lauwers, D. Hanahan and R. A. DePinho, 2006b: Smad4 is dispensable for normal pancreas development yet critical in progression and tumor biology of pancreas cancer. *Genes & development,* **20,** 3130-3146.

Beatty, G. L., E. G. Chiorean, M. P. Fishman, B. Saboury, U. R. Teitelbaum, W. Sun, R. D. Huhn, W. Song, D. Li, L. L. Sharp, D. A. Torigian, P. J. O'Dwyer and R. H. Vonderheide, 2011: CD40 agonists alter tumor stroma and show efficacy against pancreatic carcinoma in mice and humans. *Science (New York, N.Y.),* **331,** 1612-1616.

Bergmann, F., G. Moldenhauer, E. Herpel, M. M. Gaida, O. Strobel, J. Werner, I. Esposito, S. S. Muerkoster, P. Schirmacher and M. A. Kern, 2010: Expression of L1CAM, COX-2, EGFR, c-KIT and Her2/neu in anaplastic pancreatic cancer: putative therapeutic targets? *Histopathology,* **56,** 440-448.

Berrington de Gonzalez, A., S. Sweetland and E. Spencer, 2003: A meta-analysis of obesity and the risk of pancreatic cancer. *Br J Cancer,* **89,** 519-523.

Bockman, D. E., J. Guo, P. Buchler, M. W. Muller, F. Bergmann and H. Friess, 2003: Origin and development of the precursor lesions in experimental pancreatic cancer in rats. *Lab Invest,* **83,** 853-859.

Bold, R. J., C. Charnsangavej, K. R. Cleary, M. Jennings, A. Madray, S. D. Leach, J. L. Abbruzzese, P. W. Pisters, J. E. Lee and D. B. Evans, 1999: Major vascular resection as part of pancreaticoduodenectomy for cancer: radiologic, intraoperative, and pathologic analysis. *J Gastrointest Surg,* **3,** 233-243.

Burris, H. and A. M. Storniolo, 1997: Assessing clinical benefit in the treatment of pancreas cancer: gemcitabine compared to 5-fluorouracil. *European journal of cancer (Oxford, England : 1990),* **33 Suppl 1,** S18-22.

Burris, H. A., 3rd, M. J. Moore, J. Andersen, M. R. Green, M. L. Rothenberg, M. R. Modiano, M. C. Cripps, R. K. Portenoy, A. M. Storniolo, P. Tarassoff, R. Nelson, F. A. Dorr, C. D. Stephens and D. D. Von Hoff, 1997: Improvements in survival and clinical benefit with gemcitabine as first-line therapy for patients with advanced pancreas cancer: a randomized trial. *Journal of clinical oncology : official journal of the American Society of Clinical Oncology*, **15,** 2403-2413.

Cahlin, C., J. Gelin, M. Andersson, C. Lonnroth and K. Lundholm, 2005: The effects of non-selective, preferential-selective and selective COX-inhibitors on the growth of experimental and human tumors in mice related to prostanoid receptors. *Int J Oncol*, **27,** 913-923.

Caldas, C., S. A. Hahn, L. T. da Costa, M. S. Redston, M. Schutte, A. B. Seymour, C. L. Weinstein, R. H. Hruban, C. J. Yeo and S. E. Kern, 1994: Frequent somatic mutations and homozygous deletions of the p16 (MTS1) gene in pancreatic adenocarcinoma. *Nature genetics,* **8,** 27-32.

Cecconi, D., A. Scarpa, M. Donadelli, M. Palmieri, M. Hamdan, H. Astner and P. G. Righetti, 2003: Proteomic profiling of pancreatic ductal carcinoma cell lines treated with trichostatin-A. *Electrophoresis,* **24,** 1871-1878.

Chabot, J. A., W. Y. Tsai, R. L. Fine, C. Chen, C. K. Kumah, K. A. Antman and V. R. Grann, 2010: Pancreatic proteolytic enzyme therapy compared with gemcitabine-based chemotherapy for the treatment of pancreatic cancer. *Journal of clinical oncology : official journal of the American Society of Clinical Oncology*, **28,** 2058-2063.

Chari, S. T., C. L. Leibson, K. G. Rabe, L. J. Timmons, J. Ransom, M. de Andrade and G. M. Petersen, 2008: Pancreatic cancer-associated diabetes mellitus: prevalence and temporal association with diagnosis of cancer. *Gastroenterology,* **134,** 95-101.

Chen, K. T., K. Devarajan, B. N. Milestone, H. S. Cooper, C. Denlinger, S. J. Cohen, J. E. Meyer and J. P. Hoffman, 2013: Neoadjuvant Chemoradiation and Duration of Chemotherapy Before Surgical Resection for Pancreatic Cancer: Does Time Interval Between Radiotherapy and Surgery Matter? *Annals of surgical oncology.*

Chen, L., W. Fischle, E. Verdin and W. C. Greene, 2001: Duration of nuclear NF-kappaB action regulated by reversible acetylation. *Science (New York, N.Y.),* **293,** 1653-1657.

Chen, S., W. Cao, P. Yue, C. Hao, F. R. Khuri and S. Y. Sun, 2011: Celecoxib promotes c-FLIP degradation through Akt-independent inhibition of GSK3. *Cancer Res,* **71,** 6270-6281.

Chu, J., F. L. Lloyd, O. C. Trifan, B. Knapp and M. T. Rizzo, 2003: Potential involvement of the cyclooxygenase-2 pathway in the regulation of tumor-associated angiogenesis and growth in pancreatic cancer. *Mol Cancer Ther,* **2,** 1-7.

Chun, S. G., W. Zhou and N. S. Yee, 2009: Combined targeting of histone deacetylases and hedgehog signaling enhances cytoxicity in pancreatic cancer. *Cancer Biol Ther,* **8,** 1328-1339.

Colby, J. K., R. D. Klein, M. J. McArthur, C. J. Conti, K. Kiguchi, T. Kawamoto, P. K. Riggs, A. I. Pavone, J. Sawicki and S. M. Fischer, 2008: Progressive metaplastic and dysplastic changes in mouse pancreas induced by cyclooxygenase-2 overexpression. *Neoplasia,* **10,** 782-796.

Coleman, R. A., W. L. Smith and S. Narumiya, 1994: International Union of Pharmacology classification of prostanoid receptors: properties, distribution, and structure of the receptors and their subtypes. *Pharmacological reviews,* **46,** 205-229.

Collins, M. A., F. Bednar, Y. Zhang, J. C. Brisset, S. Galban, C. J. Galban, S. Rakshit, K. S. Flannagan, N. V. Adsay and M. Pasca di Magliano, 2012: Oncogenic Kras is required for both the initiation and maintenance of pancreatic cancer in mice. *J Clin Invest,* **122,** 639-653.

Crowell, P. L., C. M. Schmidt, M. T. Yip-Schneider, J. J. Savage, D. A. Hertzler, 2nd and W. O. Cummings, 2006: Cyclooxygenase-2 expression in hamster and human pancreatic neoplasia. *Neoplasia,* **8,** 437-445.

Daniluk, J., Y. Liu, D. Deng, J. Chu, H. Huang, S. Gaiser, Z. Cruz-Monserrate, H. Wang, B. Ji and C. D. Logsdon, 2012: An NF-kappaB pathway-mediated positive feedback loop amplifies Ras activity to pathological levels in mice. *J Clin Invest,* **122,** 1519-1528.

Davies, N. M., R. L. Good, K. A. Roupe and J. A. Yanez, 2004: Cyclooxygenase-3: axiom, dogma, anomaly, enigma or splice error?--Not as easy as 1, 2, 3. *J Pharm Pharm Sci,* **7,** 217-226.

de Bono, J. S., R. Kristeleit, A. Tolcher, P. Fong, S. Pacey, V. Karavasilis, M. Mita, H. Shaw, P. Workman, S. Kaye, E. K. Rowinsky, W. Aherne, P. Atadja, J. W. Scott and A. Patnaik, 2008: Phase I pharmacokinetic and pharmacodynamic study of LAQ824, a hydroxamate histone deacetylase inhibitor with a heat shock protein-90 inhibitory profile, in patients with advanced solid tumors. *Clin Cancer Res,* **14,** 6663-6673.

de Ruijter, A. J., A. H. van Gennip, H. N. Caron, S. Kemp and A. B. van Kuilenburg, 2003: Histone deacetylases (HDACs): characterization of the classical HDAC family. *Biochem J,* **370,** 737-749.

Deer, E. L., J. Gonzalez-Hernandez, J. D. Coursen, J. E. Shea, J. Ngatia, C. L. Scaife, M. A. Firpo and S. J. Mulvihill, 2010: Phenotype and genotype of pancreatic cancer cell lines. *Pancreas,* **39,** 425-435.

Ding, X. Z., W. G. Tong and T. E. Adrian, 2000: Blockade of cyclooxygenase-2 inhibits proliferation and induces apoptosis in human pancreatic cancer cells. *Anticancer Res,* **20,** 2625-2631.

Ding, X. Z., W. G. Tong and T. E. Adrian, 2001: Cyclooxygenases and lipoxygenases as potential targets for treatment of pancreatic cancer. *Pancreatology,* **1,** 291-299.

Donadelli, M., C. Costanzo, S. Beghelli, M. T. Scupoli, M. Dandrea, A. Bonora, P. Piacentini, A. Budillon, M. Caraglia, A. Scarpa and M. Palmieri, 2007: Synergistic inhibition of pancreatic adenocarcinoma cell growth by trichostatin A and gemcitabine. *Biochimica et biophysica acta,* **1773,** 1095-1106.

Donadelli, M., C. Costanzo, L. Faggioli, M. T. Scupoli, P. S. Moore, C. Bassi, A. Scarpa and M. Palmieri, 2003: Trichostatin A, an inhibitor of histone deacetylases, strongly suppresses growth of pancreatic adenocarcinoma cells. *Mol Carcinog,* **38,** 59-69.

Dovzhanskiy, D. I., S. M. Arnold, T. Hackert, I. Oehme, O. Witt, K. Felix, N. Giese and J. Werner, 2012: Experimental in vivo and in vitro treatment with a new histone deacetylase inhibitor belinostat inhibits the growth of pancreatic cancer. *BMC Cancer,* **12,** 226.

Dragovich, T., M. Huberman, D. D. Von Hoff, E. K. Rowinsky, P. Nadler, D. Wood, M. Hamilton, G. Hage, J. Wolf and A. Patnaik, 2007: Erlotinib plus gemcitabine in patients with unresectable pancreatic cancer and other solid tumors: phase IB trial. *Cancer chemotherapy and pharmacology,* **60,** 295-303.

Dumartin, L., C. Quemener, H. Laklai, J. Herbert, R. Bicknell, C. Bousquet, S. Pyronnet, V. Castronovo, M. K. Schilling, A. Bikfalvi and M. Hagedorn, 2010: Netrin-1 mediates early events in pancreatic adenocarcinoma progression, acting on tumor and endothelial cells. *Gastroenterology*, 2010 Apr;2138(2014):1595-2606, 1606.e2011-2018.

Eibl, G., D. Bruemmer, Y. Okada, J. P. Duffy, R. E. Law, H. A. Reber and O. J. Hines, 2003: PGE(2) is generated by specific COX-2 activity and increases VEGF production in COX-2-expressing human pancreatic cancer cells. *Biochem Biophys Res Commun, 306,* 887-897.

Eibl, G., Y. Takata, L. G. Boros, J. Liu, Y. Okada, H. A. Reber and O. J. Hines, 2005: Growth stimulation of COX-2-negative pancreatic cancer by a selective COX-2 inhibitor. *Cancer Res, 65,* 982-990.

Erkinheimo, T. L., H. Lassus, P. Finne, B. P. van Rees, A. Leminen, O. Ylikorkala, C. Haglund, R. Butzow and A. Ristimaki, 2004: Elevated cyclooxygenase-2 expression is associated with altered expression of p53 and SMAD4, amplification of HER-2/neu, and poor outcome in serous ovarian carcinoma. *Clin Cancer Res, 10,* 538-545.

Evans, A., E. Costello, S. Togo, U. M. Polanska, Y. Horimoto and A. Orimo, 2012: The role of inflammatory cells in fostering pancreatic cancer cell growth and invasion

Carcinoma-Associated Fibroblasts Are a Promising Therapeutic Target. *Frontiers in Physiology, 3,* 149-169.

Farrow, B., D. Albo and D. H. Berger, 2008: The role of the tumor microenvironment in the progression of pancreatic cancer. *J Surg Res, 149,* 319-328.

Feldmann, G., C. Karikari, M. dal Molin, S. Duringer, P. Volkmann, D. K. Bartsch, S. Bisht, J. B. Koorstra, P. Brossart, A. Maitra and V. Fendrich, 2011: Inactivation of Brca2 cooperates with Trp53(R172H) to induce invasive pancreatic ductal adenocarcinomas in mice: a mouse model of familial pancreatic cancer. *Cancer Biol Ther, 11,* 959-968.

Fischer, D. D., R. Cai, U. Bhatia, F. A. Asselbergs, C. Song, R. Terry, N. Trogani, R. Widmer, P. Atadja and D. Cohen, 2002: Isolation and characterization of a novel class II histone deacetylase, HDAC10. *J Biol Chem, 277,* 6656-6666.

Fournel, M., C. Bonfils, Y. Hou, P. T. Yan, M. C. Trachy-Bourget, A. Kalita, J. Liu, A. H. Lu, N. Z. Zhou, M. F. Robert, J. Gillespie, J. J. Wang, H. Ste-Croix, J. Rahil, S. Lefebvre, O. Moradei, D. Delorme, A. R. Macleod, J. M. Besterman and Z. Li, 2008: MGCD0103, a novel isotype-selective histone deacetylase inhibitor, has broad spectrum antitumor activity in vitro and in vivo. *Mol Cancer Ther, 7,* 759-768.

Friend, C., W. Scher, J. G. Holland and T. Sato, 1971: Hemoglobin Synthesis in Murine Virus-Induced Leukemic Cells In Vitro: Stimulation of Erythroid Differentiation by Dimethyl Sulfoxide. *Proc Natl Acad Sci U S A, 68,* 378-382.

Fritsche, P., B. Seidler, S. Schuler, A. Schnieke, M. Gottlicher, R. M. Schmid, D. Saur and G. Schneider, 2009: HDAC2 mediates therapeutic resistance of pancreatic cancer cells via the BH3-only protein NOXA. *Gut*, 2009 Oct;2058(2010):1399-2409.

Fuchs, C. S., G. A. Colditz, M. J. Stampfer, E. L. Giovannucci, D. J. Hunter, E. B. Rimm, W. C. Willett and F. E. Speizer, 1996: A prospective study of cigarette smoking and the risk of pancreatic cancer. *Archives of internal medicine, 156,* 2255-2260.

Funahashi, H., M. Satake, D. Dawson, N. A. Huynh, H. A. Reber, O. J. Hines and G. Eibl, 2007: Delayed progression of pancreatic intraepithelial neoplasia in a conditional Kras(G12D) mouse model by a selective cyclooxygenase-2 inhibitor. *Cancer Res*, 2007 Aug 2001;2067(2015):7068-2071.

Furukawa, F., A. Nishikawa, I. S. Lee, K. Kanki, T. Umemura, K. Okazaki, T. Kawamori, K. Wakabayashi and M. Hirose, 2003: A cyclooxygenase-2 inhibitor, nimesulide, inhibits postinitiation phase of N-nitrosobis(2-oxopropyl)amine-induced pancreatic carcinogenesis in hamsters. *Int J Cancer*, **104,** 269-273.

Gao, D. J., M. Xu, Y. Q. Zhang, Y. Q. Du, J. Gao, Y. F. Gong, X. H. Man, H. Y. Wu, J. Jin, G. M. Xu and Z. S. Li, 2010: Upregulated histone deacetylase 1 expression in pancreatic ductal adenocarcinoma and specific siRNA inhibits the growth of cancer cells. *Pancreas,* **39,** 994-1001.

Gao, L., M. A. Cueto, F. Asselbergs and P. Atadja, 2002: Cloning and functional characterization of HDAC11, a novel member of the human histone deacetylase family. *J Biol Chem*, **277,** 25748-25755.

Gao, Z., P. Chiao, X. Zhang, X. Zhang, M. Lazar, E. Seto, H. A. Young and J. Ye, 2005: COACTIVATORS AND COREPRESSORS OF NF-KB IN IkB ALPHA GENE PROMOTER. *J Biol Chem*, **280,** 21091-21098.

Garcia-Morales, P., A. Gomez-Martinez, A. Carrato, I. Martinez-Lacaci, V. M. Barbera, J. L. Soto, E. Carrasco-Garcia, M. P. Menendez-Gutierrez, M. D. Castro-Galache, J. A. Ferragut and M. Saceda, 2005: Histone deacetylase inhibitors induced caspase-independent apoptosis in human pancreatic adenocarcinoma cell lines. *Mol Cancer Ther,* **4,** 1222-1230.

Genkinger, J. M., D. Spiegelman, K. E. Anderson, L. Bergkvist, L. Bernstein, P. A. van den Brandt, D. R. English, J. L. Freudenheim, C. S. Fuchs, G. G. Giles, E. Giovannucci, S. E. Hankinson, P. L. Horn-Ross, M. Leitzmann, S. Mannisto, J. R. Marshall, M. L. McCullough, A. B. Miller, D. J. Reding, K. Robien, T. E. Rohan, A. Schatzkin, V. L. Stevens, R. Z. Stolzenberg-Solomon, B. A. Verhage, A. Wolk, R. G. Ziegler and S. A. Smith-Warner, 2009: Alcohol intake and pancreatic cancer risk: a pooled analysis of fourteen cohort studies. *Cancer epidemiology, biomarkers & prevention : a publication of the American Association for Cancer Research, cosponsored by the American Society of Preventive Oncology*, **18,** 765-776.

Giovannucci, E., Y. Liu, E. B. Rimm, B. W. Hollis, C. S. Fuchs, M. J. Stampfer and W. C. Willett, 2006: Prospective study of predictors of vitamin D status and cancer incidence and mortality in men. *J Natl Cancer Inst,* **98,** 451-459.

Glaser, K. B., M. J. Staver, J. F. Waring, J. Stender, R. G. Ulrich and S. K. Davidsen, 2003: Gene expression profiling of multiple histone deacetylase (HDAC) inhibitors: defining a common gene set produced by HDAC inhibition in T24 and MDA carcinoma cell lines. *Mol Cancer Ther,* **2,** 151-163.

Gnagnarella, P., S. Gandini, C. La Vecchia and P. Maisonneuve, 2008: Glycemic index, glycemic load, and cancer risk: a meta-analysis. *The American journal of clinical nutrition,* **87,** 1793-1801.

Goel, A., M. L. Grossbard, S. Malamud, P. Homel, M. Dietrich, T. Rodriguez, T. Mirzoyev and P. Kozuch, 2007: Pooled efficacy analysis from a phase I-II study of biweekly irinotecan in combination with gemcitabine, 5-fluorouracil, leucovorin and cisplatin in patients with metastatic pancreatic cancer. *Anti-cancer drugs,* **18,** 263-271.

Gojo, I., A. Jiemjit, J. B. Trepel, A. Sparreboom, W. D. Figg, S. Rollins, M. L. Tidwell, J. Greer, E. J. Chung, M. J. Lee, S. D. Gore, E. A. Sausville, J. Zwiebel and J. E. Karp, 2007: Phase 1 and pharmacologic study of MS-275, a histone deacetylase inhibitor, in adults with refractory and relapsed acute leukemias. *Blood,* **109,** 2781-2790.

Gore, L., M. L. Rothenberg, C. L. O'Bryant, M. K. Schultz, A. B. Sandler, D. Coffin, C. McCoy, A. Schott, C. Scholz and S. G. Eckhardt, 2008: A Phase I and Pharmacokinetic Study of the Oral Histone Deacetylase Inhibitor, MS-275, in Patients with Refractory Solid Tumors and Lymphomas. *Clin Cancer Res,* **14,** 4517.

Grant, W. B. and S. B. Mohr, 2009: Ecological studies of ultraviolet B, vitamin D and cancer since 2000. *Annals of epidemiology,* **19,** 446-454.

Greer, J. B. and D. C. Whitcomb, 2009: Inflammation and pancreatic cancer: an evidence-based review. *Current opinion in pharmacology,* **9,** 411-418.

Gregoretti, I. V., Y. M. Lee and H. V. Goodson, 2004: Molecular evolution of the histone deacetylase family: functional implications of phylogenetic analysis. *Journal of molecular biology,* **338,** 17-31.

Haddad, A., G. Flint-Ashtamker, W. Minzel, R. Sood, G. Rimon and L. Barki-Harrington, 2012: Prostaglandin EP1 receptor down-regulates expression of cyclooxygenase-2 by facilitating its proteasomal degradation. *J Biol Chem*, 2012 May 2018;2287(2021):17214-17223.

Haefner, M., T. Bluethner, M. Niederhagen, C. Moebius, C. Wittekind, J. Mossner, K. Caca and M. Wiedmann, 2008: Experimental treatment of pancreatic cancer with two novel histone deacetylase inhibitors. *World J Gastroenterol,* **14,** 3681-3692.

Hahn, S. A., M. Schutte, A. T. Hoque, C. A. Moskaluk, L. T. da Costa, E. Rozenblum, C. L. Weinstein, A. Fischer, C. J. Yeo, R. H. Hruban and S. E. Kern, 1996: DPC4, a candidate tumor suppressor gene at human chromosome 18q21.1. *Science (New York, N.Y.),* **271,** 350-353.

Hart, A. R., H. Kennedy and I. Harvey, 2008: Pancreatic cancer: a review of the evidence on causation. *Clinical gastroenterology and hepatology : the official clinical practice journal of the American Gastroenterological Association,* **6,** 275-282.

Heinemann, V., M. Reni, M. Ychou, D. J. Richel, T. Macarulla and M. Ducreux, 2014: Tumour-stroma interactions in pancreatic ductal adenocarcinoma: rationale and current evidence for new therapeutic strategies. *Cancer treatment reviews,* **40,** 118-128.

Hermanova, M., P. Karasek, R. Nenutil, M. Kyr, J. Tomasek, I. Baltasova and P. Dite, 2009: Clinicopathological correlations of cyclooxygenase-2, MDM2, and p53 expressions in surgically resectable pancreatic invasive ductal adenocarcinoma. *Pancreas,* **38,** 565-571.

Hermanova, M., P. Karasek, J. Tomasek, J. Lenz, J. Jarkovsky and P. Dite, 2010: Comparative analysis of clinicopathological correlations of cyclooxygenase-2 expression in resectable pancreatic cancer. *World J Gastroenterol,* **16,** 1879-1884.

Hess-Stumpp, H., T. U. Bracker, D. Henderson and O. Politz, 2007: MS-275, a potent orally available inhibitor of histone deacetylases--the development of an anticancer agent. *The international journal of biochemistry & cell biology,* **39,** 1388-1405.

Hill, R., Y. Li, L. M. Tran, S. Dry, J. H. Calvopina, A. Garcia, C. Kim, Y. Wang, T. R. Donahue, H. R. Herschman and H. Wu, 2012: Cell intrinsic role of COX-2 in pancreatic cancer development. *Mol Cancer Ther,* **11,** 2127-2137.

Hirokawa, Y., A. Levitzki, G. Lessene, J. Baell, Y. Xiao, H. Zhu and H. Maruta, 2007: Signal therapy of human pancreatic cancer and NF1-deficient breast cancer xenograft in mice by a combination of PP1 and GL-2003, anti-PAK1 drugs (Tyr-kinase inhibitors). *Cancer Lett,* **245,** 242-251.

Horner, M. J. e. a., 2009: SEER Cancer Statistics Review, 1975-2006, National Cancer Institute.

Hruban, R. H., N. V. Adsay, J. Albores-Saavedra, M. R. Anver, A. V. Biankin, G. P. Boivin, E. E. Furth, T. Furukawa, A. Klein, D. S. Klimstra, G. Kloppel, G. Y. Lauwers, D. S. Longnecker, J. Luttges, A. Maitra, G. J. Offerhaus, L. Perez-Gallego, M. Redston and D. A. Tuveson, 2006: Pathology of genetically engineered mouse models of pancreatic exocrine cancer: consensus report and recommendations. *Cancer Res,* **66,** 95-106.

Hruban, R. H., R. E. Wilentz and S. E. Kern, 2000: Genetic progression in the pancreatic ducts. *Am J Pathol,* **156,** 1821-1825.

Huxley, R., A. Ansary-Moghaddam, A. Berrington de Gonzalez, F. Barzi and M. Woodward, 2005: Type-II diabetes and pancreatic cancer: a meta-analysis of 36 studies. *Br J Cancer,* **92,** 2076-2083.

Hwang, R. F., T. Moore, T. Arumugam, V. Ramachandran, K. D. Amos, A. Rivera, B. Ji, D. B. Evans and C. D. Logsdon, 2008: Cancer-associated stromal fibroblasts promote pancreatic tumor progression. *Cancer Res,* **68,** 918-926.

Ioka, T., K. Katayama, S. Tanaka, R. Takakura, R. Ashida, N. Kobayashi and H. Taniai, 2013: Safety and effectiveness of gemcitabine in 855 patients with pancreatic cancer under Japanese clinical practice based on post-marketing surveillance in Japan. *Japanese journal of clinical oncology,* **43,** 139-145.

Ito, H., M. Duxbury, E. Benoit, T. E. Clancy, M. J. Zinner, S. W. Ashley and E. E. Whang, 2004: Prostaglandin E2 enhances pancreatic cancer invasiveness through an Ets-1-dependent induction of matrix metalloproteinase-2. *Cancer Res,* **64,** 7439-7446.

Ito, T., H. Igarashi and R. T. Jensen, 2012: Pancreatic neuroendocrine tumors: clinical features, diagnosis and medical treatment: advances. *Best practice & research. Clinical gastroenterology,* **26,** 737-753.

Jaboin, J., J. Wild, H. Hamidi, C. Khanna, C. J. Kim, R. Robey, S. E. Bates and C. J. Thiele, 2002: MS-27-275, an inhibitor of histone deacetylase, has marked in vitro and in vivo antitumor activity against pediatric solid tumors. *Cancer Res,* **62,** 6108-6115.

Jacobetz, M. A., D. S. Chan, A. Neesse, T. E. Bapiro, N. Cook, K. K. Frese, C. Feig, T. Nakagawa, M. E. Caldwell, H. I. Zecchini, M. P. Lolkema, P. Jiang, A. Kultti, C. B. Thompson, D. C. Maneval, D. I. Jodrell, G. I. Frost, H. M. Shepard, J. N. Skepper and D. A. Tuveson, 2013: Hyaluronan impairs vascular function and drug delivery in a mouse model of pancreatic cancer. *Gut,* **62,** 112-120.

Jamieson, N. B., C. R. Carter, C. J. McKay and K. A. Oien, 2011: Tissue biomarkers for prognosis in pancreatic ductal adenocarcinoma: a systematic review and meta-analysis. *Clin Cancer Res*, 2011 May 2015;2017(2010):3316-2031.

Jason, L. J., S. C. Moore, J. D. Lewis, G. Lindsey and J. Ausio, 2002: Histone ubiquitination: a tagging tail unfolds? *BioEssays : news and reviews in molecular, cellular and developmental biology*, **24,** 166-174.

Jenuwein, T. and C. D. Allis, 2001: Translating the histone code. *Science (New York, N.Y.)*, **293,** 1074-1080.

Jeong, S., D. H. Lee, J. I. Lee, J. W. Lee, K. S. Kwon, P. S. Kim, H. G. Kim, Y. W. Shin, Y. S. Kim and Y. B. Kim, 2005: Expression of Ki-67, p53, and K-ras in chronic pancreatitis and pancreatic ductal adenocarcinoma. *World J Gastroenterol,* **11,** 6765-6769.

Jiang, J. and R. Dingledine, 2013: Role of prostaglandin receptor EP2 in the regulations of cancer cell proliferation, invasion, and inflammation. *The Journal of pharmacology and experimental therapeutics,* **344,** 360-367.

Jiao, L., D. T. Silverman, C. Schairer, A. C. Thiebaut, A. R. Hollenbeck, M. F. Leitzmann, A. Schatzkin and R. Z. Stolzenberg-Solomon, 2009: Alcohol use and risk of pancreatic cancer: the NIH-AARP Diet and Health Study. *American journal of epidemiology,* **169,** 1043-1051.

Jones, S., X. Zhang, D. W. Parsons, J. C. Lin, R. J. Leary, P. Angenendt, P. Mankoo, H. Carter, H. Kamiyama, A. Jimeno, S. M. Hong, B. Fu, M. T. Lin, E. S. Calhoun, M. Kamiyama, K. Walter, T. Nikolskaya, Y. Nikolsky, J. Hartigan, D. R. Smith, M. Hidalgo, S. D. Leach, A. P. Klein, E. M. Jaffee, M. Goggins, A. Maitra, C. Iacobuzio-Donahue, J. R. Eshleman, S. E. Kern, R. H. Hruban, R. Karchin, N. Papadopoulos, G. Parmigiani, B. Vogelstein, V. E. Velculescu and K. W. Kinzler, 2008: Core signaling pathways in human pancreatic cancers revealed by global genomic analyses. *Science (New York, N.Y.),* **321,** 1801-1806.

Juuti, A., J. Louhimo, S. Nordling, A. Ristimaki and C. Haglund, 2006: Cyclooxygenase-2 expression correlates with poor prognosis in pancreatic cancer. *Journal of clinical pathology,* **59,** 382-386.

Kanda, M., H. Matthaei, J. Wu, S. M. Hong, J. Yu, M. Borges, R. H. Hruban, A. Maitra, K. Kinzler, B. Vogelstein and M. Goggins, 2012: Presence of somatic mutations in most early-stage pancreatic intraepithelial neoplasia. *Gastroenterology,* **142,** 730-733 e739.

Kasper, H. U., H. Wolf, U. Drebber, H. K. Wolf and M. A. Kern, 2004: Expression of inducible nitric oxide synthase and cyclooxygenase-2 in pancreatic adenocarcinoma: correlation with microvessel density. *World J Gastroenterol,* **10,** 1918-1922.

Kim, H. J. and S. C. Bae, 2011: Histone deacetylase inhibitors: molecular mechanisms of action and clinical trials as anti-cancer drugs. *American journal of translational research,* **3,** 166-179.

Kinoshita, S., Y. Wagatsuma and M. Okada, 2007: Geographical distribution for malignant neoplasm of the pancreas in relation to selected climatic factors in Japan. *International journal of health geographics,* **6,** 34.

Ko, A. H., E. Dito, B. Schillinger, A. P. Venook, E. K. Bergsland and M. A. Tempero, 2006: Phase II study of fixed dose rate gemcitabine with cisplatin for metastatic adenocarcinoma of the pancreas. *Journal of clinical oncology : official journal of the American Society of Clinical Oncology*, **24,** 379-385.

Kojima, K., S. M. Vickers, N. V. Adsay, N. C. Jhala, H. G. Kim, T. R. Schoeb, W. E. Grizzle and C. A. Klug, 2007: Inactivation of Smad4 accelerates Kras(G12D)-mediated pancreatic neoplasia. *Cancer Res,* **67,** 8121-8130.

Kollmannsberger, C., H. D. Peters and U. Fink, 1998: Chemotherapy in advanced pancreatic adenocarcinoma. *Cancer treatment reviews,* **24,** 133-156.

Kong, G., E. K. Kim, W. S. Kim, K. T. Lee, Y. W. Lee, J. K. Lee, S. W. Paik and J. C. Rhee, 2002: Role of cyclooxygenase-2 and inducible nitric oxide synthase in pancreatic cancer. *J Gastroenterol Hepatol,* **17,** 914-921.

Korc, M., 2007: Pancreatic cancer associated stroma production. *American journal of surgery,* **194,** s84-86.

Koshiba, T., R. Hosotani, Y. Miyamoto, M. Wada, J. U. Lee, K. Fujimoto, S. Tsuji, S. Nakajima, R. Doi and M. Imamura, 1999: Immunohistochemical analysis of cyclooxygenase-2 expression in pancreatic tumors. *Int J Pancreatol,* **26,** 69-76.

Kumagai, T., N. Wakimoto, D. Yin, S. Gery, N. Kawamata, N. Takai, N. Komatsu, A. Chumakov, Y. Imai and H. P. Koeffler, 2007: Histone deacetylase inhibitor, suberoylanilide hydroxamic acid (Vorinostat, SAHA) profoundly inhibits the growth of human pancreatic cancer cells. *Int J Cancer,* **121,** 656-665.

Kummar, S., M. Gutierrez, E. R. Gardner, E. Donovan, K. Hwang, E. J. Chung, M. J. Lee, K. Maynard, M. Kalnitskiy, A. Chen, G. Melillo, Q. C. Ryan, B. Conley, W. D. Figg, J. B. Trepel, J. Zwiebel, J. H. Doroshow and A. J. Murgo, 2007: Phase I trial of MS-275, a histone deacetylase inhibitor, administered weekly in refractory solid tumors and lymphoid malignancies. *Clin Cancer Res,* **13,** 5411-5417.

Lachner, M. and T. Jenuwein, 2002: The many faces of histone lysine methylation. *Current opinion in cell biology,* **14,** 286-298.

Larsson, S. C., N. Orsini and A. Wolk, 2007: Body mass index and pancreatic cancer risk: A meta-analysis of prospective studies. *Int J Cancer,* **120,** 1993-1998.

Lee, M. J., H. S. Lee, W. H. Kim, Y. Choi and M. Yang, 2003: Expression of mucins and cytokeratins in primary carcinomas of the digestive system. *Mod Pathol,* **16,** 403-410.

Lehmann, A., C. Denkert, J. Budczies, A. C. Buckendahl, S. Darb-Esfahani, A. Noske, B. M. Muller, M. Bahra, P. Neuhaus, M. Dietel, G. Kristiansen and W. Weichert, 2009: High class I HDAC activity and expression are associated with RelA/p65 activation in pancreatic cancer in vitro and in vivo. *BMC Cancer,* **9,** 395.

Lenoir, O., K. Flosseau, F. X. Ma, B. Blondeau, A. Mai, R. Bassel-Duby, P. Ravassard, E. N. Olson, C. Haumaitre and R. Scharfmann, 2011: Specific Control of Pancreatic Endocrine ?- and ?-Cell Mass by Class IIa Histone Deacetylases HDAC4, HDAC5, and HDAC9. *Diabetes,* **60,** 2861-2871.

Lev-Ari, S., H. Zinger, D. Kazanov, D. Yona, R. Ben-Yosef, A. Starr, A. Figer and N. Arber, 2005: Curcumin synergistically potentiates the growth inhibitory and pro-apoptotic effects of celecoxib in pancreatic adenocarcinoma cells. *Biomed Pharmacother,* **59 Suppl 2,** S276-280.

Li, D., K. Xie, R. Wolff and J. L. Abbruzzese, 2004: Pancreatic cancer. *Lancet,* **363,** 1049-1057.

Li, G., T. Yang and J. Yan, 2002: Cyclooxygenase-2 increased the angiogenic and metastatic potential of tumor cells. *Biochem Biophys Res Commun,* **299,** 886-890.

Mai, A. and L. Altucci, 2009: Epi-drugs to fight cancer: from chemistry to cancer treatment, the road ahead. *The international journal of biochemistry & cell biology,* **41,** 199-213.

Maier, T. J., S. Schiffmann, I. Wobst, K. Birod, C. Angioni, M. Hoffmann, J. J. Lopez, C. Glaubitz, D. Steinhilber, G. Geisslinger and S. Grosch, 2009: Cellular membranes function as a storage compartment for celecoxib. *Journal of molecular medicine (Berlin, Germany),* **87,** 981-993.

Malka, D., P. Hammel, F. Maire, P. Rufat, I. Madeira, F. Pessione, P. Levy and P. Ruszniewski, 2002: Risk of pancreatic adenocarcinoma in chronic pancreatitis. *Gut,* **51,** 849-852.

Malumbres, M. and M. Barbacid, 2003: RAS oncogenes: the first 30 years. *Nature reviews. Cancer,* **3,** 459-465.

Marengo, E., E. Robotti, D. Cecconi, M. Hamdan, A. Scarpa and P. G. Righetti, 2004: Identification of the regulatory proteins in human pancreatic cancers treated with Trichostatin A by 2D-PAGE maps and multivariate statistical analysis. *Analytical and bioanalytical chemistry,* **379,** 992-1003.

Marks, P. A. and R. Breslow, 2007: Dimethyl sulfoxide to vorinostat: development of this histone deacetylase inhibitor as an anticancer drug. *Nature biotechnology,* **25,** 84-90.

Matsubayashi, H., J. R. Infante, J. Winter, A. P. Klein, R. Schulick, R. Hruban, K. Visvanathan and M. Goggins, 2007: Tumor COX-2 expression and prognosis of patients with resectable pancreatic cancer. *Cancer Biol Ther,* 2007 Oct;2006(2010):1569-2075.

Matsumoto, G., M. Muta, K. Tsuruta, S. Horiguchi, K. Karasawa and A. Okamoto, 2007: Tumor size significantly correlates with postoperative liver metastases and COX-2 expression in patients with resectable pancreatic cancer. *Pancreatology,* **7,** 167-173.

McAdam, B. F., F. Catella-Lawson, I. A. Mardini, S. Kapoor, J. A. Lawson and G. A. FitzGerald, 1999: Systemic biosynthesis of prostacyclin by cyclooxygenase (COX)-2: the human pharmacology of a selective inhibitor of COX-2. *Proc Natl Acad Sci U S A,* **96,** 272-277.

Merati, K., M. said Siadaty, A. Andea, F. Sarkar, E. Ben-Josef, R. Mohammad, P. Philip, A. F. Shields, V. Vaitkevicius, D. J. Grignon and N. V. Adsay, 2001: Expression of inflammatory modulator COX-2 in pancreatic ductal adenocarcinoma and its relationship to pathologic and clinical parameters. *Am J Clin Oncol,* **24,** 447-452.

Miller, T. A., D. J. Witter and S. Belvedere, 2003: Histone deacetylase inhibitors. *Journal of medicinal chemistry,* **46,** 5097-5116.

Miyake, K., T. Yoshizumi, S. Imura, K. Sugimoto, E. Batmunkh, H. Kanemura, Y. Morine and M. Shimada, 2008: Expression of hypoxia-inducible factor-1alpha, histone deacetylase 1, and metastasis-associated protein 1 in pancreatic carcinoma: correlation with poor prognosis with possible regulation. *Pancreas,* **36,** e1-9.

Molina, M. A., M. Sitja-Arnau, M. G. Lemoine, M. L. Frazier and F. A. Sinicrope, 1999: Increased cyclooxygenase-2 expression in human pancreatic carcinomas and cell lines: growth inhibition by nonsteroidal anti-inflammatory drugs. *Cancer Res,* **59,** 4356-4362.

Moore, P. S., S. Barbi, M. Donadelli, C. Costanzo, C. Bassi, M. Palmieri and A. Scarpa, 2004: Gene expression profiling after treatment with the histone deacetylase inhibitor trichostatin A reveals altered expression of both pro- and anti-apoptotic genes in pancreatic adenocarcinoma cells. *Biochimica et biophysica acta,* **1693,** 167-176.

Moore, P. S., B. Sipos, S. Orlandini, C. Sorio, F. X. Real, N. R. Lemoine, T. Gress, C. Bassi, G. Kloppel, H. Kalthoff, H. Ungefroren, M. Lohr and A. Scarpa, 2001: Genetic profile of 22 pancreatic carcinoma cell lines. Analysis of K-ras, p53, p16 and DPC4/Smad4. *Virchows Arch,* **439,** 798-802.

Mottet, D. and V. Castronovo, 2008: [Histone deacetylases: a new class of efficient anti-tumor drugs]. *Medecine sciences : M/S,* **24,** 742-746.

Muller-Decker, K., G. Furstenberger, N. Annan, D. Kucher, A. Pohl-Arnold, B. Steinbauer, I. Esposito, S. Chiblak, H. Friess, P. Schirmacher and I. Berger, 2006: Preinvasive duct-derived neoplasms in pancreas of keratin 5-promoter cyclooxygenase-2 transgenic mice. *Gastroenterology,* **130,** 2165-2178.

Naito, Y., H. Kinoshita, Y. Okabe, R. Kawahara, T. Sakai, H. Suga, S. Arikawa, K. Oshima and M. Kojiro, 2006: CD56 (NCAM) expression in pancreatic carcinoma and the surrounding pancreatic tissue. *The Kurume medical journal,* **53,** 59-62.

Nakagawa, M., Y. Oda, T. Eguchi, S. Aishima, T. Yao, F. Hosoi, Y. Basaki, M. Ono, M. Kuwano, M. Tanaka and M. Tsuneyoshi, 2007: Expression profile of class I histone deacetylases in human cancer tissues. *Oncol Rep,* **18,** 769-774.

Narumiya, S., Y. Sugimoto and F. Ushikubi, 1999: Prostanoid receptors: structures, properties, and functions. *Physiological reviews,* **79,** 1193-1226.

Nathan, D., D. E. Sterner and S. L. Berger, 2003: Histone modifications: Now summoning sumoylation. *Proc Natl Acad Sci U S A,* **100,** 13118-13120.

Natoni, F., L. Diolordi, C. Santoni and M. S. Gilardini Montani, 2005: Sodium butyrate sensitises human pancreatic cancer cells to both the intrinsic and the extrinsic apoptotic pathways. *Biochimica et biophysica acta,* **1745,** 318-329.

Nawrocki, S. T., J. S. Carew, M. S. Pino, R. A. Highshaw, R. H. Andtbacka, K. Dunner, Jr., A. Pal, W. G. Bornmann, P. J. Chiao, P. Huang, H. Xiong, J. L. Abbruzzese and D. J. McConkey, 2006: Aggresome disruption: a novel strategy to enhance bortezomib-induced apoptosis in pancreatic cancer cells. *Cancer Res,* **66,** 3773-3781.

Neesse, A., P. Michl, K. K. Frese, C. Feig, N. Cook, M. A. Jacobetz, M. P. Lolkema, M. Buchholz, K. P. Olive, T. M. Gress and D. A. Tuveson, 2011: Stromal biology and therapy in pancreatic cancer. *Gut,* **60,** 861-868.

Neri, B., G. Cipriani, R. Grifoni, E. Molinara, P. Pantaleo, S. Rangan, A. Vannini, P. Tonelli, A. Valeri, D. Pantalone, A. Taddei and P. Bechi, 2009: Gemcitabine plus irinotecan as first-line weekly therapy in locally advanced and/or metastatic pancreatic cancer. *Oncology research,* **17,** 559-564.

Nishikawa, A., F. Furukawa, I. S. Lee, T. Tanaka and M. Hirose, 2004: Potent chemopreventive agents against pancreatic cancer. *Current cancer drug targets,* **4,** 373-384.

Nowak, S. J. and V. G. Corces, 2004: Phosphorylation of histone H3: a balancing act between chromosome condensation and transcriptional activation. *Trends in genetics : TIG,* **20,** 214-220.

Okami, J., S. Nakamori, N. Hiraoka, M. Tsujie, N. Hayashi, H. Yamamoto, Y. Fujiwara, H. Nagano, K. Dono, K. Umeshita, M. Sakon and M. Monden, 2003: Suppression of pancreatic cancer cell invasion by a cyclooxygenase-2-specific inhibitor. *Clin Exp Metastasis,* **20,** 577-584.

Okami, J., H. Yamamoto, Y. Fujiwara, M. Tsujie, M. Kondo, S. Noura, S. Oshima, H. Nagano, K. Dono, K. Umeshita, O. Ishikawa, M. Sakon, N. Matsuura, S. Nakamori and M. Monden, 1999: Overexpression of cyclooxygenase-2 in carcinoma of the pancreas. *Clin Cancer Res,* **5,** 2018-2024.

Okusaka, T., H. Ishii, A. Funakoshi, H. Ueno, J. Furuse and T. Sumii, 2006: A phase I/II study of combination chemotherapy with gemcitabine and 5-fluorouracil for advanced pancreatic cancer. *Japanese journal of clinical oncology,* **36,** 557-563.

Olive, K. P., M. A. Jacobetz, C. J. Davidson, A. Gopinathan, D. McIntyre, D. Honess, B. Madhu, M. A. Goldgraben, M. E. Caldwell, D. Allard, K. K. Frese, G. Denicola, C. Feig, C. Combs, S. P. Winter, H. Ireland-Zecchini, S. Reichelt, W. J. Howat, A. Chang, M. Dhara, L. Wang, F. Ruckert, R. Grutzmann, C. Pilarsky, K. Izeradjene, S. R. Hingorani, P. Huang, S. E. Davies, W. Plunkett, M. Egorin, R. H. Hruban, N. Whitebread, K. McGovern, J. Adams, C. Iacobuzio-Donahue, J. Griffiths and D. A. Tuveson, 2009: Inhibition of Hedgehog signaling enhances delivery of chemotherapy in a mouse model of pancreatic cancer. *Science (New York, N.Y.),* **324,** 1457-1461.

Omura, N., M. Griffith, A. Vincent, A. Li, S. M. Hong, K. Walter, M. Borges and M. Goggins, 2010: Cyclooxygenase-deficient pancreatic cancer cells use exogenous sources of prostaglandins. *Mol Cancer Res,* 2010 Jun;2018(2016):2821-2032.

Ouaïssi, S. Francoise, C. L. Sofia, G. Urs, Z. Kevin, S. Bernard, S. Igor, C. D. Anabela, L. Dominique, M. Eric and O. Ali, 2012: HDAC gene expression in pancreatic tumor cell lines following treatment with the HDAC inhibitors panobinostat (LBH589) and trichostatine (TSA). *Pancreatology,* **12,** 146-155.

Ouaissi, M., U. Giger, G. Louis, I. Sielezneff, O. Farges and B. Sastre, 2012: Ductal adenocarcinoma of the pancreatic head: A focus on current diagnostic and surgical concepts. *World J Gastroenterol,* **18,** 3058-3069.

Ouaissi, M., C. Hubert, R. Verhelst, P. Astarci, C. Sempoux, A. Jouret-Mourin, A. Loundou and J. F. Gigot, 2010: Vascular reconstruction during pancreatoduodenectomy for ductal adenocarcinoma of the pancreas improves resectability but does not achieve cure. *World journal of surgery,* **34,** 2648-2661.

Ouaissi, M., I. Sielezneff, R. Silvestre, B. Sastre, J. P. Bernard, J. S. Lafontaine, M. J. Payan, L. Dahan, N. Pirro, J. F. Seitz, E. Mas, D. Lombardo and A. Ouaissi, 2008: High histone deacetylase 7 (HDAC7) expression is significantly associated with adenocarcinomas of the pancreas. *Annals of surgical oncology,* **15,** 2318-2328.

Park, J. H., Y. Jung, T. Y. Kim, S. G. Kim, H. S. Jong, J. W. Lee, D. K. Kim, J. S. Lee, N. K. Kim, T. Y. Kim and Y. J. Bang, 2004: Class I histone deacetylase-selective novel synthetic inhibitors potently inhibit human tumor proliferation. *Clin Cancer Res,* **10,** 5271-5281.

Patel, A. V., C. Rodriguez, L. Bernstein, A. Chao, M. J. Thun and E. E. Calle, 2005: Obesity, recreational physical activity, and risk of pancreatic cancer in a large U.S. Cohort. *Cancer epidemiology, biomarkers & prevention : a publication of the American Association for Cancer Research, cosponsored by the American Society of Preventive Oncology,* **14,** 459-466.

Pham, H., M. Chen, A. Li, J. King, E. Angst, D. W. Dawson, J. Park, H. A. Reber, O. J. Hines and G. Eibl, 2010: Loss of 15-hydroxyprostaglandin dehydrogenase increases prostaglandin E2 in pancreatic tumors. *Pancreas,* **39,** 332-339.

Pili, R., B. Salumbides, M. Zhao, S. Altiok, D. Qian, J. Zwiebel, M. A. Carducci and M. A. Rudek, 2012: Phase I study of the histone deacetylase inhibitor entinostat in combination with 13-cis retinoic acid in patients with solid tumours. *Br J Cancer,* **106,** 77-84.

Polyak, K., I. Haviv and I. G. Campbell, 2009: Co-evolution of tumor cells and their microenvironment. *Trends in genetics : TIG,* **25,** 30-38.

Poplin, E., Y. Feng, J. Berlin, M. L. Rothenberg, H. Hochster, E. Mitchell, S. Alberts, P. O'Dwyer, D. Haller, P. Catalano, D. Cella and A. B. Benson, 3rd, 2009: Phase III, randomized study of gemcitabine and oxaliplatin versus gemcitabine (fixed-dose rate infusion) compared with gemcitabine (30-minute infusion) in patients with pancreatic carcinoma E6201: a trial of the Eastern Cooperative Oncology Group. *Journal of clinical oncology : official journal of the American Society of Clinical Oncology,* **27,** 3778-3785.

Pour, P., J. Althoff, F. W. Kruger and U. Mohr, 1977: A potent pancreatic carcinogen in Syrian hamsters: N-nitrosobis(2-oxopropyl)amine. *J Natl Cancer Inst,* **58,** 1449-1453.

Qiu, W., F. Sahin, C. A. Iacobuzio-Donahue, D. Garcia-Carracedo, W. M. Wang, C. Y. Kuo, D. Chen, D. E. Arking, A. M. Lowy, R. H. Hruban, H. E. Remotti and G. H. Su, 2011: Disruption of p16 and activation of Kras in pancreas increase ductal adenocarcinoma formation and metastasis in vivo. *Oncotarget,* **2,** 862-873.

Raderer, M., F. Wrba, G. Kornek, T. Maca, D. Y. Koller, G. Weinlaender, M. Hejna and W. Scheithauer, 1998: Association between Helicobacter pylori infection and pancreatic cancer. *Oncology,* **55,** 16-19.

Rasmuson, A., A. Kock, O. M. Fuskevag, B. Kruspig, J. Simon-Santamaria, V. Gogvadze, J. I. Johnsen, P. Kogner and B. Sveinbjornsson, 2012: Autocrine prostaglandin E2 signaling promotes tumor cell survival and proliferation in childhood neuroblastoma. *PLoS One,* 2012;2017(2011):e29331.

Reid, M. D., P. Bagci and N. V. Adsay, 2013: Histopathologic assessment of pancreatic cancer: does one size fit all? *J Surg Oncol,* **107,** 67-77.

Renehan, A. G., M. Tyson, M. Egger, R. F. Heller and M. Zwahlen, 2008: Body-mass index and incidence of cancer: a systematic review and meta-analysis of prospective observational studies. *Lancet,* **371,** 569-578.

Renouf, D. J., M. J. Moore, D. Hedley, S. Gill, D. Jonker, E. Chen, D. Walde, R. Goel, B. Southwood, I. Gauthier, W. Walsh, L. McIntosh and L. Seymour, 2012: A phase I/II study of the Src inhibitor saracatinib (AZD0530) in combination with gemcitabine in advanced pancreatic cancer. *Investigational new drugs,* **30,** 779-786.

Richards, D. A., K. A. Boehm, D. M. Waterhouse, D. J. Wagener, S. S. Krishnamurthi, A. Rosemurgy, W. Grove, K. Macdonald, S. Gulyas, M. Clark and K. D. Dasse, 2006: Gemcitabine plus CI-994 offers no advantage over gemcitabine alone in the treatment of patients with advanced pancreatic cancer: results of a phase II randomized, double-blind, placebo-controlled, multicenter study. *Annals of oncology : official journal of the European Society for Medical Oncology / ESMO,* **17,** 1096-1102.

Rohrmann, S., J. Linseisen, A. Vrieling, P. Boffetta, R. Z. Stolzenberg-Solomon, A. B. Lowenfels, M. K. Jensen, K. Overvad, A. Olsen, A. Tjonneland, M. C. Boutron-Ruault, F. Clavel-Chapelon, G. Fagherazzi, G. Misirli, P. Lagiou, A. Trichopoulou, R. Kaaks, M. M. Bergmann, H. Boeing, S. Bingham, K. T. Khaw, N. Allen, A. Roddam, D. Palli, V. Pala, S. Panico, R. Tumino, P. Vineis, P. H. Peeters, A. Hjartaker, E. Lund, M. L. Redondo Cornejo, A. Agudo, L. Arriola, M. J. Sanchez, M. J. Tormo, A. Barricarte Gurrea, B. Lindkvist, J. Manjer, I. Johansson, W. Ye, N. Slimani, E. J. Duell, M. Jenab, D. S. Michaud, T. Mouw, E. Riboli and H. B. Bueno-de-Mesquita, 2009: Ethanol intake and the risk of pancreatic cancer in the European Prospective Investigation into Cancer and Nutrition (EPIC). *Cancer causes & control : CCC,* **20,** 785-794.

Rundlett, S. E., A. A. Carmen, R. Kobayashi, S. Bavykin, B. M. Turner and M. Grunstein, 1996: HDA1 and RPD3 are members of distinct yeast histone deacetylase complexes that regulate silencing and transcription. *Proc Natl Acad Sci U S A,* **93,** 14503-14508.

Ryan, Q. C., D. Headlee, M. Acharya, A. Sparreboom, J. B. Trepel, J. Ye, W. D. Figg, K. Hwang, E. J. Chung, A. Murgo, G. Melillo, Y. Elsayed, M. Monga, M. Kalnitskiy, J. Zwiebel and E. A. Sausville, 2005: Phase I and pharmacokinetic study of MS-275, a histone deacetylase inhibitor, in patients with advanced and refractory solid tumors or lymphoma. *Journal of clinical oncology : official journal of the American Society of Clinical Oncology,* **23,** 3912-3922.

Ryu, J. K., W. J. Lee, K. H. Lee, J. H. Hwang, Y. T. Kim, Y. B. Yoon and C. Y. Kim, 2006: SK-7041, a new histone deacetylase inhibitor, induces G2-M cell cycle arrest and apoptosis in pancreatic cancer cell lines. *Cancer Lett,* **237,** 143-154.

Saif, M. W., 2013: Advancements in the management of pancreatic cancer: 2013. *JOP : Journal of the pancreas,* **14,** 112-118.

Saif, M. W., L. Karapanagiotou and K. Syrigos, 2007: Genetic alterations in pancreatic cancer. *World J Gastroenterol*, **13,** 4423-4430.

Saito, A., T. Yamashita, Y. Mariko, Y. Nosaka, K. Tsuchiya, T. Ando, T. Suzuki, T. Tsuruo and O. Nakanishi, 1999: A synthetic inhibitor of histone deacetylase, MS-27-275, with marked in vivo antitumor activity against human tumors. *Proc Natl Acad Sci U S A*, **96,** 4592-4597.

Sato, N., T. Ohta, H. Kitagawa, M. Kayahara, I. Ninomiya, S. Fushida, T. Fujimura, G. Nishimura, K. Shimizu and K. Miwa, 2004: FR901228, a novel histone deacetylase inhibitor, induces cell cycle arrest and subsequent apoptosis in refractory human pancreatic cancer cells. *Int J Oncol*, **24,** 679-685.

Saunders, L. R. and E. Verdin, 2007: Sirtuins: critical regulators at the crossroads between cancer and aging. *Oncogene,* **26,** 5489-5504.

Schneider, G. and R. M. Schmid, 2003: Genetic alterations in pancreatic carcinoma. *Mol Cancer,* **2,** 15.

Shi, G., D. DiRenzo, C. Qu, D. Barney, D. Miley and S. F. Konieczny, 2013: Maintenance of acinar cell organization is critical to preventing Kras-induced acinar-ductal metaplasia. *Oncogene,* **32,** 1950-1958.

Sierra, J. C., S. S. Hobbs, R. Chaturvedi, F. Yan, K. T. Wilson, R. M. Peek, Jr. and D. B. Polk, 2013: Induction of COX-2 expression by Helicobacter pylori is mediated by activation of epidermal growth factor receptor in gastric epithelial cells. *American journal of physiology. Gastrointestinal and liver physiology*.

Silverman, D. T., R. N. Hoover, L. M. Brown, G. M. Swanson, M. Schiffman, R. S. Greenberg, R. B. Hayes, K. D. Lillemoe, J. B. Schoenberg, A. G. Schwartz, J. Liff, L. M. Pottern and J. F. Fraumeni, Jr., 2003: Why do Black Americans have a higher risk of pancreatic cancer than White Americans? *Epidemiology (Cambridge, Mass.),* **14,** 45-54.

Sipos, B., S. Moser, H. Kalthoff, V. Torok, M. Lohr and G. Kloppel, 2003: A comprehensive characterization of pancreatic ductal carcinoma cell lines: towards the establishment of an in vitro research platform. *Virchows Arch,* **442,** 444-452.

Stathopoulos, G. P., K. Syrigos, G. Aravantinos, A. Polyzos, P. Papakotoulas, G. Fountzilas, A. Potamianou, N. Ziras, J. Boukovinas, J. Varthalitis, N. Androulakis, A. Kotsakis, G. Samonis and V. Georgoulias, 2006: A multicenter phase III trial comparing irinotecan-gemcitabine (IG) with gemcitabine (G) monotherapy as first-line treatment in patients with locally advanced or metastatic pancreatic cancer. *Br J Cancer,* **95,** 587-592.

Sugimoto, Y. and S. Narumiya, 2007: Prostaglandin E receptors. *J Biol Chem*, 2007 Apr 2020;2282(2016):11613-11617.

Sun, C., D. Ansari, R. Andersson and D. Q. Wu, 2012: Does gemcitabine-based combination therapy improve the prognosis of unresectable pancreatic cancer? *World J Gastroenterol*, **18,** 4944-4958.

Sung, V., N. Richard, H. Brady, A. Maier, G. Kelter and C. Heise, 2011: Histone deacetylase inhibitor MGCD0103 synergizes with gemcitabine in human pancreatic cells. *Cancer Sci,* **2011 Jun;102(6):1201-7. doi,** 10.1111/j.1349-7006.2011.01921.x.

Takahashi, H., A. Li, D. W. Dawson, O. J. Hines, H. A. Reber and G. Eibl, 2011: Cyclooxygenase-2 confers growth advantage to syngeneic pancreatic cancer cells. *Pancreas,* **40,** 453-459.

Takahashi, M., F. Furukawa, K. Toyoda, H. Sato, R. Hasegawa, K. Imaida and Y. Hayashi, 1990: Effects of various prostaglandin synthesis inhibitors on pancreatic carcinogenesis in hamsters after initiation with N-nitrosobis(2-oxopropyl)amine. *Carcinogenesis,* **11,** 393-395.

Tanabe, T. and N. Tohnai, 2002: Cyclooxygenase isozymes and their gene structures and expression. *Prostaglandins & other lipid mediators,* **68-69,** 95-114.

Tatamiya, T., A. Saito, T. Sugawara and O. Nakanishi, 2004: Isozyme-selective activity of the HDAC inhibitor MS-275. *AACR Meeting Abstracts,* **2004,** 567-a-.

Taunton, J., C. A. Hassig and S. L. Schreiber, 1996: A mammalian histone deacetylase related to the yeast transcriptional regulator Rpd3p. *Science (New York, N.Y.),* **272,** 408-411.

Tinari, N., M. De Tursi, A. Grassadonia, M. Zilli, L. Stuppia, S. Iacobelli and C. Natoli, 2012: An epigenetic approach to pancreatic cancer treatment: the prospective role of histone deacetylase inhibitors. *Current cancer drug targets,* **12,** 439-452.

Tong, M., Y. Ding and H. H. Tai, 2006: Histone deacetylase inhibitors and transforming growth factor-beta induce 15-hydroxyprostaglandin dehydrogenase expression in human lung adenocarcinoma cells. *Biochemical pharmacology,* **72,** 701-709.

Tonini, G., B. Vincenzi, D. Santini, S. Scarpa, T. Vasaturo, C. Malacrino, R. Coppola, P. Magistrelli, D. Borzomati, A. Baldi, A. Antinori, M. Caricato, G. Nuzzo and A. Picciocchi, 2005: Nuclear and cytoplasmic expression of survivin in 67 surgically resected pancreatic cancer patients. *Br J Cancer,* **92,** 2225-2232.

Toomey, D. P., E. Manahan, C. McKeown, A. Rogers, H. McMillan, M. Geary, K. C. Conlon and J. F. Murphy, 2010: Vascular endothelial growth factor and not cyclooxygenase 2 promotes endothelial cell viability in the pancreatic tumor microenvironment. *Pancreas,* **39,** 595-603.

Trikudanathan, G., A. Philip, C. A. Dasanu and W. L. Baker, 2011: Association between Helicobacter pylori infection and pancreatic cancer. A cumulative meta-analysis. *JOP : Journal of the pancreas,* **12,** 26-31.

Tsuchiya, S., S. Tanaka, Y. Sugimoto, M. Katsuyama, R. Ikegami and A. Ichikawa, 2003: Identification and characterization of a novel progesterone receptor-binding element in the mouse prostaglandin E receptor subtype EP2 gene. *Genes to cells : devoted to molecular & cellular mechanisms,* **8,** 747-758.

Tucker, O. N., A. J. Dannenberg, E. K. Yang, F. Zhang, L. Teng, J. M. Daly, R. A. Soslow, J. L. Masferrer, B. M. Woerner, A. T. Koki and T. J. Fahey, 3rd, 1999: Cyclooxygenase-2 expression is up-regulated in human pancreatic cancer. *Cancer Res,* **59,** 987-990.

Turtoi, A., D. Musmeci, Y. Wang, B. Dumont, J. Somja, G. Bevilacqua, E. De Pauw, P. Delvenne and V. Castronovo, 2011: Identification of novel accessible proteins bearing diagnostic and therapeutic potential in human pancreatic ductal adenocarcinoma. *Journal of proteome research,* **10,** 4302-4313.

Ueki, T., M. Toyota, T. Sohn, C. J. Yeo, J. P. Issa, R. H. Hruban and M. Goggins, 2000: Hypermethylation of multiple genes in pancreatic adenocarcinoma. *Cancer Res,* **60,** 1835-1839.

Uwagawa, T., T. Misawa, T. Sakamoto, R. Ito, T. Gocho, H. Shiba, S. Wakiyama, S. Hirohara, S. Sadaoka and K. Yanaga, 2009: A phase I study of full-dose gemcitabine and regional arterial infusion of nafamostat mesilate for advanced pancreatic cancer. *Annals of oncology : official journal of the European Society for Medical Oncology / ESMO,* **20,** 239-243.

Verdin, E., F. Dequiedt and H. G. Kasler, 2003: Class II histone deacetylases: versatile regulators. *Trends in genetics : TIG,* **19,** 286-293.

Vincent, A., J. Herman, R. Schulick, R. H. Hruban and M. Goggins, 2011: Pancreatic cancer. *Lancet,* **378,** 607-620.

Vonlaufen, A., S. Joshi, C. Qu, P. A. Phillips, Z. Xu, N. R. Parker, C. S. Toi, R. C. Pirola, J. S. Wilson, D. Goldstein and M. V. Apte, 2008: Pancreatic stellate cells: partners in crime with pancreatic cancer cells. *Cancer Res,* **68,** 2085-2093.

Vrieling, A., H. B. Bueno-de-Mesquita, H. C. Boshuizen, D. S. Michaud, M. T. Severinsen, K. Overvad, A. Olsen, A. Tjonneland, F. Clavel-Chapelon, M. C. Boutron-Ruault, R. Kaaks, S. Rohrmann, H. Boeing, U. Nothlings, A. Trichopoulou, E. Moutsiou, V. Dilis, D. Palli, V. Krogh, S. Panico, R. Tumino, P. Vineis, C. H. van Gils, P. H. Peeters, E. Lund, I. T. Gram, L. Rodriguez, A. Agudo, N. Larranaga, M. J. Sanchez, C. Navarro, A. Barricarte, J. Manjer, B. Lindkvist, M. Sund, W. Ye, S. Bingham, K. T. Khaw, A. Roddam, T. Key, P. Boffetta, E. J. Duell, M. Jenab, V. Gallo and E. Riboli, 2010: Cigarette smoking, environmental tobacco smoke exposure and pancreatic cancer risk in the European Prospective Investigation into Cancer and Nutrition. *Int J Cancer,* **126,** 2394-2403.

Wang, G., J. He, J. Zhao, W. Yun, C. Xie, J. W. Taub, A. Azmi, R. M. Mohammad, Y. Dong, W. Kong, Y. Guo and Y. Ge, 2012a: Class I and class II histone deacetylases are potential therapeutic targets for treating pancreatic cancer. *PLoS One,* **7,** e52095.

Wang, W., J. Gao, X. H. Man, Z. S. Li and Y. F. Gong, 2009: Significance of DNA methyltransferase-1 and histone deacetylase-1 in pancreatic cancer. *Oncol Rep,* **21,** 1439-1447.

Wang, X., G. Li, A. Wang, Z. Zhang, J. R. Merchan and B. Halmos, 2013: Combined histone deacetylase and cyclooxygenase inhibition achieves enhanced antiangiogenic effects in lung cancer cells. *Mol Carcinog,* **52,** 218-228.

Wang, Z., S. Ali, S. Banerjee, B. Bao, Y. Li, A. S. Azmi, M. Korc and F. H. Sarkar, 2012b: Activated K-Ras and INK4a/Arf deficiency promote aggressiveness of pancreatic cancer by induction of EMT consistent with cancer stem cell phenotype. *J Cell Physiol,* **228,** 556-562.

Wei, D., L. Wang, Y. He, H. Q. Xiong, J. L. Abbruzzese and K. Xie, 2004: Celecoxib inhibits vascular endothelial growth factor expression in and reduces angiogenesis and metastasis of human pancreatic cancer via suppression of Sp1 transcription factor activity. *Cancer Res,* **64,** 2030-2038.

Wheater, Young and Heath, 2004: Histologie fonctionnelle. *de Boeck edition.*

Whiteside, T. L., 2008: The tumor microenvironment and its role in promoting tumor growth. *Oncogene,* **27,** 5904-5912.

Williams, C. S., M. Tsujii, J. Reese, S. K. Dey and R. N. DuBois, 2000: Host cyclooxygenase-2 modulates carcinoma growth. *J Clin Invest,* **105,** 1589-1594.

Witt, O., H. E. Deubzer, T. Milde and I. Oehme, 2009: HDAC family: What are the cancer relevant targets? *Cancer Lett,* **277,** 8-21.

Wu, S., R. W. Li, W. Li and C. J. Li, 2012: Transcriptome characterization by RNA-seq unravels the mechanisms of butyrate-induced epigenomic regulation in bovine cells. *PLoS One,* **7,** e36940.

Xu, W. S., R. B. Parmigiani and P. A. Marks, 2007: Histone deacetylase inhibitors: molecular mechanisms of action. *Oncogene,* **26,** 5541-5552.

Yip-Schneider, M. T., D. S. Barnard, S. D. Billings, L. Cheng, D. K. Heilman, A. Lin, S. J. Marshall, P. L. Crowell, M. S. Marshall and C. J. Sweeney, 2000: Cyclooxygenase-2 expression in human pancreatic adenocarcinomas. *Carcinogenesis,* **21,** 139-146.

Yonezawa, S., M. Higashi, N. Yamada and M. Goto, 2008: Precursor lesions of pancreatic cancer. *Gut and Liver,* **2,** 137-154.

Yoshida, M., A. Matsuyama, Y. Komatsu and N. Nishino, 2003: From discovery to the coming generation of histone deacetylase inhibitors. *Current medicinal chemistry,* **10,** 2351-2358.

Yoshida, S., M. Ujiki, X. Z. Ding, C. Pelham, M. S. Talamonti, R. H. Bell, Jr., W. Denham and T. E. Adrian, 2005: Pancreatic stellate cells (PSCs) express cyclooxygenase-2 (COX-2) and pancreatic cancer stimulates COX-2 in PSCs. *Mol Cancer,* **4,** 27.

Zafar, S. F., G. P. Nagaraju and B. El-Rayes, 2012: Developing histone deacetylase inhibitors in the therapeutic armamentarium of pancreatic adenocarcinoma. *Expert opinion on therapeutic targets,* **16,** 707-718.

Zhan, Y., K. Gong, C. Chen, H. Wang and W. Li, 2012: P38 MAP kinase functions as a switch in MS-275-induced reactive oxygen species-dependent autophagy and apoptosis in human colon cancer cells. *Free radical biology & medicine,* **53,** 532-543.

Zhong, B., X. Cai, S. Chennamaneni, X. Yi, L. Liu, J. J. Pink, A. Dowlati, Y. Xu, A. Zhou and B. Su, 2012a: From COX-2 inhibitor nimesulide to potent anti-cancer agent: synthesis, in vitro, in vivo and pharmacokinetic evaluation. *European journal of medicinal chemistry,* **47,** 432-444.

Zhong, Y., Z. Xia, J. Liu, Y. Lin and H. Zan, 2012b: The effects of cyclooxygenase-2 gene silencing by siRNA on cell proliferation, cell apoptosis, cell cycle and tumorigenicity of Capan-2 human pancreatic cancer cells. *Oncol Rep,* **27,** 1003-1010.

Zhou, W., I. C. Liang and N. S. Yee, 2011: Histone deacetylase 1 is required for exocrine pancreatic epithelial proliferation in development and cancer. *Cancer Biol Ther,* **11,** 659-670.

Zhu, C., Q. Chen, Z. Xie, J. Ai, L. Tong, J. Ding and M. Geng, 2011: The role of histone deacetylase 7 (HDAC7) in cancer cell proliferation: regulation on c-Myc. *J Mol Med,* 2011 Mar;2089(2013):2279-2089.

VII. ANNEXES

Annexes

Annexe 1

Effect of HDAC Inhibition in a Human Pancreas Cancer Model Is Significantly Improved by the Simultaneous Inhibition of Cyclooxygenase 2.

Peulen, O[*]. Gonzalez, A[*]. Peixoto, P. Turtoi, A. Mottet, D. Delvenne, P. and Castronovo, V.

PlosOne, 2013. 8(9).

Annexe 2

HDAC5 is required for maintenance of pericentric heterochromatin, and controls cell-cycle progression and survival of human cancer cells.

Peixoto, P. Castronovo, V. Matheus, N. Polese, C. Peulen, O. Gonzalez, A. Boxus, M. Verdin, E. Thiry, M. Dequiedt, F. and Mottet, D.

Cell death and differenciation 2012. 19(7): p 1239-52.

Annexe 3

Revealing the anti-tumoral effect of Algerian Glaucium flavum roots against human cancer cells.

Bournine, L. Bensalem, S. Peixoto, P. Gonzalez, A. Maiza-Benabdesselam, F. Bedjou, F. Wauters, J. Tits, M. Frédérich, M. Castronovo, V. and Bellahcène, A.

Phytomedicine, 2013: p. 1211-8.

Effect of HDAC Inhibition in a Human Pancreas Cancer Model Is Significantly Improved by the Simultaneous Inhibition of Cyclooxygenase 2.

Peulen, O. Gonzalez, A. Peixoto, P. Turtoi, A. Mottet, D. Delvenne, P. and Castronovo, V.

PlosOne, 2013. 8(9).

PLOS ONE

The Anti-Tumor Effect of HDAC Inhibition in a Human Pancreas Cancer Model Is Significantly Improved by the Simultaneous Inhibition of Cyclooxygenase 2

Olivier Peulen[1,9], Arnaud Gonzalez[1,9], Paul Peixoto[1], Andrei Turtoi[1], Denis Mottet[1], Philippe Delvenne[2], Vincent Castronovo[1]*

1 Metastasis Research Laboratory, GIGA-Cancer, University of Liege, Liege, Belgium, 2 Laboratory of Experimental Pathology, GIGA-Cancer, University of Liege, Liege, Belgium

Abstract

Pancreatic ductal adenocarcinoma is the fourth leading cause of cancer death worldwide, with no satisfactory treatment to date. In this study, we tested whether the combined inhibition of cyclooxygenase-2 (COX-2) and class I histone deacetylase (HDAC) may results in a better control of pancreatic ductal adenocarcinoma. The impact of the concomitant HDAC and COX-2 inhibition on cell growth, apoptosis and cell cycle was assessed first *in vitro* on human pancreas BxPC-3, PANC-1 or CFPAC-1 cells treated with chemical inhibitors (SAHA, MS-275 and celecoxib) or HDAC1/2/3/7 siRNA. To test the potential antitumoral activity of this combination *in vivo*, we have developed and characterized, a refined chick chorioallantoic membrane tumor model that histologically and proteomically mimics human pancreatic ductal adenocarcinoma. The combination of HDAC1/3 and COX-2 inhibition significantly impaired proliferation of BxPC-3 cells *in vitro* and stalled entirely the BxPC-3 cells tumor growth onto the chorioallantoic membrane *in vivo*. The combination was more effective than either drug used alone. Consistently, we showed that both HDAC1 and HDAC3 inhibition induced the expression of COX-2 via the NF-kB pathway. Our data demonstrate, for the first time in a Pancreatic Ductal Adenocarcinoma (PDAC) model, a significant action of HDAC and COX-2 inhibitors on cancer cell growth, which sets the basis for the development of potentially effective new combinatory therapies for pancreatic ductal adenocarcinoma patients.

Introduction

Pancreatic ductal adenocarcinoma (PDAC) lists among the most deadly form of cancers [1]. Early-stage of the disease is clinically silent and the diagnosis of the disease is mostly made at an advanced stage. This late diagnosis contributes to one of the lowest 5-year survival rate (only 3%) [2]. Today PDAC are treated by surgery and/or adjuvant therapy with gemcitabine, increasing only slightly the median survival of the patients. There is therefore an urgent need to develop new effective therapies for PDAC patients.

There are abundant evidence indicating that deregulation of histone acetylation contributes to pancreas cancer development and progression [3]. Histone deacetylases (HDAC) represent a family of enzymes that regulate paramount cellular activities including epigenetic silencing of tumor suppressor genes and modulation of protein functions. We and others have shown that HDAC inhibition exerts both anti-cancer and anti-angiogenesis activities [4–6]. HDAC expression is altered in PDAC, including HDAC1, HDAC2, HDAC3 and HDAC7 [7–10]. Preclinical studies have suggested that HDAC inhibition hold significant

potential for the development of new anticancer therapies [11]. Accordingly, several HDAC inhibitors have been recently approved by the Food and Drug Administration for the treatment of Cutaneous T-Cell Lymphoma while new molecules are currently in phase III clinical trials. However, when used in monotherapy, HDAC inhibitors showed limited efficacy in various solid malignancies, including PDAC [3,12,13]. Indeed, LAQ824 or MS-275 have been evaluated in phase I clinical trials in solid cancers, including PDAC, without any objective clinical response [14,15]. Alternatively, HDAC inhibitors have been used in combined therapy strategies [16,17], with some combinations generating promising effects for human PDAC *in vitro* [18–21] or in experimental tumors [22]. Unfortunately, these results do not translate in clinical trials [23,24].

The lack of efficacy of HDAC inhibitors in pancreatic cancer could be linked to the pleiotropic activities of HDACs in cell biology [25,26] leading to undesired pro-cancer effects. For example, a recent study demonstrated that pan-HDAC inhibitors induce cyclooxygenase-2 (COX-2) expression in lung cancer cells, leading to a stimulation of endothelial cell proliferation [27]. Since

COX-2 has been also associated to pancreatic cancer cell proliferation [28] or tumor growth [29–31], we hypothesized that COX-2 overexpression may also be induced in PDAC when treated with HDAC inhibitors, leading to reduced efficiency and hence therapeutic failure.

To test the biological relevance of combining class I HDAC and COX-2 inhibitors *in vivo*, we devised a refined PDAC chick chorioallantoic membrane (CAM) model based on our previous work [32]. The CAM model has been successfully used with several cell lines to produce tumors [33,34]. Similarly to the murine model, most steps of tumor progression are recapitulated in a very short period of time [35]. Previously, BxPC-3 pancreatic cancer cells were already demonstrated to produce vascularized 100 μm long tumor nodes on CAM [32]. However, the small size of the nodules represented a significant limitation for structural observation, accurate volume evaluation and study of drug efficacy. Here, we have established and implemented a refined BxPC-3 PDAC model featuring a dramatic increase (64-fold) in tumor size and displaying structural architecture and protein expression mimicking human PDAC. This model was successfully exploited to demonstrate that the combination of class I HDAC and COX-2 inhibitors result in a complete tumor growth inhibition.

Materials and Methods

Cells and chemicals

BxPC-3 (ATCC CRL-1687), PANC-1 (ATCC CRL-1469) and CFPAC-1 (ATCC CRL-1918) are human pancreatic cancer cell lines derived respectively from PDAC [36], pancreas duct epithelioid carcinoma [37] and PDAC liver metastasis [38]. BxPC-3 were a generous gift from Prof. Bikfalvi (Inserm u1029, Bordeaux, France), Panc-1 were a generous gift from Prof. Muller and Burtea (NMR Laboratory, University of Mons, Belgium). CFPAC-1 were bought from ATCC. Celecoxib was obtained from the University Pharmacy (Kemprotec Ltd, Middlesbrough, UK). MS-275 and SAHA were purchased from Enzo Life Sciences (Antwerpen, Belgium). Other chemicals were purchased from Sigma (Bornem, Belgium).

Cell culture

BxPC-3 human pancreatic cancer cell line were maintained in RPMI1640 medium supplemented with glucose (2.5 g/L), sodium pyruvate (1 mM) and FBS (10%). PANC-1 were maintained in DMEM supplemented with FBS (10%). CFPAC-1 were maintained in Iscove's Modified Dulbecco's Medium with FBS (10%). Cells were treated with MS-275, celecoxib or combination of both as well as with suberoylanilide hydroxamic acid (SAHA) solubilized in medium with 0.1% DMSO.

Small interfering RNA transfection

HDAC-specific small interfering RNA (siRNA) were synthesized by Eurogentec (Seraing, Belgium). NF-kB p65 SMARTpool siRNA were bought from Thermo Fisher-Dharmacon (Whaltham, MA). Lipofectamine-mediated transfections were performed at a siRNA concentration of 40 nM following manufacturer's recommendations (Life Technologies, Carlsbad, NM). GL3 was an irrelevant siRNA targeting luciferase. siRNA sequences were published previously [5].

Cell growth

Equal densities of cells were seeded in complete medium and were harvested at the indicated time-points. The cell numbers were indirectly determined using Hoechst incorporation. Results were expressed as DNA content.

Western-blotting

BxPC-3 cells or frozen tumors were disrupted in lysis buffer (1% SDS, 40 mM Tris-HCl pH7.5) in the presence of protease and phosphatase inhibitors. Proteins were separated by SDS-PAGE (6–12.5%) then electrotransfered on nitrocellulose membranes. Following primary antibodies were used: anti-COX-2 (Cayman Chemicals, Ann Arbor, MI), anti-HDAC1 (Cell Signalling, Danvers, MA), anti-HDAC2 (Santa Cruz Biotechnology, Santa Cruz, CA), anti-HDAC3 (Cell Signalling, Danvers, MA), anti-acetylated-Histone-3 (Millipore, Billerica, MA), anti-HDAC7 (Santa Cruz Biotechnology, Santa Cruz, CA), anti-phospho-IkBα (Cell Signalling, Danvers, MA), anti-p65 (Cell signaling, Danvers, MA), anti-p21 (Santa Cruz Biotechnology, Santa Cruz, CA), anti-p27 (BD Biosciences, Franklin Lakes, NJ), anti-pRB (BD Biosciences, Franklin Lakes, NJ), anti-E2F1 (Santa Cruz Biotechnology, Santa Cruz, CA), anti-MEK2 (Cell signaling, Danvers, MA), anti-ORC2 (Cell signaling, Danvers, MA), anti-caspase-3 (Cell Signalling, Danvers, MA) and anti-HSC70 (Santa Cruz Biotechnology, Santa Cruz, CA). Immunodetection was performed using appropriate secondary antibody conjugated with horseradish peroxidase.

Quantitative real-time RT-PCR

Total RNA extraction and quantitative real-time RT-PCR were performed as previously described [39]. Human COX-2 expression was detected using a commercial RT-qPCR TaqMan assay (Hs00153133-m1; Applied Biosystems, Carlsbad, NM). Human IL-8 expression was detected using specific forward (5′-GAAG-GAACCATCTCACTGTGTGTAA-3′) and reverse (5′-ATCAG-GAAGGCTGCCAAGAG-3′) primers synthesized by Eurogentec (Seraing, Belgium).

Annexin V/propidium iodide staining

Apoptotic cells were determined by annexin V-FITC and non-vital dye propidium iodide (PI) staining with a FITC-Annexin V apoptosis detection kit I (BD Biosciences, Franklin Lakes, NJ) according to the manufacturer's instructions. Flow cytometry was performed on a FACSCalibur II™ and samples were analyzed using CellQuest™ software (BD Biosciences, Franklin Lakes, NJ).

Cell cycle analysis

The relative percentage of cells in each stage of the cell cycle was analyzed as previously described [33] by flow cytometric analysis with FACSCalibur II™ and ModFit LT™program.

Tumor growth on CAM

Fertilized chicken eggs were opened as previously described [32]. On post-fertilization day 11, CAM surface was gently scratched with a needle and 3.5×10^6 BxPC-3, PANC-1 or CFPAC-1 cells in suspension with 50% matrigel in a final volume of 100 μL were grafted on the CAM enclosed by a 6-mm plastic ring. The implantation day was considered as day 0 of tumor development. Drugs (celecoxib 8 μM and/or MS-275 0.2 μM in a 30 μl final volume) were applied daily directly on tumor starting at day 2. At day 7, the tumors were excised from the CAM and digital pictures were taken using a stereomicroscope. Tumor volume was calculated using an ellipsoid formula: Volume $= (4 \times \pi x Z_1 \times Z_2 \times Z_3)/3$ where Z_{1-3} are the main radius of the tumor.

Ethics statement

All animal experiments were approved by the Animal Welfare Committee of the University of Liège (approval #1278).

Histology procedure

BxPC-3 tumors were washed in PBS and then fixed in 4% paraformaldehyde for 30min at 4°C. The tumors were embedded in paraffin and 5 µm sections were stained with Hematoxylin-eosin or Masson's trichrome.

Immunoperoxydase and amylase-periodic acid Schiff (PAS) staining were performed on 5 µm sections, respectively, with the BenchMark XT IHC/ISH automated stainer and the NexES Special Stains (Ventana Medical Systems Inc, Tucson, AZ) according to the manufacturer's instructions. Following antibodies were used: anti-cytokeratin 7 (CK7 - Dako, Glostrup, Denmark), anti-cytokeratin 19 (CK19 - Roche Diagnostics, Vilvoorde, Belgium), anti-cytokeratin 20 (CK20 - Dako, Glostrup, Denmark), anti-CD56 (Novocastra, Leica Microsystem Inc, Buffalo Grove, IL), anti-carcinoembryonic antigen (CEA - Roche Diagnostics, Vilvoorde, Belgium), anti-Ki67 (Dako, Glostrup, Denmark), anti-latent transforming growth factor-beta binding protein 2 (LTBP2 – Santa Cruz Biotchnology, Santa Cruz, CA), anti-transforming
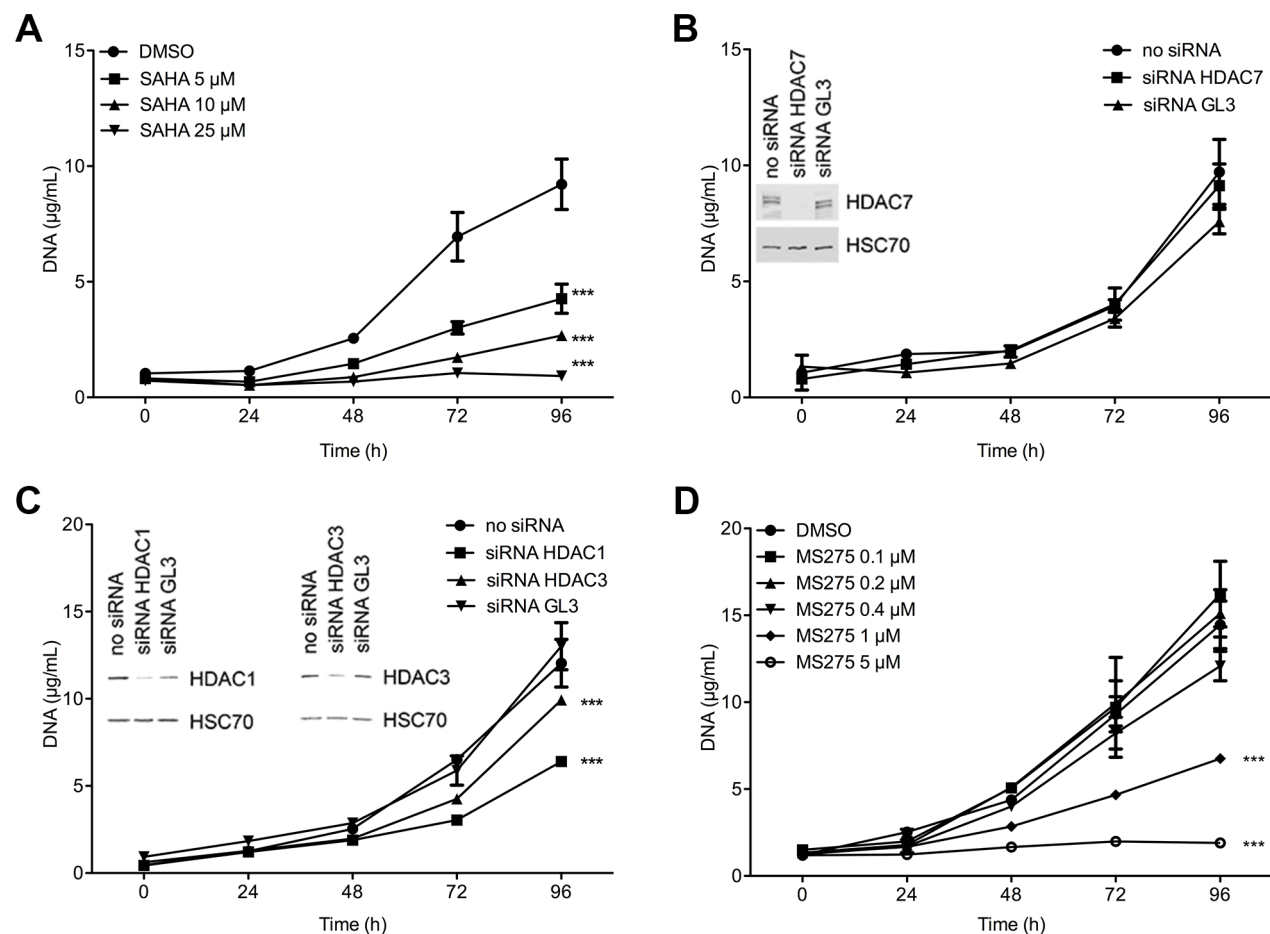
growth factor beta-induced (TGFBI - Cell Signalling, Danvers, MA), anti-myoferlin (Sigma, Bornem, Belgium) and anti-desmin (Dako, Glostrup, Denmark) were used for the primary reaction.

Ki67 quantification was performed on randomly taken pictures (3 pictures from each tumor, 3 tumors in each experimental group). After channel splitting, blue channel pictures were binarized according to the brightness. The size of the area occupied by all cells or by Ki67-positive cells was measured using imageJ 1.46r software.

In order to visualize the tumor vasculature, thick rehydrated tissue sections (35 µm) were incubated for 30min in the dark with 0.05% Triton X-100 in PBS containing 5 µg/mL *Sambucus nigra* agglutinin (SNA, Vector Laboratories, Burlingame, CA). The sections were washed with 0.05% Triton X-100 in PBS and visualized with confocal microscope (Leica SP2). Three-dimensional images were reconstructed with Imaris software (Bitplane Scientific Software, Zurich, Switzerland).

Statistical analysis

All results were reported as means with standard deviation. Statistical analysis was performed using one-way or two-way ANOVA depending on the number of grouping factors. Group

Figure 1. Effect of HDAC silencing or inhibition on BxPC-3 cell proliferation. (A) Time-dependent and dose-dependent effects of SAHA on cell proliferation. (B) Time-dependent effect of class IIa HDAC7 silencing on cell proliferation. HDAC7 expression was detected by western-blot 48h after siRNA transfection. HSC70 was used as a loading control. (C) Time-dependent effect of class I HDAC1 or –3 silencing on cell proliferation.. HDAC1 and HDAC3 expression was detected by western-blot 48h after siRNA transfection. HSC70 was used as a loading control. (D) Time-dependent and dose-dependent effects of MS-275 on cell proliferation ***P<.001 versus DMSO or GL3 conditions. Results are expressed as mean ± s.d., n≥3 in each condition.
doi:10.1371/journal.pone.0075102.g001

Figure 2. Effect of HDAC silencing or inhibition on COX-2 expression in BxPC-3 cells. (A) Western-blot detection of COX-2 and HDAC in 20 μg BxPC-3 proteins 48h after HDAC1 or HDAC3 siRNA transfection. (B) Western-blot detection of COX-2 and HDAC in 20 μg BxPC-3 proteins 48h after HDAC2 siRNA transfection. (C) Dose-dependent effects of 48h MS-275 treatment on COX-2 expression. Acetylated-histone H3 was used as a control of treatment efficacy. HSC70 was used as a loading control. (D) Time-dependent relative expression of COX-2 mRNA in BxPC-3 cells treated with 1 μM MS-275. Results are expressed as mean ± s.d., n = 3.
doi:10.1371/journal.pone.0075102.g002

means were compared by a Bonferroni's post-test. P<.05 was considered as statistically significant. All experiments were performed as 3 independent biological replicates.

Results

Class I HDAC inhibition reduced pancreas cancer cell growth in vitro

BxPC-3 cells have been described to express altered levels of class I HDAC1, HDAC3 and class II HDAC7 [40,41]. To evaluate the role of these HDAC in BxPC-3 cells, we first examined their time-dependent and concentration-dependent growth in presence of SAHA, a class I/II inhibitor (Figure 1A). Our results confirmed that BxPC-3 cells were sensitive to SAHA, with a 50% growth reduction (P<.001) observed at 5 μM. Next, we selectively silenced HDAC1, –3 or –7 using siRNA to examine the individual involvement of these HDAC in the SAHA-induced growth reduction. HDAC7 silencing did not affect cell growth (Figure 1B). However, HDAC1 and HDAC3 silencing reduced significantly BxPC-3 cell growth by respectively 50% (P<.001) and

20% (P<.001) (Figure 1C). In order to evaluate this decrease in cell growth with clinically compatible drug, we evaluated the time-dependent and concentration-dependent growth of BxPC-3 cells in presence of MS-275 (HDAC1 and HDAC3 inhibitor). MS-275 (1 μM) reduced BxPC-3 cell growth by 50% (P<.001) whereas 5 μM abolished completely the growth (P<.001) (Figure 1D).

Class I HDAC inhibition induced COX-2 expression in vitro

The limited efficiency of HDAC inhibitors in clinical trials including PDAC patients could be explained, at least in part, by the potential up regulation of the expression of COX-2 in pancreatic malignant cells. To evaluate this hypothesis, we first analyzed COX-2 expression in BxPC-3 cells silenced for HDAC1, HDAC2, HDAC3 or treated with MS-275. HDAC1 or HDAC3 repression induced respectively a 6.3-fold and a 4.8-fold increase of COX-2 expression at protein level (Figure 2A) while HDAC2 silencing reduced COX-2 expression (Figure 2B). HDAC1 silencing induced an HDAC2 overexpression.
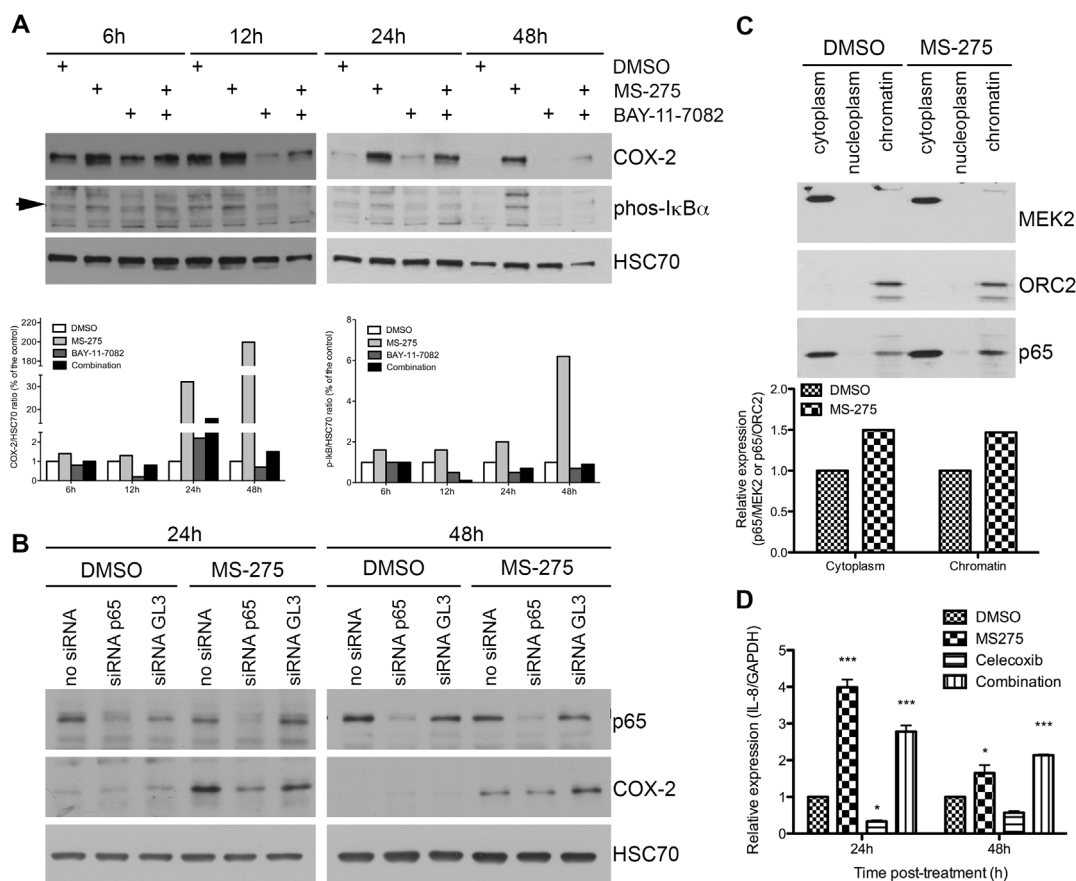
Figure 3. Effect of HDAC inhibition on NF-kB activation in BxPC-3 cells. (A) Effect of an IKK inhibitor (10 µM BAY-11-7082) on 1 µM MS-275-induced COX-2 expression. Phospho-IkBα was used as a control of BAY-11-7082 treatment efficacy. HSC70 was used as a loading control. Densitometry was expressed as a COX-2/HSC70 or IkBα/HSC70 ratio. (B) Western-blot detection of COX-2 in 20 µg BxPC-3 proteins after 1 µM MS-275 treatment and p65 siRNA transfection. HSC70 was used as a loading control. (C) Western-blot detection of p65 in 15 µg BxPC-3 cytoplasm, nucleoplasm or chromatin-associated proteins after 1 µM MS-275 treatment. MEK2 and ORC2 were used as a loading control respectively in cytoplasm and chromatin fractions. Densitometry was expressed as a p65/MEK2 or p65/ORC2 ratio. (D) Time-dependent relative expression of IL-8 mRNA in BxPC-3 cells treated with 1 µM MS-275, 10 µM Celecoxib or a combination of the drugs. Results are expressed as mean $\pm$ s.d. ***P<.001, *P<.05 versus DMSO. n≥3 in each condition.
doi:10.1371/journal.pone.0075102.g003

Treatment of BxPC-3 cells with MS-275 showed similar effects on COX-2 accumulation in a concentration-depend manner (Figure 2C). To determine whether COX-2 induction occurs at transcriptional level, we analyzed COX-2 mRNA level by RT-qPCR following 6, 12, and 24h of MS-275 treatment. We found that COX-2 gene expression was up-regulated following the MS-275 treatment in a time-dependent manner (Figure 2D).

To study the mechanisms by which class I HDAC inhibition induces COX-2, we explored the known link between NF-kB and HDAC1/3 [42,43] and tested the possibility that MS-275-induced COX-2 expression could be NF-kB dependent. Accordingly, we co-treated cells with MS-275 and BAY-11-7082, an IkBα kinase (IKK) inhibitor. BAY-11-7082 reduced by 30% to 90% the COX-2 expression following respectively 6h to 48h of MS-275 treatment (Figure 3A), suggesting the MS-275-induced expression of COX-2 is, at least in part, NF-kB dependent. This hypothesis was supported by p65-silencing and p65 translocation to the nucleus. COX-2 expression was induced by a 24h treatment with MS-275 and was prevented by p65 siRNA (Figure 3B). Moreover, 24h MS-275 treatment induced an increase by 50% of the p65 protein level in the cytoplasm and in the chromatin fraction of BxPC-3 cells

(Figure 3C). The same MS-275 treatment induced the gene expression of IL-8 (Figure 3D), a direct target of NF-kB.

Combined inhibition of class I HDAC and COX-2 inhibits cell growth in vitro

In order to validate our hypothesis that class I HDAC inhibition mediated induction of COX-2 might contribute to the low efficiency of HDAC based therapy in PDAC patients, we have combined the latter with celecoxib, a selective COX-2 inhibitor at IC50 (respectively 1 µM of MS-275 and 10 µM of celecoxib). The MS-275-induced COX-2 overexpression led to a 50% increase of PGE2 concentration in the culture media (Figure 4A). BxPC-3 cell treatment with celecoxib alone or in combination with MS-275 reduced significantly the PGE$_2$ concentration in the cell media. We then analyzed the impact of these treatments on the cell growth. The combination of the two drugs reduced significantly (>85%, P<.001) the BxPC-3 cell growth in comparison with using either drug alone (Figure 4B). We next asked the question whether this reduction is due to induction of apoptosis and performed an annexin V/propidium iodide staining at 24, 48 and 72h (Figure 4C) following the treatment. None of the individual drugs nor their combination were able to induce apoptosis. These results were
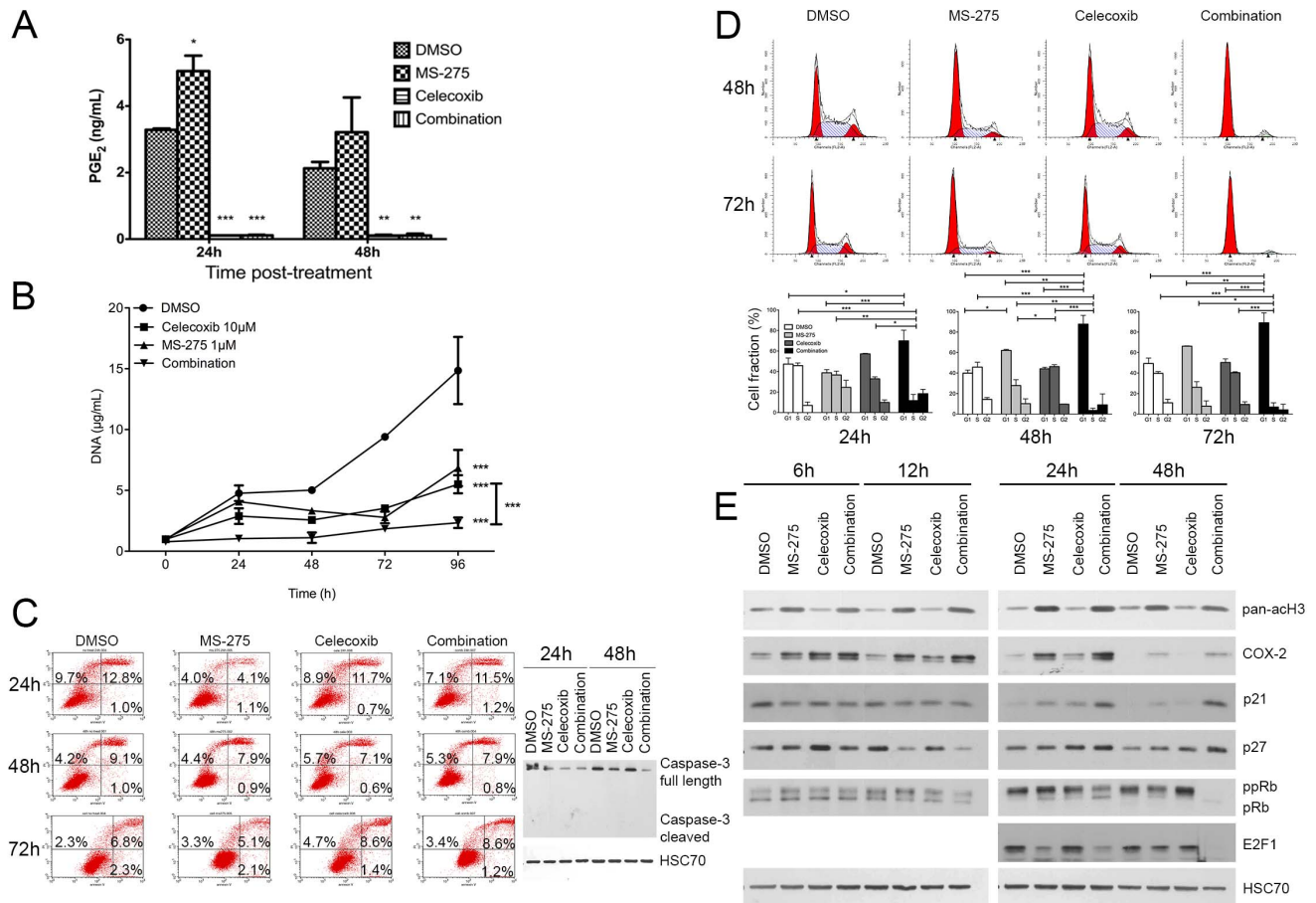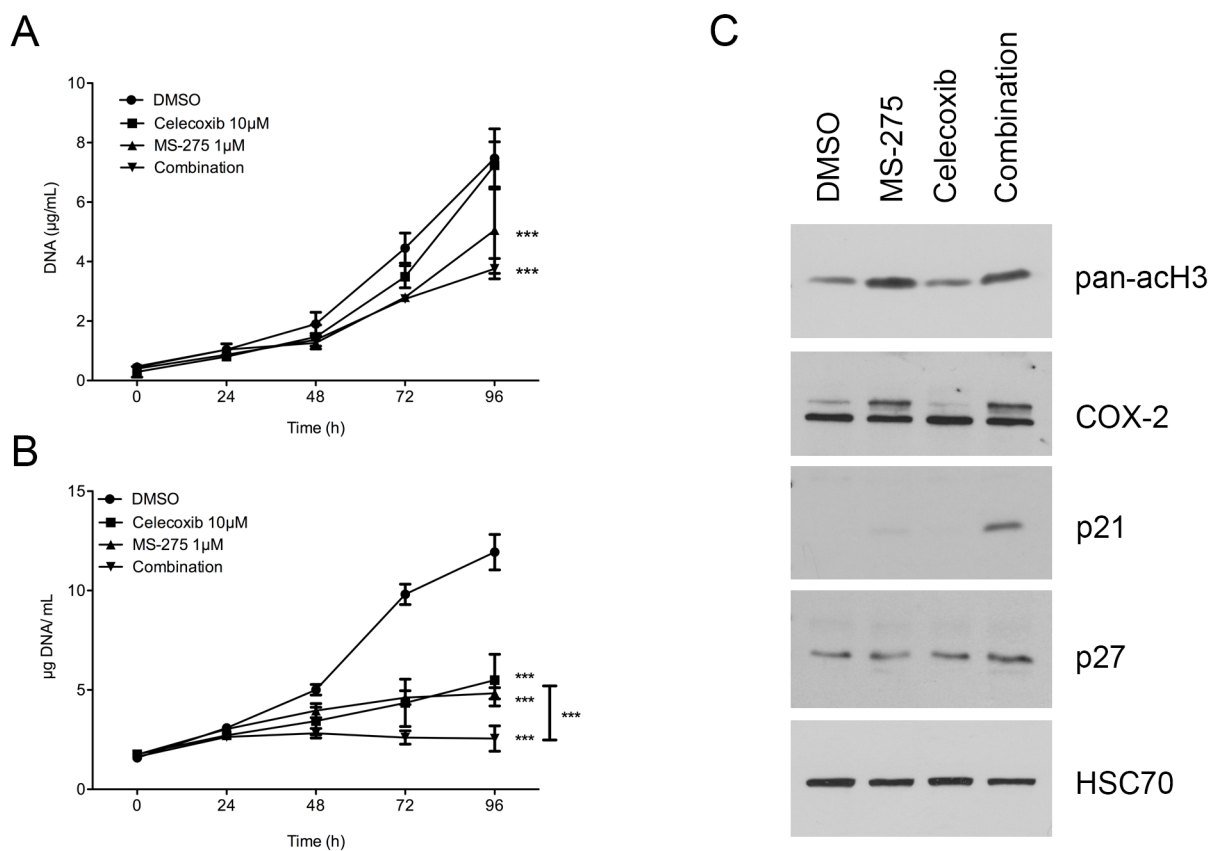
Figure 4. Effect of HDAC and COX-2 coinhibition in BxPC-3 cells. (A) ELISA assay of PGE$_2$ in cell culture media 24h and 48h after 1 μM MS-275 and 10 μM celecoxib treatment. (B) Time-dependent effects of MS-275 and celecoxib on cell growth. (C) Time-dependent effects of 1 μM MS-275 and 10 μM celecoxib on apoptotic cell ratio by annexin V/PI flow cytometry and on caspase-3 cleavage. (D) Time-dependent effects of 1 μM MS-275 and 10 μM celecoxib on cell cycle by PI incorporation. (E) Western-blot detection of p21, p27, pRb ppRb and E2F1 in 20 μg BxPC-3 proteins 6 to 48h after 1 μM MS-275 and 10 μM celecoxib treatment. HSC70 was used as a loading control. Results are expressed as mean ± s.d., ***P<.001, **P<.01, *P<.05 versus DMSO or indicated conditions. n≥3 in each condition.
doi:10.1371/journal.pone.0075102.g004

confirmed by western-blot, showing intact caspase-3 in all samples (Figure 4C). To further investigate the mechanisms of the observed cell growth arrest, we next examined the effect of MS-275/celecoxib combination on the cell cycle (Figure 4D). MS-275 alone, but not celecoxib, increased the proportion of cell in G1 by 50% at 48h. However, MS-275/celecoxib combination decreased significantly (P<.001) the proportion of cells in S phase at 24 (–74%), 48 (–92%) and 72h (–82%) and increased significantly (P<.001) the proportion in G1 phase at 24 (+48%), 48 (+119%) and 72h (+80%). To validate these results we analyzed by western blot the expression of cell cycle markers and found a clear accumulation of p21^{WAF1} and p27^{Kip1}, two cell cycle inhibitors, at 24h and 48h after the co-administration of MS-275 and celecoxib (Figure 4E). Consistently, the hyperphosphorylated form of pRb was less abundant when BxPC-3 cells were co-treated with MS-275/celecoxib. The hypophosphorylated form of pRb appeared with the co-inhibition of class I HDAC and COX-2. The whole pRb protein disappeared at 48h after the cotreatment. This disappearance was already observed by others after a p21^{WAF1} or p27^{Kip1} accumulation [44]. The E2F1 transcription factor, a S-phase orchestrator, became undetectable 48h after co-administration of MS-275 and celecoxib. These results show that cellular growth inhibition is associated to a G0/G1 phase blockage.

BxPC-3 is a PDAC cell line characterized by its KRAS wildtype, while mutations of the gene coding for this protein is the most common genetic alteration observed in human PDAC. However, BxPC-3 cells overexpress COX-2, a situation noted in 50% of human PDAC. We have decided to extend our observations regarding the interest of the combined treatment in pancreatic cancer by examining the efficiency of such combined treatment on two human pancreas cell lines with reported KRAS mutations. The first cell line was PANC-1 ([12 ASP]-KRAS) in which COX-2 was undetected at the protein level [45]. The second cell line was CFPAC-1 ([12 VAL]-KRAS) but in which COX-2 was detected at protein level [45].

PANC-1 cell line was cultured with MS-275, celecoxib or both drugs in combination. Celecoxib 10 μM did not alter cell growth when MS-275 1 μM reduced significantly (p<,001) cell growth by 32%. The combination of the two drugs reduced the PANC-1 cell growth (49%, P<.001). However, the combination-induced growth inhibition was not significantly different from the MS-275-induced one (Figure 5A). In this cell line, MS-275 did not induce the expression of COX-2 (data not shown).

CFPAC-1 cell line was cultured in the same conditions. Celecoxib 10 μM reduced cell growth by 54% (p<,001) and MS-275 1 μM reduced cell growth by 59% (p>,001). Here, the

Figure 5. Effect of HDAC and COX-2 coinhibition in PANC-1 and CFPAC-1 cells. (A) Time-dependent effects of MS-275 and celecoxib on PANC-1 cell growth. (B) Time-dependent effects of MS-275 and celecoxib on CFPAC-1 cell growth. (C) Western-blot detection of Cox-2, p21, p27 in 30 µg CFPAC-1 proteins 48h after 1 µM MS-275 and 10 µM celecoxib treatment. HSC70 was used as a loading control. Results are expressed as mean ± s.d., ***P<.001 versus DMSO or indicated conditions. n≥3 in each condition.
doi:10.1371/journal.pone.0075102.g005

combination of the two drugs reduced significantly (79%, P<.001) CFPAC-1 cell growth in comparison to either drug alone (Figure 5B). We then analyzed by western blot the expression of COX-2 and cell cycle markers in CFPAC-1 cells 48h after drugs administration. We showed an MS-275-induced accumulation of COX-2 like in BxPC-3 cells (Figure 5C). We found also an accumulation of p21^{WAF1} and p27^{Kip1} after the co-administration of MS-275 and celecoxib (Figure 5C), suggesting a cell cycle arrest.

BxPC-3 CAM tumor mimics human PDAC

The evaluation of new drugs or drug combinations for pancreas cancer will be eased by the availability of easy, ethically and economically sustainable animal models. Thus, we have undertaken to refine a human pancreas chorioallantoic membrane (CAM) model based on our initial work [32]. Embedding BxPC-3 cells into matrigel prior to CAM implantation generated a major improvement in the tumor volume. Indeed, following implantation, the tumor volume increased linearly ($r^2 = 0.87$) until day 7 (Figure 6A). At the time of tumor collection (day 7), an average tumor volume of 59.95±15.34 mm^3 (n = 10) was observed. BxPC-3 CAM tumors grew inside the CAM connective tissue as a unique spheric nodule. The same procedure was followed for BxPC-3, PANC-1 and CFPAC-1 cell lines. PANC-1 did not grow on CAM when CFPAC-1 grew as very small nodules (1 mm long).

BxPC-3 CAM tumor histology (Figure 6B) revealed large islets of cohesive cells, some of which showed a nascent central lumen and were isolated from each other by a collagen-containing

extracellular matrix with several sparse fibroblast-like cells demonstrating the presence of an interstitial stroma.

To further validate our human pancreas cancer CAM model, we compared the expression of the cytokeratin-7, -19, -20, CD56, CEA and Ki67 using immunohistochemistry to human PDAC. We also checked for mucin and proteoglycan production utilizing the PAS staining. Tumoral cells from both BxPC-3 CAM tumor and PDAC samples were strongly positive for cytokeratin-7 and -19, CEA and Ki67 (Figure 6C) but negative for cytokeratin-20 and CD56 (data not shown). Both tumors were positive for PAS staining. Altogether, the data showed remarkable histology and biomarker expression similarities between the BxPC-3 CAM model and PDAC from human patients.

Furthermore, our recent work on targetable biomarkers in human PDAC [46] identified several biomarker candidates among which myoferlin, transforming growth factor beta-induced and latent-transforming growth factor beta-binding protein 2. Immunohistochemistry and western-blot confirmed the presence of these new PDAC biomarkers in the BxPC-3 CAM tumors (Figure 7A–B). Finally, using western blot we confirmed that HDAC1, HDAC2, HDAC3 and COX-2 are expressed in the BxPC-3 CAM tumor (Figure 7A).

We next demonstrated that tumors were functionally vascularized. BxPC-3 CAM blood vessels were stained by FITC-conjugated SNA and 3D reconstructed after confocal acquisition. BxPC-3 CAM tumors displayed blood vessels around pancreatic islets (Figure 8A). The fluorescence of tumor stroma after
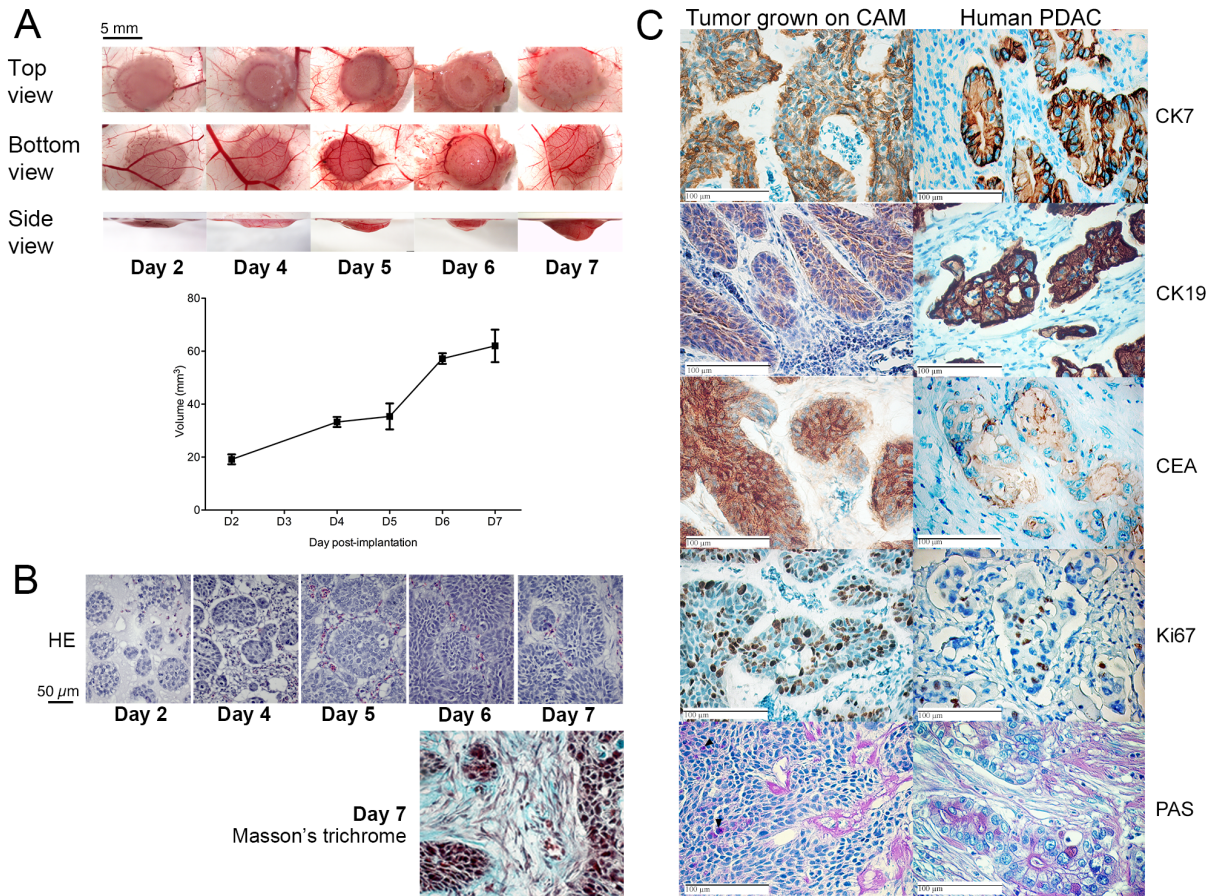
Figure 6. Growth curve and immunohistologic characterization of BxPC-3 tumors grown on CAM. (A) Cells were implanted on CAM at embryonic day 11 and collected 2, 4, 5, 6 or 7 days after implantation. Macroscopic pictures were obtained at the same magnification from top, bottom and side view. Results are expressed as mean ± s.d., n>5 at each time-point. (B) Histologic (Haematoxylin-Eosin or Masson's trichrome staining) analysis of tumors collected 2, 4, 5, 6 or 7 days after implantation. (C) Immunohistology of tumors 7 days after BxPC-3 implantation on CAM and human PDAC tumors. CK7 = Cytokeratin-7, CK19 = cytokeratin-19, CEA = Carcinoembryonic antigen, PAS = Amylase-periodic acid Schiff staining.

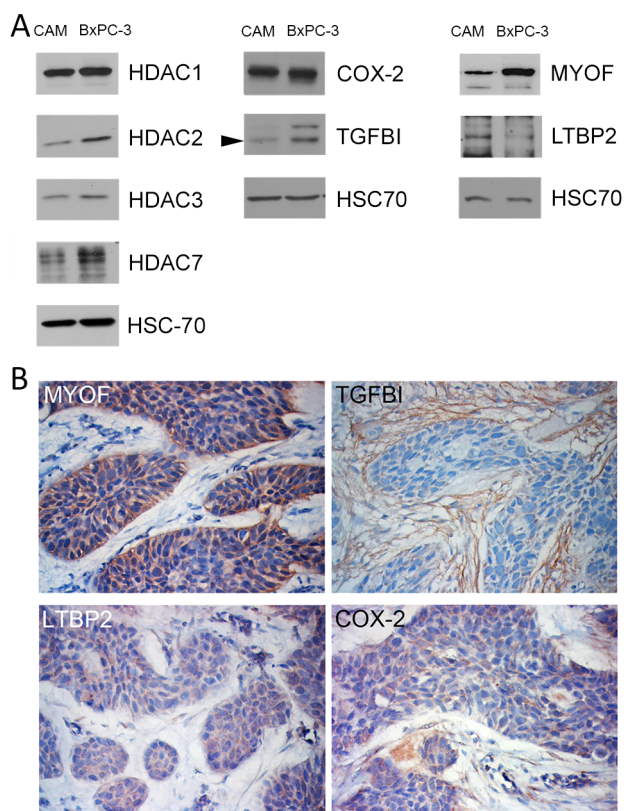doi:10.1371/journal.pone.0075102.g006

fluorescent dye injection in the CAM vasculature confirms that the vessels are functional (Figure 8B) and the detection of desmin positive pericytes suggests vessel stabilization (Figure 8C).

Next, BxPC-3 tumors were treated beginning day 2 either with 8 µM celecoxib or 0.2 µM MS-275 or with a combination of two drugs at their respective concentrations. MS-275 concentration was chosen to fit with the plasmatic concentration measured in Human in a 5 mg/m^2 weekly dosing schedule [15]. While celecoxib alone did not affect tumor growth, MS-275 alone induced a decreased of tumor growth by 50% (P<.001) and induced the expression of COX-2. Combination of celecoxib and MS-275 completely abolished (P<.001) tumor growth, leading to no change in tumor volume compared to the beginning of treatment (Figure 9A-B). Tumors treated with MS-275 overexpressed COX-2 (Figure 9C). Tumors treated with combination of celecoxib and MS-275 revealed empty spaces inside the tumor. (Figure 9D). We then asked the question whether this reduction of tumor volume is due to induction of apoptosis or to proliferation arrest. Tumors treated with MS-275, celecoxib or both drugs were submitted to a cleaved caspase-3 detection and were labeled for Ki67. The full-length caspase-3 was detected in all samples but no cleaved caspase-3 was observed (Figure 9E). The relative Ki67-

positive area was slightly but significantly reduced by the combination of HDAC and COX-2 inhibitors (Figure 9F).

Discussion

The potential interest of anti-HDAC treatment strategies for PDAC is supported by several preclinical studies [18,19,22,47–50]. In agreement with these studies, we showed that pan-HDAC inhibitor SAHA was able to reduce significantly pancreatic cancer cell growth. Following the rationale that HDAC7, HDAC3 and HDAC1 have been reported to be over-expressed in the PDAC [8–10] we have examined their individual roles with respect to their ability to control BxPC-3 cell growth. The results demonstrated that HDAC7 silencing was unable to decrease the cell growth while HDAC1 and HDAC3 inhibition or silencing reduced significantly the BxPC-3 cell growth highlighting the importance of these enzymes in PDAC patients. However, the results of clinical studies where HDAC inhibitors are used show only limited or no ability to affect tumor development [3,13]. This is likely to be related to the pleiotropic activities of HDAC including some that might promote tumor progression. In this line, HDAC1, –2 and –3 may have been shown to regulate the function of RelA/p65 subunits of NF-kB. Class I HDAC1 can indeed interact with RelA/p65 acting as a corepressor to negatively
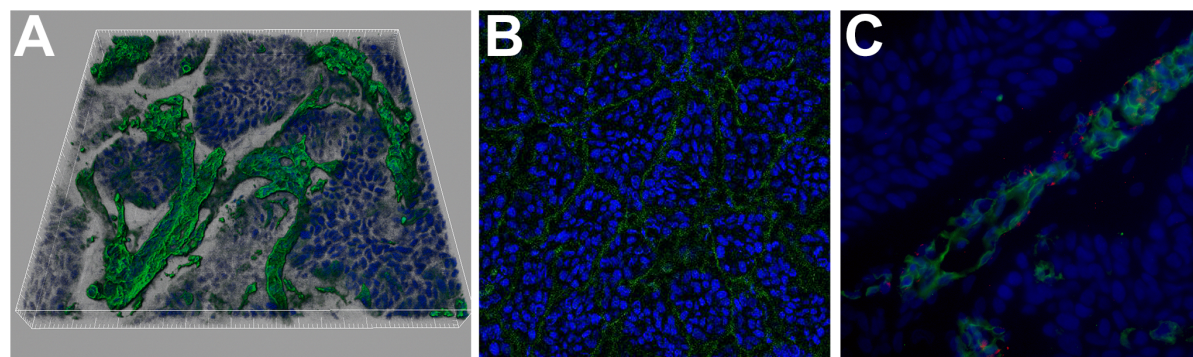
Figure 7. Biomarker detection in tumors 7 days after BxPC-3 implantation on CAM. (A) Western-blot detection of HDAC1, HDAC2, HDAC3, HDAC7, COX-2, TGFBI, MYOF, LTBP2 in 20 µg PDAC-CAM or BxPC-3 proteins. HSC70 was used as a loading control. (B) Immunoperoxydase labelling of MYOF, TGFBI, LTBP2, COX-2.
doi:10.1371/journal.pone.0075102.g007

cells following trichostatin A or SAHA treatment [27]. Here, we showed, for the first time, that the class I HDAC chemical inhibitor MS-275 and selective silencing of both HDAC1 and HDAC3 are able to induce the transcription of COX-2 gene and the accumulation of the functional enzyme independently of the KRAS status. Conversely, HDAC2 silencing does not elicit COX-2 accumulation but reduce its expression. COX-2 is considered to be part of the positive feedback loop amplifying *Ras* activity to a pathological level causing inflammation and cancer [51]. Moreover, COX-2 was demonstrated to confer a growth advantage to pancreatic cancer cells [52]. These results together with our findings suggest the potential interest in inhibiting COX-2 activity while subjecting COX-2 positive (about 50-60% of the cases [53]) PDAC patients to anti-HDAC treatments. This can be easily achieved because several molecules, including the celecoxib [54], were developed in order to inhibit specifically COX-2. Celecoxib was found to significantly decrease or delay pancreatic cancer progression in animal model [29,55]. Keeping these findings in mind, we combined class I HDAC and COX-2 inhibitors and test their efficiency to control tumor growth. The co-treatment reduced the pancreas cancer cell growth by blocking cells in G0/G1 state. This is probably a mechanism that could explain the effects observed *in vivo*, where the combination of two drugs completely stalled the tumor growth. Importantly, the inhibition of tumor growth was observed with drug concentrations 10-fold lower than the concentrations needed if the drugs were used individually [56,57]. This represents a considerable advantage for a putative clinical use regarding the possible undesired effects. However, the *in vivo* model used in this work remains very simple compared to the complexity of the pathology in human. Moreover, the cell line used to grow the tumor in ovo is a limitation as it does not harbor constitutively active Kras which is the most common genetic alteration in human PDAC. In consequence, *in vivo* studies in genetically-engineered mouse models of PDAC are more than necessary before entering potential clinical trials with combined treatment, especially in the case of patients harboring KRAS mutation. Several models are now available to recapitulate the disease [58].

One additional outcome of the current study is the development and characterization of a refined animal model of PDAC recapitulating all the main features observed in human tumors. We have based our development on a model we previously set-up [32] but which did not provide with the possibility to efficiently test experimental therapies. Following extensive method development

regulate its transcriptional activity [43]. HDAC3-mediated deacetylation of RelA/p65 promotes its binding to IKBα leading to cytosolic sequestration [42] and NF-kB repression. In parallel, HDAC2 was also overexpressed in PDAC and was shown to regulate NF-kB activity without direct interaction with p65 [43]. As a consequence, class I HDAC inhibition could induce the transcriptional activation of NF-kB-driven genes. Consistently, a significant COX-2 induction was recently showed in lung cancer

Figure 8. Blood vessel detection in tumors 7 days after BxPC-3 implantation on CAM. (A) Imaris 3D reconstruction from a 35 µm stacked image after SNA staining (green). Nuclei were counter stained with DAPI (blue). (B) Confocal image after FITC (green) injection in CAM blood vessels. Nuclei were counter stained with TOPRO (blue) (C) Desmin immunodetection (red) in PDAC-CAM stained with SNA (green). Nuclei were counter stained with DAPI (blue).
doi:10.1371/journal.pone.0075102.g008
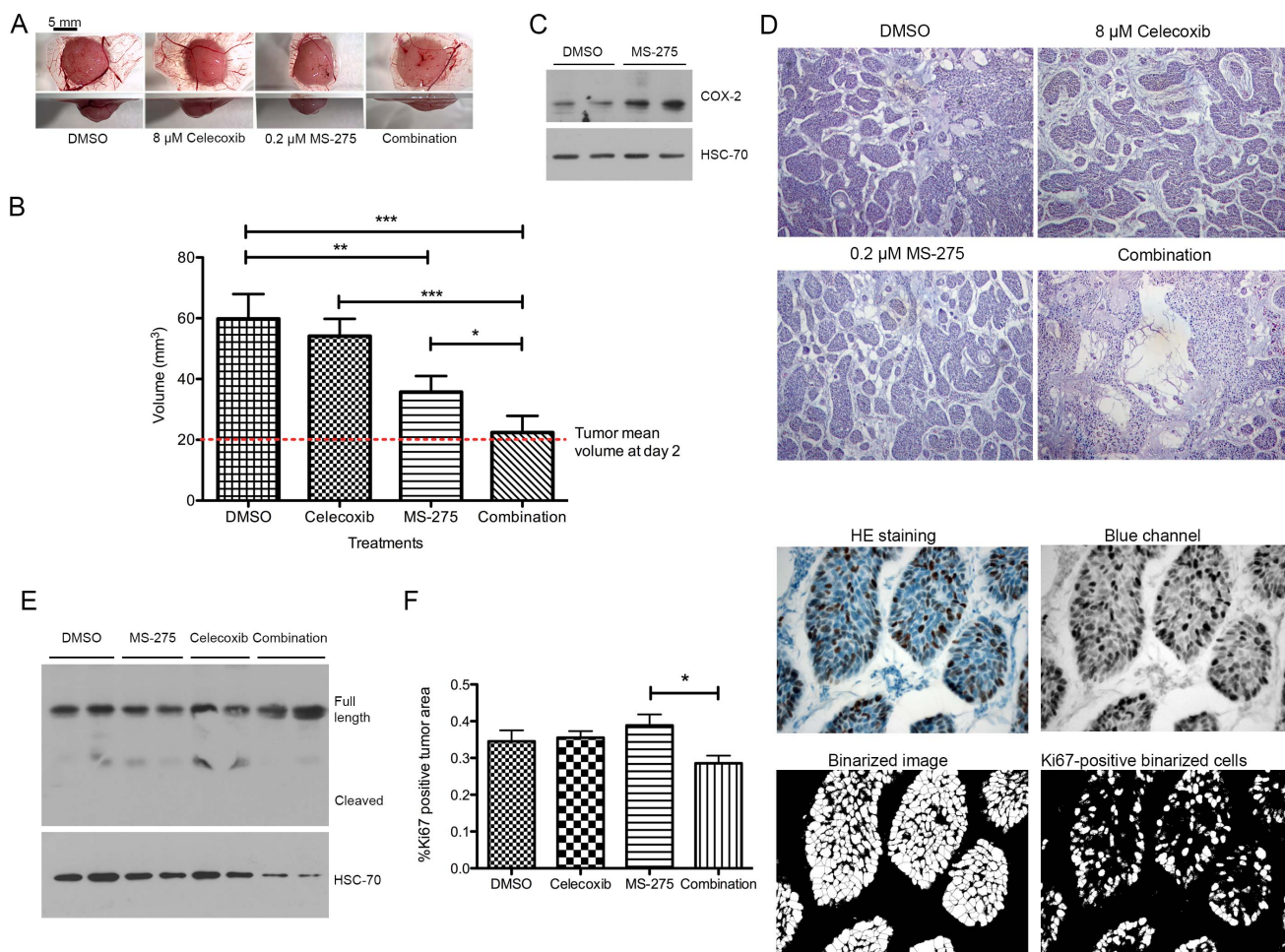
Figure 9. Effect of HDAC and COX-2 co-inhibition on BxPC-3 tumor growth on CAM. (A) Macroscopic pictures were obtained at the same magnification from bottom and side view. (B) Tumor volume at day 7 after cell implantation. Tumors were treated with 30 µl celecoxib (8 µM), MS-275 (0.2 µM) or drug combination at same concentration. (C) Western-blot detection of COX-2 in 20 µg proteins isolated from tumors grown on CAM and treated with MS-275 (0.2 µM). HSC70 was used as a loading control. (D) Histological aspect of tumors grown on CAM during 7 days and treated with 30 µl celecoxib (8 µM), MS-275 (0.2 µM) or drug combination at same concentration. (E) Western-blot detection of caspase-3 in 40 µg proteins isolated from tumors grown on CAM and treated with MS-275 (0.2 µM) or celecoxib (8 µM). HSC70 was used as a loading control. (F) Ki67 immunostaining and associated quantification of tumors grown on CAM during 7 days and treated with 30 µl celecoxib (8 µM), MS-275 (0.2 µM) or drug combination at same concentration. Results are expressed as mean ± s.d. ***P<.001, **P<.01, *P>.05. n≥3 in each condition.
doi:10.1371/journal.pone.0075102.g009

we have established means to produce larger tumors, bearing fully functional blood vessels. The clinical relevance of this improved model is supported by the CK7^{+}/CK19^{+}/CK20^{-}/CEA^{+}/Ki67^{+}/CD56^{-} immunodetection. CK7 and CK20 expression has been shown to be useful in the differential diagnosis of several carcinomas of epithelial origin. According to Lee et al. [59] 95% of PDAC are CK7^{+}, 100% are CK19^{+} and 73% are CK20^{-}. In pancreas carcinomas the proportion of cells stained for CEA and the Ki-67 index were respectively increased 3-fold and 10-fold in comparison with the normal tissue [60,61]. CD56 staining was found negative in all cases of human PDAC [62]. These biomarkers, together with the presence of mucin are the main hallmarks of PDAC [63].

Recently, we have discovered several biomarkers of human PDAC that bare therapeutic potential [46]. These antigens were also present in our CAM tumor model, supporting its similarity with human cancer and providing the research community with a

rapid and cost effective model for pancreas cancer research such as our present demonstration of the benefit to combine COX-2 and HDAC inhibition for optimal anti tumor activity.

Acknowledgments

Author Contributions

Conceived and designed the experiments: OP VC. Performed the experiments: AG PP PD. Analyzed the data: OP AG DM AT VC. Contributed reagents/materials/analysis tools: PD. Wrote the paper: OP VC. Obtained the permission to use the PANC-1 cell line: OP.

References

1. Jemal A, Siegel R, Xu J, Ward E (2010) Cancer statistics, 2010. CA Cancer J Clin 60: 277–300. doi:10.3322/caac.20073.

2. Anonymous (2011) Pancreatic cancer in the UK. Lancet 378: 1050. doi:10.1016/S0140-6736(11)61465-7.

3. Tinari N, de Tursi M, Grassadonia A, Zilli M, Stuppia L, et al. (2012) An epigenetic approach to pancreatic cancer treatment: The prospective role of histone deacetylase inhibitors. Curr Cancer Drug Targets 12: 439–452.

4. Mottet D, Pirotte S, Lamour V, Hagedorn M, Javerzat S, et al. (2008) HDAC4 represses p21WAF1/Cip1 expression in human cancer cells through a Sp1-dependent, p53-independent mechanism. Oncogene 28: 243–256. doi:10.1038/onc.2008.371.

5. Mottet D, Bellahcène A, Pirotte S, Waltregny D, Deroanne C, et al. (2007) Histone deacetylase 7 silencing alters endothelial cell migration, a key step in angiogenesis. Circ Res 101: 1237–1246. doi:10.1161/CIRCRE-SAHA.107.149377.

6. Deroanne CF, Bonjean K, Servotte S, Devy L, Colige A, et al. (2002) Histone deacetylases inhibitors as anti-angiogenic agents altering vascular endothelial growth factor signaling. Oncogene 21: 427–436. doi:10.1038/sj.onc.1205108.

7. Fritsche P, Seidler B, Schüler S, Schnieke A, Göttlicher M, et al. (2009) HDAC2 mediates therapeutic resistance of pancreatic cancer cells via the BH3-only protein NOXA. Gut 58: 1399–1409. doi:10.1136/gut.2009.180711.

8. Lehmann A, Denkert C, Budczies J, Buckendahl AC, Darb-Esfahani S, et al. (2009) High class I HDAC activity and expression are associated with RelA/p65 activation in pancreatic cancer in vitro and in vivo. BMC Cancer 9: 395. doi:10.1186/1471-2407-9-395.

9. Miyake K, Yoshizumi T, Imura S, Sugimoto K, Batmunkh E, et al. (2008) Expression of hypoxia-inducible factor-1alpha, histone deacetylase 1, and metastasis-associated protein 1 in pancreatic carcinoma: correlation with poor prognosis with possible regulation. Pancreas 36: e1–e9. doi:10.1097/MPA.0-b013e31815f2c2a.

10. Ouaïssi M, Sielezneff I, Silvestre R, Sastre B, Bernard JP, et al. (2008) High histone deacetylase 7 (HDAC7) expression is significantly associated with adenocarcinomas of the pancreas. Ann Surg Oncol 15: 2318–2328. doi:10.1245/s10434-008-9940-z.

11. Khan O, La Thangue NB (2012) HDAC inhibitors in cancer biology: Emerging mechanisms and clinical applications. Immunol Cell Biol 90: 85–94.

12. Kim H-J, Bae S-C (2011) Histone deacetylase inhibitors: molecular mechanisms of action and clinical trials as anti-cancer drugs. Am J Transl Res 3: 166–179.

13. Zafar SF, Nagaraju GP, El-Rayes B (2012) Developing histone deacetylase inhibitors in the therapeutic armamentarium of pancreatic adenocarcinoma. Expert Opin Ther Targets 16: 707–718. doi:10.1517/14728222.2012.691473.

14. de Bono JS, Kristeleit R, Tolcher A, Fong P, Pacey S, et al. (2008) Phase I pharmacokinetic and pharmacodynamic study of LAQ824, a hydroxamate histone deacetylase inhibitor with a heat shock protein-90 inhibitory profile, in patients with advanced solid tumors. Clin Cancer Res 14: 6663–6673. doi:10.1158/1078-0432.CCR-08-0376.

15. Gore L, Rothenberg ML, O'Bryant CL, Schultz MK, Sandler AB, et al. (2008) A phase I and pharmacokinetic study of the oral histone deacetylase inhibitor, MS-275, in patients with refractory solid tumors and lymphomas. Clin Cancer Res 14: 4517–4525. doi:10.1158/1078-0432.CCR-07-1461.

16. Ellis L, Pili R (2010) Histone deacetylase inhibitors: Advancing therapeutic strategies in hematological and solid malignancies. Pharmaceuticals 3: 2441–2469. doi:10.3390/ph3082441.

17. Bots M, Johnstone RW (2009) Rational combinations using HDAC inhibitors. Clin Cancer Res 15: 3970–3977. doi:10.1158/1078-0432.CCR-08-2786.

18. Chun SG, Zhou W, Yee NS (2009) Combined targeting of histone deacetylases and hedgehog signaling enhances cytoxicity in pancreatic cancer. Cancer Biol Ther 8: 19–30.

19. Iwahashi S, Ishibashi H, Utsunomiya T, Morine Y, Ochir TL, et al. (2011) Effect of histone deacetylase inhibitor in combination with 5-fluorouracil on pancreas cancer and cholangiocarcinoma cell lines. J Med Invest 58: 106–109. doi:10.2152/jmi.58.106.

20. Bai J, Demirjian A, Sui J, Marasco W, Callery MP (2006) Histone deacetylase inhibitor trichostatin A and proteasome inhibitor PS-341 synergistically induce apoptosis in pancreatic cancer cells. Biochem Biophys Res Commun 348: 1245–1253. doi:10.1016/j.bbrc.2006.07.185.

21. Piacentini P, Donadelli M, Costanzo C, Moore PS, Palmieri M, et al. (2006) Trichostatin A enhances the response of chemotherapeutic agents in inhibiting pancreatic cancer cell proliferation. Virchows Arch 448: 797–804. doi:10.1007/s00428-006-0173-x.

22. Donadelli M, Costanzo C, Beghelli S, Scupoli MT, Dandrea M, et al. (2007) Synergistic inhibition of pancreatic adenocarcinoma cell growth by trichostatin A and gemcitabine. Biochim Biophys Acta 1773: 1095–1106. doi:10.1016/j.bbamcr.2007.05.002.

23. Richards DA, Boehm KA, Waterhouse DM, Wagener DJ, Krishnamurthi SS, et al. (2006) Gemcitabine plus CI-994 offers no advantage over gemcitabine alone in the treatment of patients with advanced pancreatic cancer: results of a phase II randomized, double-blind, placebo-controlled, multicenter study. Ann Oncol 17: 1096–1102. doi:10.1093/annonc/mdl081.

24. Pili R, Salumbides B, Zhao M, Altiok S, Qian D, et al. (2012) Phase I study of the histone deacetylase inhibitor entinostat in combination with 13-cis retinoic acid in patients with solid tumours. Br J Cancer 106: 77–84. doi:10.1038/bjc.2011.527.

25. Wu S, Li RW, Li W, Li CJ (2012) Transcriptome characterization by RNA-seq unravels the mechanisms of butyrate-induced epigenomic regulation in bovine cells. PLoS ONE 7: e36940. doi:10.1371/journal.pone.0036940.

26. Glaser KB, Staver MJ, Waring JF, Stender J, Ulrich RG, et al. (2003) Gene expression profiling of multiple histone deacetylase (HDAC) inhibitors: defining a common gene set produced by HDAC inhibition in T24 and MDA carcinoma cell lines. Mol Cancer Ther 2: 151–163.

27. Wang X, Li G, Wang A, Zhang Z, Merchan JR, et al. (2013) Combined histone deacetylase and cyclooxygenase inhibition achieves enhanced antiangiogenic effects in lung cancer cells. Mol Carcinog 52: 218–228. doi:10.1002/mc.21846.

28. Sun WH, Chen G-S, Ou XL, Yang Y, Luo C, et al. (2009) Inhibition of COX-2 and activation of peroxisome proliferator-activated receptor gamma synergistically inhibits proliferation and induces apoptosis of human pancreatic carcinoma cells. Cancer Lett 275: 247–255. doi:10.1016/j.canlet.2008.10.023.

29. Colby JKL, Klein RD, McArthur MJ, Conti CJ, Kiguchi K, et al. (2008) Progressive metaplastic and dysplastic changes in mouse pancreas induced by cyclooxygenase-2 overexpression. Neoplasia 10: 782–796.

30. Mukherjee P, Basu GD, Tinder TL, Subramani DB, Bradley JM, et al. (2009) Progression of pancreatic adenocarcinoma is significantly impeded with a combination of vaccine and COX-2 inhibition. J Immunol 182: 216–224.

31. Hill R, Li Y, Tran LM, Dry S, Calvopina JH, et al. (2012) Cell intrinsic role of COX-2 in pancreatic cancer development. Mol Cancer Ther 11: 2127–2137. doi:10.1158/1535-7163.MCT-12-0342.

32. Dumartin L, Quemener C, Laklai H, Herbert J, Bicknell R, et al. (2010) Netrin-1 mediates early events in pancreatic adenocarcinoma progression, acting on tumor and endothelial cells. Gastroenterology 137: 1595–1606. doi:10.1053/j.gastro.2009.12.061.

33. Peixoto P, Castronovo V, Matheus N, Polese C, Peulen OJ, et al. (2012) HDAC5 is required for maintenance of pericentric heterochromatin, and controls cell-cycle progression and survival of human cancer cells. Cell Death Differ 19: 1239–1252. doi:10.1038/cdd.2012.3.

34. Lamour V, Le Mercier M, Lefranc F, Hagedorn M, Javerzat S, et al. (2010) Selective osteopontin knockdown exerts anti-tumoral activity in a human glioblastoma model. Int J Cancer 126: 1797–1805. doi:10.1002/ijc.24751.

35. Deryugina EI, Quigley JP (2008) Chick embryo chorioallantoic membrane model systems to study and visualize human tumor cell metastasis. Histochem Cell Biol 130: 1119–1130. doi:10.1007/s00418-008-0536-2.

36. Tan MH, Nowak NJ, Rueyming L (1986) Characterization of a new primary human pancreatic tumor line. Cancer Invest 4: 15–23.

37. Lieber M, Mazzetta J, Nelson-Rees W, Kaplan M, Todaro G (1975) Establishment of a continuous tumor-cell line (PANC-1) from a human carcinoma of the exocrine pancreas. Int J Cancer 15: 741–747. doi:10.1002/ijc.2910150505.

38. Schoumacher RA, Ram J, Iannuzzi MC, Bradbury NA, Wallace RW, et al. (1990) A cystic fibrosis pancreatic adenocarcinoma cell line. Proc Natl Acad Sci U S A 87: 4012–4016.

39. Detry C, Lamour V, Castronovo V, Bellahcène A (2008) CREB-1 and AP-1 transcription factors JunD and Fra-2 regulate bone sialoprotein gene expression in human breast cancer cells. Bone 42: 422–431. doi:10.1016/j.bone.2007.10.016.

40. Ouaïssi M, Cabral S, Tavares J, da Silva AC, Mathieu Daude F, et al. (2008) Histone deacetylase (HDAC) encoding gene expression in pancreatic cancer cell lines and cell sensitivity to HDAC inhibitors. Cancer Biol Ther 7: 523–531.

41. Mehdi O, Françoise S, Sofia CL, Urs G, Kevin Z, et al. (2012) HDAC gene expression in pancreatic tumor cell lines following treatment with the HDAC inhibitors panobinostat (LBH589) and trichostatine (TSA). Pancreatology 12: 146–155. doi:10.1016/j.pan.2012.02.013.

42. Chen LF, Fischle W, Verdin E, Greene WC (2001) Duration of nuclear NF-κB action regulated by reversible acetylation. Science 293: 1653–1657. doi:10.1126/science.1062374.

43. Ashburner BP, Westerheide SD, Baldwin AS (2001) The p65 (RelA) subunit of NF-kappaB interacts with the histone deacetylase (HDAC) corepressors HDAC1 and HDAC2 to negatively regulate gene expression. Mol Cell Biol 21: 7065–7077. doi:10.1128/MCB.21.20.7065-7077.2001.

44. Broude EV, Swift ME, Vivo C, Chang BD, Davis BM, et al. (2007) p21Waf1/Cip1/Sdi1 mediates retinoblastoma protein degradation. Oncogene 26: 6954–6958. doi:10.1038/sj.onc.1210516.

45. Deer EL, González-Hernández J, Coursen JD, Shea JE, Ngatia J, et al. (2010) Phenotype and genotype of pancreatic cancer cell lines. Pancreas 39: 425–435. doi:10.1097/MPA.0b013e3181c15963.

46. Turtoi A, Musmeci D, Wang Y, Dumont B, Somja J, et al. (2011) Identification of novel accessible proteins bearing diagnostic and therapeutic potential in human pancreatic ductal adenocarcinoma. J Proteome Res 10: 4302–4313. doi:10.1021/pr200527z.

47. Kumagai T, Wakimoto N, Yin D, Gery S, Kawamata N, et al. (2007) Histone deacetylase inhibitor, suberoylanilide hydroxamic acid (Vorinostat, SAHA) profoundly inhibits the growth of human pancreatic cancer cells. Int J Cancer 121: 656–665. doi:10.1002/ijc.22558.

48. Zhou W, Liang IC, Yee NS (2011) Histone deacetylase 1 is required for exocrine pancreatic epithelial proliferation in development and cancer. Cancer Biol Ther 11: 659–670. doi:10.4161/cbt.11.7.14720.

49. Iwahashi S, Shimada M, Utsunomiya T, Morine Y, Imura S, et al. (2011) Histone deacetylase inhibitor augments anti-tumor effect of gemcitabine and pegylated interferon-α on pancreatic cancer cells. Int J Clin Oncol 16: 671–678. doi:10.1007/s10147-011-0246-y.

50. Jones J, Bentas W, Blaheta RA, Makarevic J, Hudak L, et al. (2008) Modulation of adhesion and growth of colon and pancreatic cancer cells by the histone deacetylase inhibitor valproic acid. Int J Mol Med 22: 293–299. doi:10.3892/ijmm_00000022.

51. Daniluk J, Liu Y, Deng D, Chu J, Huang H, et al. (2012) An NF-κB pathway-mediated positive feedback loop amplifies Ras activity to pathological levels in mice. J Clin Invest 122: 1519–1528. doi:10.1172/JCI59743DS1.

52. Takahashi H, Li A, Dawson DW, Hines OJ, Reber HA, et al. (2011) Cyclooxygenase-2 confers growth advantage to syngeneic pancreatic cancer cells. Pancreas 40: 453–459. doi:10.1097/MPA.0b013e31820b9733.

53. Molina MA, Sitja-Arnau M, Lemoine MG, Frazier ML, Sinicrope FA (1999) Increased cyclooxygenase-2 expression in human pancreatic carcinomas and cell lines: growth inhibition by nonsteroidal anti-inflammatory drugs. Cancer Res 59: 4356–4362.

54. Penning TD, Talley JJ, Bertenshaw SR, Carter JS, Collins PW, et al. (1997) Synthesis and biological evaluation of the 1,5-diarylpyrazole class of cyclooxygenase-2 inhibitors: identification of 4-[5-(4-methylphenyl)-3-(trifluoromethyl)-1H-pyrazol-1-yl]benze nesulfonamide (SC-58635, celecoxib). J Med Chem 40: 1347–1365. doi:10.1021/jm960803q.

55. Padillo FJ, Ruiz-Rabelo JF, Cruz A, Perea MD, Tasset I, et al. (2010) Melatonin and celecoxib improve the outcomes in hamsters with experimental pancreatic cancer. J Pineal Res 49: 264–270. doi:10.1111/j.1600-079X.2010.00791.x.

56. Rosendahl AH, Gundewar C, Said K, Karnevi E, Andersson R (2012) Celecoxib synergizes human pancreatic ductal adenocarcinoma cells to sorafenib-induced growth inhibition. Pancreatology 12: 219–226.

57. Zhang H, Chen P, Bai S, Huang C (2007) The histone deacetylase inhibitor MS-275 induces p21WAF1/Cip1 expression in human Hep3B hepatoma cells. Drug Dev Res 68: 61–70. doi:10.1002/ddr.20167.

58. Ijichi H (2011) Genetically-engineered mouse models for pancreatic cancer: Advances and current limitations. World J Clin Oncol 2: 195. doi:10.5306/wjco.v2.i5.195.

59. Lee MJ, Lee HS, Kim WH, Choi Y, Yang M (2003) Expression of mucins and cytokeratins in primary carcinomas of the digestive system. Mod Pathol 16: 403–410. doi:10.1097/01.MP.0000067683.84284.66.

60. Allum WH, Stokes HJ, Macdonald F, Fielding JWL (1986) Demonstration of carcinoembryonic antigen (CEA) expression in normal, chronically inflamed, and malignant pancreatic tissue by immunohistochemistry. J Clin Pathol 39: 610–614.

61. Jeong S, Lee DH, Lee JI, Lee JW, Kwon KS, et al. (2005) Expression of Ki-67, p53, and K-ras in chronic pancreatitis and pancreatic ductal adenocarcinoma. World J Gastroenterol 11: 6765–6769.

62. Naito Y, Kinoshita H, Okabe Y, Kawahara R, Sakai T, et al. (2006) CD56 (NCAM) expression in pancreatic carcinoma and the surrounding pancreatic tissue. Kurume Med J 53: 59–62.

63. Reid MD, Bagci P, Adsay NV (2013) Histopathologic assessment of pancreatic cancer: Does one size fit all? J Surg Oncol 107: 67–77.

HDAC5 is required for maintenance of pericentric heterochromatin, and controls cell-cycle progression and survival of human cancer cells.

Peixoto, P. Castronovo, V. Matheus, N. Polese, C. Peulen, O. Gonzalez, A. Boxus, M. Verdin, E. Thiry, M. Dequiedt, F. and Mottet, D.

Cell death and differenciation 2012. 19(7): p 1239-52.

ANNEXE 2

npg

HDAC5 is required for maintenance of pericentric heterochromatin, and controls cell-cycle progression and survival of human cancer cells

P Peixoto[1,6], V Castronovo[1,6], N Matheus[1,6], C Polese[1,6], O Peulen[1,6], A Gonzalez[1,6], M Boxus[2], E Verdin[3], M Thiry[4,6], F Dequiedt[5,6] and D Mottet*[,1,6]

Histone deacetylases (HDACs) form a family of enzymes, which have fundamental roles in the epigenetic regulation of gene expression and contribute to the growth, differentiation, and apoptosis of cancer cells. In this study, we further investigated the biological function of HDAC5 in cancer cells. We found HDAC5 is associated with actively replicating pericentric heterochromatin during late S phase. We demonstrated that specific depletion of HDAC5 by RNA interference resulted in profound changes in the heterochromatin structure and slowed down ongoing replication forks. This defect in heterochromatin maintenance and assembly are sensed by DNA damage checkpoint pathways, which triggered cancer cells to autophagy and apoptosis, and arrested their growth both *in vitro* and *in vivo*. Finally, we also demonstrated that HDAC5 depletion led to enhanced sensitivity of DNA to DNA-damaging agents, suggesting that heterochromatin de-condensation induced by histone HDAC5 silencing may enhance the efficacy of cytotoxic agents that act by targeting DNA *in vitro*. Together, these results highlighted for the first time an unrecognized link between HDAC5 and the maintenance/assembly of heterochromatin structure, and demonstrated that its specific inhibition might contribute to increase the efficacy of DNA alteration-based cancer therapies in clinic.

Histone deacetylases (HDACs) are enzymes that modulate the acetylation level of histones and non-histone proteins to regulate gene expression and chromatin structure. Eighteen human HDACs are divided into four classes: class I (HDAC1, 2, 3, 8); class II (HDAC4, 5, 6, 7, 9, 10), subdivided into class IIa (HDAC4, 5, 7) and class IIb (HDAC6 and 10); class III, also called sirtuin proteins (SIRT1–7); and class IV (HDAC11).[1] Several compounds were identified as broad-spectrum inhibitors of class-I and -II HDAC (HDACi).[2] These HDACis can cause cell-cycle arrest, activation of programmed cell death (apoptosis/autophagy), or inhibition of angiogenesis. Based on their potent anticancer effects *in vitro*, several HDACis are currently being investigated in clinical trials in cancer patients, both as single agents and in combination with other drugs. The FDA (Food and Drug Administration)

approval of SAHA (suberoylanilide hydroxamic acid; Zolinza) for treatment of cutaneous T-cell lymphoma[3] validates the concept of HDAC inhibition to treat cancer.

Generally, HDACis are well tolerated when compared with most of the currently used antitumor treatments. However, some side effects have been reported. So, by targeting the most relevant HDAC members, it may be possible to improve efficacy by removing undesirable toxicities. Preclinical investigations by targeted knockdown of individual HDAC members demonstrated the roles of class IIa HDACs in tumorigenesis. Indeed, we and others have demonstrated that silencing of HDAC4 inhibited cancer cell proliferation *in vitro* and arrested tumor growth *in vivo* through epigenetic regulation of p21[WAF1/Cip1] gene expression.[4,5] Recently, Zhu *et al.*[6] also demonstrated HDAC7 is a crucial player in

cancer cell proliferation. Together, these findings would suggest that inhibition of class IIa HDACs might be a sufficient strategy to treat cancer. However, the contribution of HDAC5 to tumor progression is largely ignored and needs to be further characterized to determine whether class IIa HDAC members are the most relevant targets in cancer therapy.

The human HDAC5 gene is located on chromosome 17q21, a region which is characterized by losses of chromosomal material in different cancers.[7] Moreover, HDAC5 expression is frequently reduced in cancer such as colon cancer and acute myeloid leukemia,[8–10] and is associated with poor clinical outcome of lung cancer patients.[11] In contrary, an upregulation of HDAC5 has been observed in high-risk medulloblastoma and its expression is associated with poor survival.[12] Like for many HDACs, HDAC5 is then aberrantly expressed in tumors, suggesting that this HDAC may have a role in tumor progression.

Here, we investigated the function of HDAC5 in cancer cells. We found that its sub-nuclear localization changed during S phase progression, with HDAC5 colocalizing with actively replicating heterochromatic regions during late S phase. We demonstrated that its specific depletion by RNA interference (RNAi) induced a defect in pericentric heterochromatin assembly and slowed down an ongoing replication fork, which consequently induced DNA-damage checkpoint pathways, which leads to cell-cycle blocking, inhibition of cell proliferation, induction of apoptosis as well as autophagy, and, consequently, decreased tumor growth *in vivo*. Altogether, these findings implicate HDAC5 in the maintenance/assembly of pericentric heterochromatin structure and demonstrate that class IIa HDAC5 can represent a potential target for anticancer therapies.

Results

HDAC5 localizes to pericentromeric heterochromatin primarily during late S phase. To explore the function of HDAC5, we first examined its localization in HeLa cells. Confocal microscopy showed that approximately 85% of asynchronous cells showed a nuclear localization, with more intense foci around the nucleolus (Figure 1A). This localization was observed in different cell types, including MCF-7, MDA-MB-231, endothelial cells, and fibroblasts (data not shown). Transfection with two different efficient HDAC5 small interfering RNA (siRNA) correlated with loss of nuclear HDAC5 foci, excluding a non-specific staining (Supplementary Figures S1A, and S1B–S2). This localization was also confirmed with a second anti-HDAC5 antibody (Supplementary Figure S1C). To further characterize the intra-nuclear localization of HDAC5, we performed electron microscopy. Endogenous HDAC5 was detected as individual foci in the nucleus and the clusters showed a preferential colocalization of HDAC5 with pericentric (pericentromeric) heterochromatin (Figure 1B and Supplementary Figure S3). As fluorescence-activated cell sorting (FACS) analysis (see Figure 2a) revealed that an asynchronous population of HeLa cells is composed of 65–70% of cells in G_1, 20–25% of cells in S, and 5–10% of cells in G_2/M phase, we hypothesized that HDAC5 could target pericentric

heterochromatin during different phases of the cell cycle. First, we monitored the localization and expression of HDAC5 during S phase. In early S phase, HDAC5 shows a diffuse nuclear staining, but in late S phase, the patterns were strikingly different, with HDAC5 now colocalizing with proliferating cell nuclear antigen (PCNA) to punctuate foci that are characteristic of late-replicating pericentric heterochromatin (Figure 1C). A colocalization between HDAC5 and heterochromatin protein 1 (HP-1), a heterochromatin marker, in late S phase confirmed that HDAC5 is localized to heterochromatic regions (Figure 1D). The re-entry into S phase was monitored by both FACS (see Figure 1C) and western blotting against cyclin E and phospho-histone H3 on Ser10, two markers of S phase progression,[13,14] a period during which the global level of HDAC5 did not change (Figure 1E). During mitosis, HDAC5 was not detectable with mitotic chromosome. However, we observed that HDAC5 also associated with heterochromatin in the G_1 phase (Supplementary Figure S4). Bearing in mind the importance of HDAC for chromatin condensation, we assessed the impact of HDAC5 depletion on the organization of pericentric heterochromatin by electron microscopy. Electron micrographs of GL3 siRNA/mock-transfected cells revealed dense nucleoli and a condensed pattern of heterochromatin. By contrast, HDAC5-depleted cells showed a reduced number of dense heterochromatin clusters at the periphery of the nucleolus, demonstrating failure of appropriate assembly/maintenance of chromatin structure at pericentric heterochromatin (Figure 1F). To determine whether HDAC5 depletion exerted a more global influence on chromatin organization, we performed a MNaseI (micrococcal nuclease 1) assay. No defects in wrapping of DNA by the histone octamer were observed in the absence of HDAC5 (Figure 1G), suggesting that HDAC5 did not have a role in the assembly/maintenance of nucleosome organization.

HDAC5 depletion affects DNA replication efficiency and cell-cycle progression. Because heterochromatin assembly and DNA replication are tightly coupled, we examined the consequences of HDAC5 depletion on DNA replication and S phase progression. To identify the effect of HDAC5 depletion on global S phase, asynchronous cells were transfected with an HDAC5 siRNA for 24, 48, and 72 h, and then pulsed with 5-bromo-2′-deoxyuridine (BrdU) before FACS analysis. After 24 h, the number of replicating cells in HDAC5-depleted cells was 28.8% lower compared with mock-transfected cells, and most of the cells were blocked in the G_1 phase (Figures 2a and b). Forty-eight hours after transfection, the percentage of replicating cells was significantly higher in HDAC5-depleted cells (28.23%) compared with control conditions (Figures 2c and d). After 72 h, no significant changes were observed (Figures 2e and f). These data show that HDAC5 siRNA-transfected cells are first blocked in G_1/S and then re-enter S phase later despite still efficient HDAC5 inhibition (Figure 2g). However, this reversible cell-cycle blocking was not observed in MCF-7 cells (data not shown).

To further investigate whether HDAC5 depletion altered cell-cycle progression, HDAC5-depleted cells were treated with the mitotic inhibitor nocodazole 24 h before harvesting
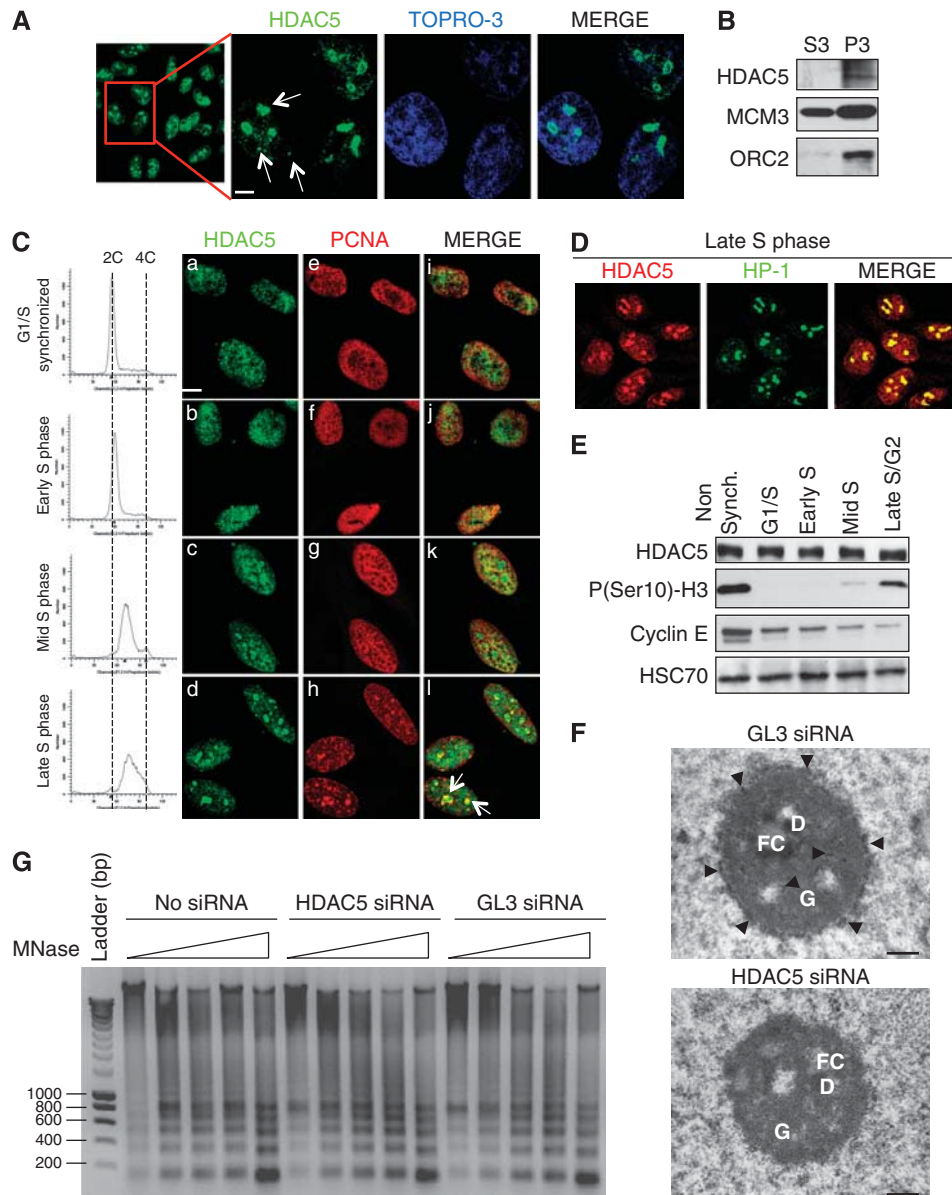
Figure 1 (**A**) Intracellular localization of endogenous HDAC5 protein in HeLa cells was addressed by indirect immunofluorescence and confocal microscopy using primary antibodies against HDAC5 recognized by secondary antibodies conjugated with Alexa 488 (green). DNA was counterstained with TOPRO-3 (blue) (original magnification: × 630; bar: 5 μm). The insets show individual cells from the field at a higher magnification. (**B**) HDAC5 is present in the fraction of chromatin-bound proteins. The fraction of chromatin-bound proteins was prepared as described under Materials and Methods, and the level of HDAC5 was assessed by western blotting. MCM3 and ORC2 proteins were used as fractionation control for the nuclear soluble proteins (S3) and the chromatin-enriched fraction (P3), respectively. (**C**) HDAC5 colocalized with heterochromatin in late S phase. Double immunostaining for HDAC5 (a–d) and PCNA (e–h), and merged images (i–l) in G_1/S (a, e and i) early S (b, f and j) mid-S (c, g and k), and late-S phase (d, h and l) (original magnification: × 630; bar: 5 μm). (**D**) HDAC5 colocalized with HP-1 in late S phase. Late-S phase cells were stained with an anti-HDAC5 antibody, followed by Alexa 546-conjugated secondary antibodies (red, top panel). The same cells were stained with an anti-HP-1 antibody, followed by an Alexa 488-conjugated secondary antibody (green, middle panel). The confocal merge image of HDAC5 and HP-1 staining shows colocalization (yellow, right panel) of HDAC5 and HP-1 in the nucleus (original magnification: × 630; bar: 15 μm). (**E**) Levels of HDAC5 protein during S phase progression. Whole-cell lysates were prepared from asynchronous, early S, mid-S, or late S phase, and the lysates were analyzed by western blotting using anti-HDAC5, anti-cyclin E, and anti-phosphoSer10 H3 antibodies. HSC70 was used as a loading control. (**F**) HDAC5 depletion alters chromatin structure. Electron microscopic analysis of MCF-7 cells transfected with either a GL3 siRNA or with an HDAC5 siRNA for 24 h. GL3 siRNA-transfected cells showed dense nucleoli and a condensed pattern of heterochromatin (black arrows). By contrast, HDAC5-depleted cells showed an even dispersion of the chromatin. FC, fibrillar center; D, dense fibrillar components; G, granular components (bar: 0.5 μm).(**G**) Nuclei extracted from MCF-7 cells transfected with No siRNA, GL3 siRNA, or with HDAC5 siRNA for 48 h were digested with increasing concentrations of MNase and analyzed by gel electrophoresis

(Figure 3a). Addition of nocodazole resulted in accumulation of cells in M phase in mock- or GL3 siRNA-transfected cells. By contrast, HDAC5 depletion led to a decreased number of cells in M phase after nocodazole treatment, in favor of an accumulation of cells in both G_1 and S phase. This demonstrated that HDAC5 depletion caused a defect in cell-cycle progression. However, after 48 or 72 h of transfection, HDAC5-depleted cells progressed through their cell cycle like
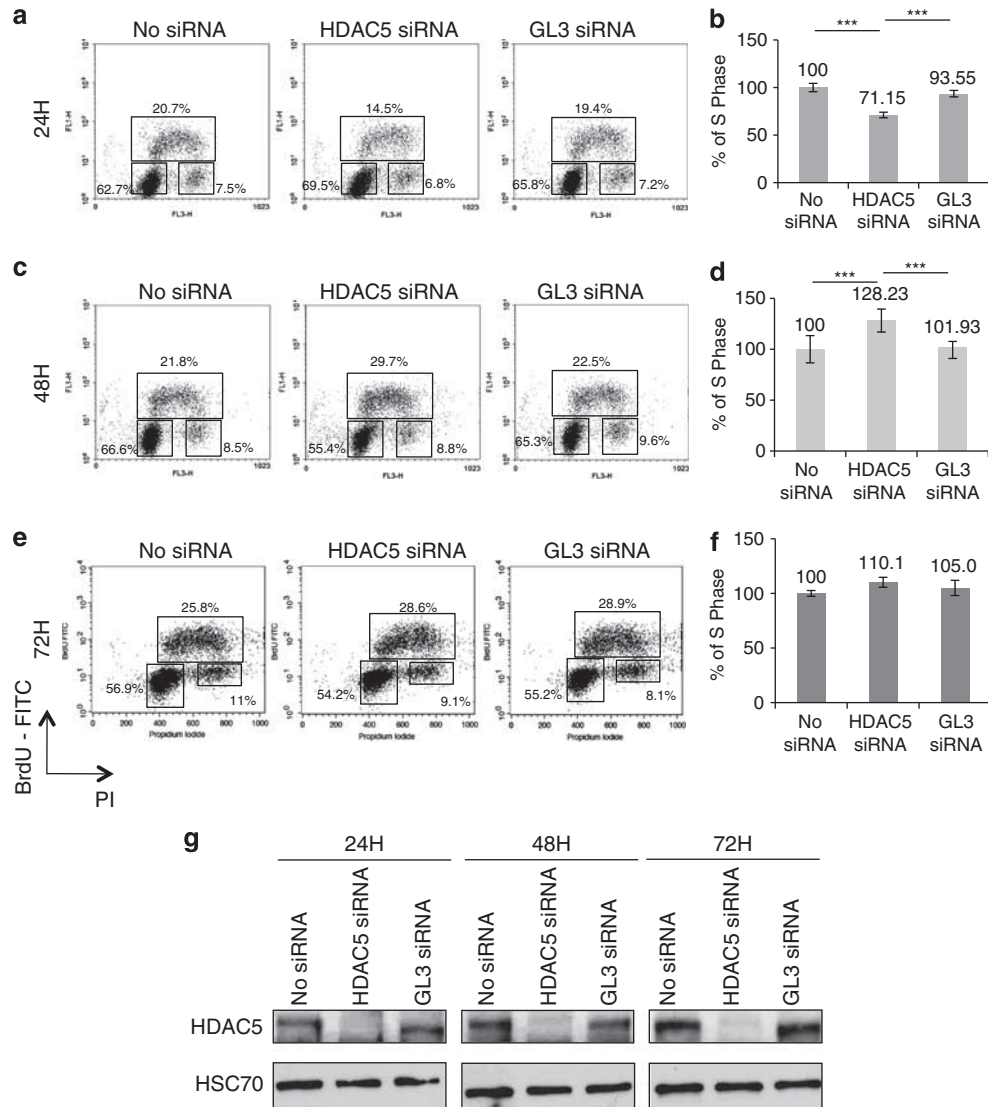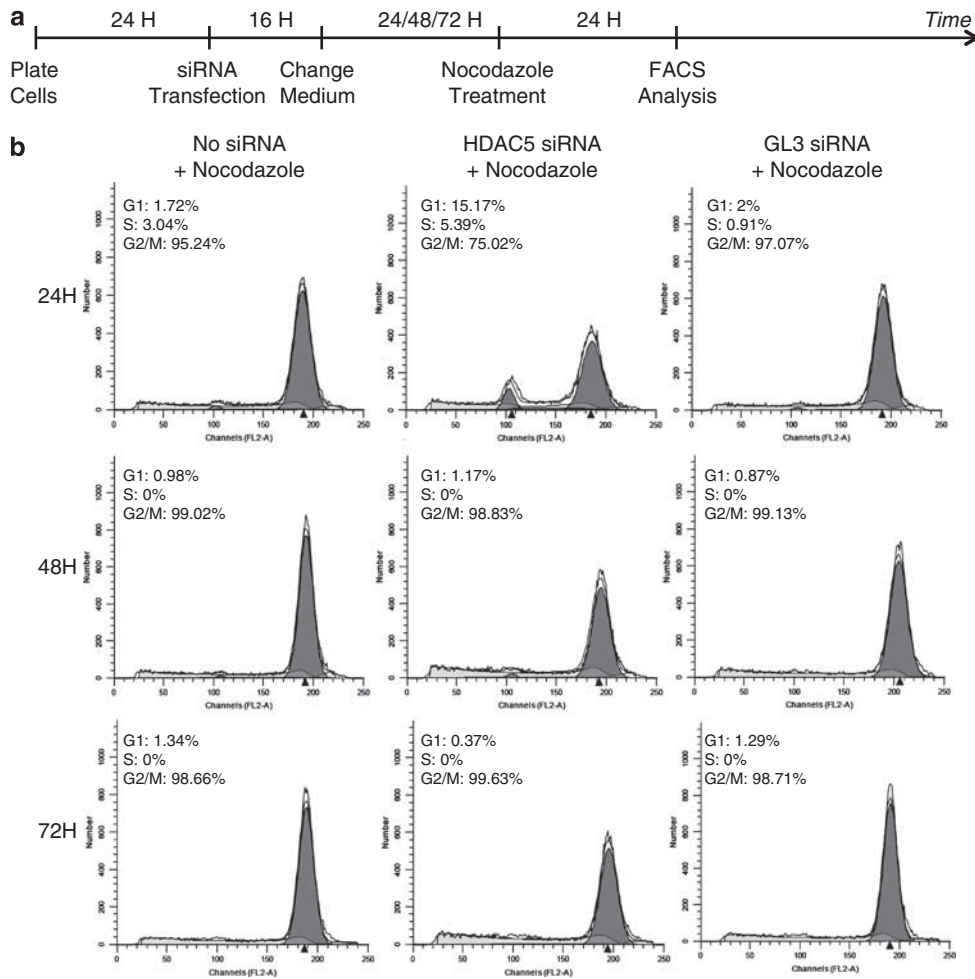
Figure 2 (**a–f**) HDAC5 depletion decreases DNA replication. HeLa cells were mock-transfected (No siRNA) or transfected with a siRNA directed against either HDAC5 or GL3 for 24 (**a**), 48 h (**c**), or 72 h (**e**); pulse-labeled for 30 min with the nucleotide analog BrdU; fixed; stained with an anti-BrdU antibody and PI; and analyzed by flow cytometry. The distributions of cell-cycle phases (G$_1$–S–G$_2$/M) are shown as percentage and are representative of three independent experiments. (**b**, **d** and **f**) In the bar graph, results are expressed as percentage of BrdU-positive cells arbitrarily fixed as 100% under the No siRNA condition. The values represent the mean ± S.D. of three independent experiments. Statistical analysis was performed by two-way ANOVA with a 95% interval of confidence followed by Bonferroni's post-test. ***$P < 0.001$. (**g**) Western blot analysis of HDAC5 expression level in protein lysates from HeLa cells cultured in parallel

control cells, suggesting that cells seem to adapt or recover from HDAC5 loss, thus ensuring normal cell-cycle progression (Figure 3).

HDAC5 depletion inhibits replication fork progression. The inability to remove histones in front of the replication fork or to load nucleosomes behind the fork can impede replication progression. To test whether HDAC5 depletion affected replication fork progression, we performed DNA fiber assay (Figure 4a). A comparison of DNA fibers from control- and HDAC5 siRNA-transfected cells revealed a striking difference in the overall length of their replication tracks (Figure 4b) and stalled replication fork were commonly observed when HDAC5 is depleted (Supplementary Figure S5). When distribution of fibers length was

quantified and plotted, the entire distribution of fiber length in HDAC5-depleted cells shifted leftward to shorter fibers (Figure 4c). Quantification of the doubly labeled fibers indicated that the average rate of fork progression in HDAC5-depleted cells was 1.26-fold slower than in control cells, suggesting that replication forks progressed at a slower rate in the absence of HDAC5 (Figure 4d).

DNA replication is a multi-step process, which first requires loading of DNA replication licensing factors. The chromatin association of ORC (origin recognition complex) and MCM (mini-chromosome maintenance protein) subunits, and PCNA, which are DNA replication licensing factors—was not altered in the absence of HDAC5 (Figure 4e), suggesting that replication factors were assembled normally and the replication defect occurred downstream from replication factor recruitment.

Figure 3 (**a** and **b**) HDAC5 depletion delays cell-cycle progression. HeLa cells were mock-transfected (No siRNA) or transfected with a siRNA directed against either HDAC5 or GL3 for 24, 48, or 72 h. Nocodazole, a mitotic inhibitor, was added 24 h before harvest. Samples were stained with PI and analyzed by flow cytometry. The distributions of cell-cycle phases (G$_1$–S–M) are shown as percentage and are representative of three independent experiments

Analysis of the activities of lamin B2, an early replication origin, and, Ors8, a late replication origin, demonstrated that HDAC5 depletion affected the firing of origins. Indeed, firing from both origins was reduced by approximately 40% at 24 h after transfection, whereas it was significantly increased after 48 h of transfection (Figures 4f and g).

HDAC5 depletion induces DNA damages and activates DNA-damage checkpoint pathways. Changes in heterochromatin structure alter fork progression. DNA double-strand breaks (DSBs) arise frequently as a consequence of replication fork stalling. One of the first molecules to appear following DSB formation is the phosphorylated form of H2AX histone variant on Serine[139] (γ-H2AX). Inhibition of HDAC5 expression led to a significant increase in γ-H2AX as early as 24 h after transfection as shown by western blotting and single-cell electrophoresis assay (Figures 5a and b), suggesting that HDAC5 depletion leads to DNA damages. A co-staining between γ-H2AX and BrdU revealed that these DNA damages occur at replication sites mainly in mid- to late S phase (Figure 5c and Supplementary Figure S6).

DNA damages during S phase activate the intra-S phase checkpoint and involve transducer kinases such as checkpoint kinase 1 (Chk1) and/or Chk2.[15,16] The active form of Chk1 but not Chk2 was detected in HDAC5-depleted cells. The level of p53, a downstream target of Chk1, is slightly increased 24 h after HDAC5 depletion, but it declined thereafter, and reached the basal level after 32 h. In HDAC5-depleted cells, the p53 target gene p21[WAF1/Cip1] also showed a similar rise and fall, although it faded off more slowly. Similarly, upregulation of p27[kip1] and p16INK4A, two other cyclin-dependent kinase (CDK) inhibitors (CDKi), was transient and not sustained over time. As attempted, these CDKis inhibit the phosphorylation of retinoblastoma protein (pRb), thereby preventing E2F1 from transcribing genes that are required for cell-cycle progression such as cyclin A or E2F1 itself (Figure 5d). However, induction of these CDKis and accumulation of hypo-phosphorylated pRB were not maintained after 72 or 96 h (Figure 5e), showing that HDAC5 depletion caused a transient induction of CDKis that decline slightly at basal level later.

To see whether induction of both p53 and p21[WAF1/Cip1] was similar in other cell types, we explored the consequences of
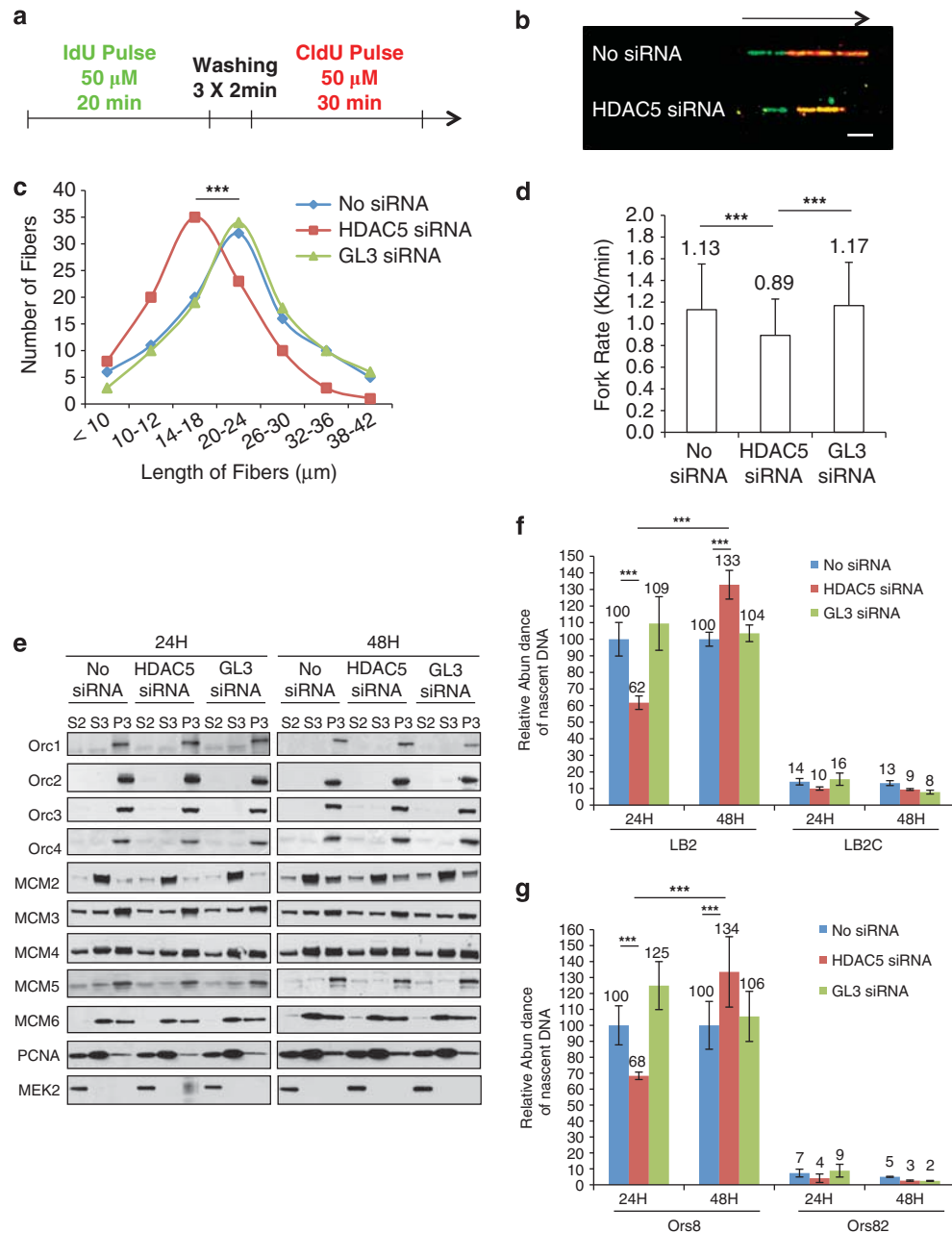
Figure 4 (**a–d**) HDAC5 depletion inhibits replication forks. (**a**) A schematic representation showing the principle of the DNA fiber assay. (**b**) Representative images of replication tracks in mock (No siRNA)- and HDAC5 siRNA-transfected cells pulse-labeled with 50 μM IdU for 20 min (green track) followed by 50 μM CldU for 30 min (red track), and then processed for DNA fiber spreads as described under Materials and Methods. Fork direction is indicated by a black arrow. All track photos are shown at identical magnifications (original magnification: × 630; bar: 5 μm). (**c**) The numbers of fibers for each specified length in mock (No siRNA)-, HDAC5 siRNA-, and GL3 siRNA-transfected cells were compared. The data were derived from one of two independent experiments in which at least 100 fibers were analyzed per experiment. Results are expressed as a frequency distribution of fiber length. Fiber length means were compared by one-way ANOVA with a 95% interval of confidence followed by Bonferroni's post-test. (**d**) Mean fork rates (kb/min) ± S.D. in each condition were calculated from the data shown in panel **c**, and compared by one-way ANOVA with a 95% interval of confidence. (**e**) HDAC5 depletion does not alter the chromatin loading of DNA replication licensing factors. HeLa cells were mock-transfected (No siRNA) or transfected with a siRNA directed against either HDAC5 or GL3 for 24 or 48 h. Fractions of chromatin-bound proteins were prepared as described under Materials and Methods, and the level of different DNA replication licensing factors was assessed by western blotting. The MEK2 protein was used as a fractionation control. S2, cytoplasmic fraction; S3, nuclear soluble proteins; P3, chromatin-enriched fraction. (**f** and **g**) HDAC5 depletion inhibits the firing of origins. Histogram plots of the lamin B2 (**f**) and Ors8 (**g**) origin activities in mock-transfected cells or cells transfected with a siRNA directed against either HDAC5 or GL3 for 24 or 48 h as measured by nascent-strand DNA abundance. Results are expressed as a percentage of the nascent-DNA strand abundance mean under the No siRNA condition. The values represent the mean ± S.D. of two independent experiments, each with three technical replicates. Statistical analysis was performed by two-way ANOVA with a 95% interval of confidence followed by Bonferroni's post-test. ***$P < 0.001$
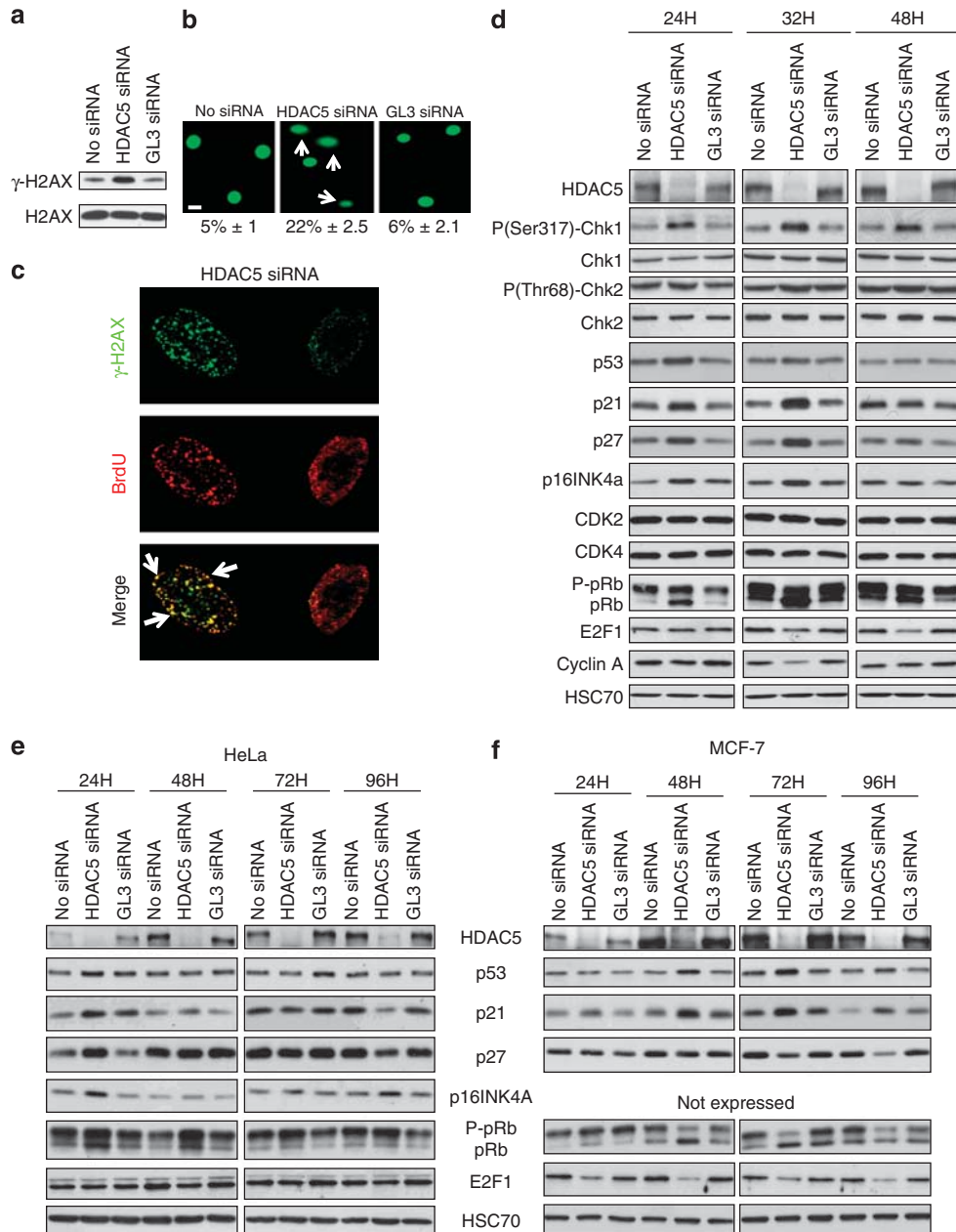
Figure 5 HDAC5 depletion leads to DNA damages and activates the DNA-damage checkpoint pathway. (**a**) HeLa cells were mock-transfected (No siRNA) or transfected with a siRNA directed against either HDAC5 or GL3 for 24 h, and western blotting was performed using anti-γ-H2AX antibodies. (**b**) HeLa cells were mock-transfected (No siRNA) or transfected with a siRNA directed against either HDAC5 or GL3 for 24 h, and the presence of DNA damages was assayed by the Oxiselect Comet Assay Kit according to the manufacturer's instructions (Cellbiolabs, San Diego, CA, USA). Representative cells are shown for each condition. A higher number of nuclei in HDAC5-depleted cells showed the presence of the characteristic comet tail, indicating the presence of DNA damages. The arrows indicate cell nuclei with tail (original magnification: × 630; bar: 10 μm). The average comet tail moment length was scored for at least 100 nuclei per slide by using the CASP software, version 1.2.2 (www.casp.of.pl). Results are expressed as mean ± S.D. and are indicated under the pictures. (**c**) HeLa cells were transfected as in panel **a**, pulse-labeled for 30 min with the nucleotide analog BrdU, fixed, and double immunostained for γ-H2AX (green) and BrdU (red). Representative pictures of HDAC5-depleted cells from two independent experiments are shown. The white arrows indicate colocalization foci into the nucleus. (**d**) HeLa cells were mock-transfected (No siRNA) or transfected with a siRNA directed against either HDAC5 or GL3 for 24, 32 or 48 h. Total protein extracts were prepared and processed for western blotting using the indicated antibodies. HSC70 was used as a loading control. HeLa cells (**e**) or MCF-7 cells (**f**) were mock-transfected (No siRNA) or transfected with a siRNA directed against either HDAC5 or GL3 for 24, 48, 72, or 96 h. Total protein extracts were prepared and processed for western blotting using the indicated antibodies. HSC70 was used as a loading control

HDAC5 depletion in MCF-7 cells, which also harbors wild-type p53 and pRb genes. In those cells, HDAC5 depletion also induced activation of the p53–p21[WAF1/Cip1] and pRb pathways, but the induction was more persistent compared with HeLa cells (Figure 5f).

HDAC5 depletion induced both apoptosis and autophagy. HDAC5 depletion induced a DNA-damage response, which engages both the p53–p21[WAF1/Cip1] and the p16INK4A–pRb pathways. These pathways can establish and maintain the growth arrest that is typical

of senescence and/or induce apoptosis. Any blue staining indicative of SA-β-gal (senescence-associated β-galactosidase) activity, a typical marker of senescence, was observed in both HeLa and MCF-7 cells in the absence of HDAC5 (data not shown). However, HDAC5 depletion drives cells into apoptosis. By 48 h after transfection, there was a nearly two-fold increase of cells undergoing apoptosis (Figures 6a and b). Apoptosis in both cell types was confirmed by caspase-7 activation (Figures 6c and d, and Supplementary Figures S7A and S7B) as well as microscopic analysis showing typical apoptotic morphology (Supplementary Figure S8).

As autophagy and apoptosis can share common components and inhibitory/activating signaling pathways, we next determined whether HDAC5 depletion could also induce autophagy by analyzing the level of LC3, an autophagosomal marker. LC3-II levels (compared with β-actin loading controls) increased in both HeLa and MCF-7 cells depleted for HDAC5 (Figures 6c and d, bottom panels), suggesting concomitant induction of apoptosis and autophagy. This amount of LC3-II further accumulates in the presence of a lysosomal inhibitor, indicating enhancement of the autophagic flux (Supplementary Figure S9A). To further confirm activation of autophagy, both HeLa and MCF-7 cells were stained with an LC3 antibody
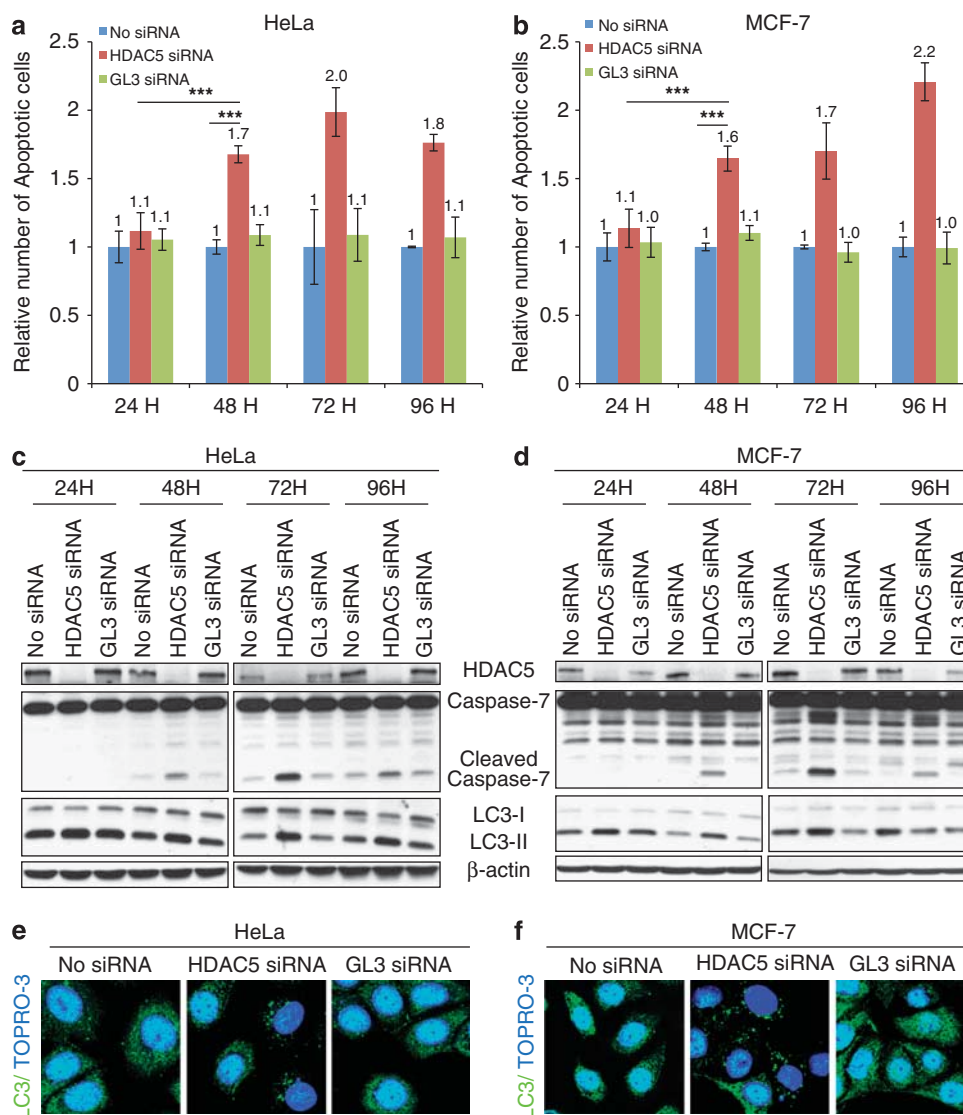
Figure 6 HDAC5 depletion induces both apoptosis and autophagy. HeLa (**a**) or MCF-7 cells (**b**) were mock-transfected (No siRNA) or transfected with a siRNA directed against either HDAC5 or GL3 for 24, 48, 72, and 96 h. Apoptotic cells were quantified by Annexin V staining as described under Materials and Methods. Results are presented as a relative number of apoptotic cells arbitrarily fixed as 1 under the No siRNA condition. The values represent the mean ± S.D. of three independent experiments. Statistical analysis was performed by two-way ANOVA with a 95% interval of confidence followed by Bonferroni's post-test. ***$P < 0.001$. HeLa (**c**) or MCF-7 cells (**d**) were mock-transfected (No siRNA) or transfected with a siRNA directed against either HDAC5 or GL3 for 24–48–72 or 96 h. Both floating and adherent cells were collected and lysed. Western blotting was performed using anti-HDAC5, anti-caspase-7, and anti-LC3 antibodies. β-Actin was used as a loading control. (**e** and **f**) Both HeLa and MCF-7 cells were mock-transfected (No siRNA) or transfected with a siRNA directed against either HDAC5 or GL3 for 48 h. Autophagic vacuoles (white arrows) were detected by confocal microscopy after LC3 staining. Representative cells are shown for each condition (original magnification: × 630; bar: 5 μm)

and presence of autophagic vacuoles was analyzed by confocal microscopy. Figures 6e and f showed the presence of autophagic vacuoles in both HeLa and MCF-7 depleted for HDAC5. This formation/accumulation of autophagic vacuoles was confirmed by electron microscopy (Supplementary Figure S9B).

HDAC5 depletion globally reduces cancer cell proliferation, survival, and inhibits tumor growth *in vivo*. Because HDAC5 depletion affects cell-cycle progression, and induces both apoptosis and autophagy, we assessed the effect of HDAC5 depletion on the global cancer cell proliferation, survival, and tumor growth. *In vitro*, HDAC5 depletion significantly decreased proliferation (Figures 7a and b) as well as survival (Figures 7c and d) of both HeLa and MCF-7 cells. To examine the effect of HDAC5 depletion on tumor cell growth, we used an *in vivo* model in which cancer cells are engrafted onto embryonated chick chorioallantoic membrane (CAM). Tumors formed from HDAC5-depleted MCF-7 cells (Figures 7e–g) were smaller than control tumors, demonstrating the relevance of inhibiting HDAC5 in cancer cells *in vivo*.

HDAC5 depletion increases the efficacy of chemotherapeutic drugs *in vitro*. It has become increasingly clear that the chromatin compaction present in heterochromatin helps to protect DNA from damaging drugs.[17] As such, knockdown of heterochromatic proteins or induced de-condensation of chromatin sensitizes cells to DNA damages.[18] According to our data, HDAC5 depletion could expose heterochromatic regions to DNA-damaging drugs. Therefore, we examined whether HDAC5 depletion could sensitize cancer cells to chemotherapeutic drugs. MCF-7 or HeLa cells were transfected with a siRNA against HDAC5 for 24 h, and then incubated either with doxorubicin or cisplatin for an additional 24 h. Loss of HDAC5 caused 5–6 times more apoptosis compared with cisplatin or doxorubicin alone in HeLa cells (Figures 8a–c). Interestingly, the combination of HDAC5 siRNA/doxorubicin or cisplatin produces more cell death than chemotherapeutic drugs associated with trichostatin A (TSA), a broad-spectrum HDACi (Supplementary Figures S10A and S10B), demonstrating that only inhibition of HDAC5 produces better cytotoxicity than HDACi to potentiate chemotherapeutic drugs.

Using the same schedule, HDAC5 depletion in MCF-7 cells did not potentiate the activity of chemotherapeutic drugs. To test whether this schedule alters the effectiveness of combination treatment, HDAC5-depleted MCF-7 cells were exposed to DNA-damaging drugs 48 h after siRNA transfection for an additional 24 h. A better cytotoxic/apoptotic effect was observed (Figures 8d and e, and Supplementary Figure S10C) suggesting that appropriate sequencing and scheduling of the combination of HDAC5 silencing with DNA-damaging drugs is required for each cancer cell type.

Discussion

The inheritance and faithful maintenance of chromatin organization is crucial for eukaryotic cells. To orchestrate DNA replication in the context of chromatin, cells have evolved efficient nucleosome dynamics involving assembly pathways and chromatin maturation mechanisms. During replication, modified parental histones are displaced ahead of the replication fork and are randomly distributed between the two daughter strands. Concomitantly, deposition of *de novo*-synthesized histones H3 and H4 provides the full complement of histones that are needed to ensure proper assembly of the duplicated material. During its initial synthesis, histone H4 is acetylated at lysine residues 5 and 12. These residues must be deacetylated to form heterochromatin in late S phase, thus ensuring secure maintenance of the under-acetylated state of heterochromatin. This latter step is promoted through the action of HDAC-containing complexes such as Mi-2/NuRD (nucleosome-remodeling deacetylase complex) and/or the Sin3/HDAC chromatin-modifying complex,[19] which have been shown to contain both HDAC1 and HDAC2, and associate with pericentric heterochromatin during S phase.[20,21] Whereas some reports pointed to the role of HDAC2 in the rearrangement of the nucleosomes during the formation of heterochromatin in late S phase,[22] as well as the implication for HDAC3 in replication fork progression,[23,24] we demonstrated that HDAC5 is recruited to heterochromatin regions, probably with members of NuRD/Sin3 chromatin remodeling complexes as well as with other epigenetic regulators such as DNA methyltransferase 1 (DNMT1) or HP-1,[22,25–28] to participate in the establishment of the pericentric heterochromatin structure in late S phase. However, the mechanisms of action of HDAC5 in the assembly/maturation of pericentric heterochromatin remain to be identified.

The chromatin structural defect caused by HDAC5 depletion results in a slow-growth phenotype, with delayed cell-cycle progression and activation of multiple checkpoints pathways. We indeed observed: (i) activation of the Chk1-dependent intra-S phase checkpoint, which could survey alterations in chromatin structure, and serves as an efficient mechanism to slow down fork progression in the absence of appropriate chromatin assembly and block initiation of new replication forks in a global manner, consistent with reports showing that origin firing is inhibited during S phase when DNA damage or replication fork stalling activates the intra-S-phase checkpoint kinases;[29–31] and (ii) activation of a G_1/S checkpoint pathway, which prevents late-G_1 cells from entering the S period by directly or indirectly inhibiting initiation at the earliest-firing origins, with the consequence that the entire S period is delayed along the cell-cycle axis.[29,30]

In addition to cell-cycle blocking, we also observed activation of autophagy in HDAC5-depleted cells. Numerous studies suggest that autophagy may function in the regulation of cell survival and have a major role in the maintenance of genomic integrity.[32] The precise role of autophagy in response to HDAC5 depletion is not fully understood yet but is thought to be a temporary survival mechanism, which delays apoptosis as inhibition of HDAC5 silencing-induced autophagy unmasks and accelerates apoptosis (data not shown).

Activation of checkpoint pathways and consequently cell-cycle blocking in HDAC5-depleted cells should allow time for the chromatin defects to be resolved. Once repair is accomplished, these checkpoint/repair pathways are usually
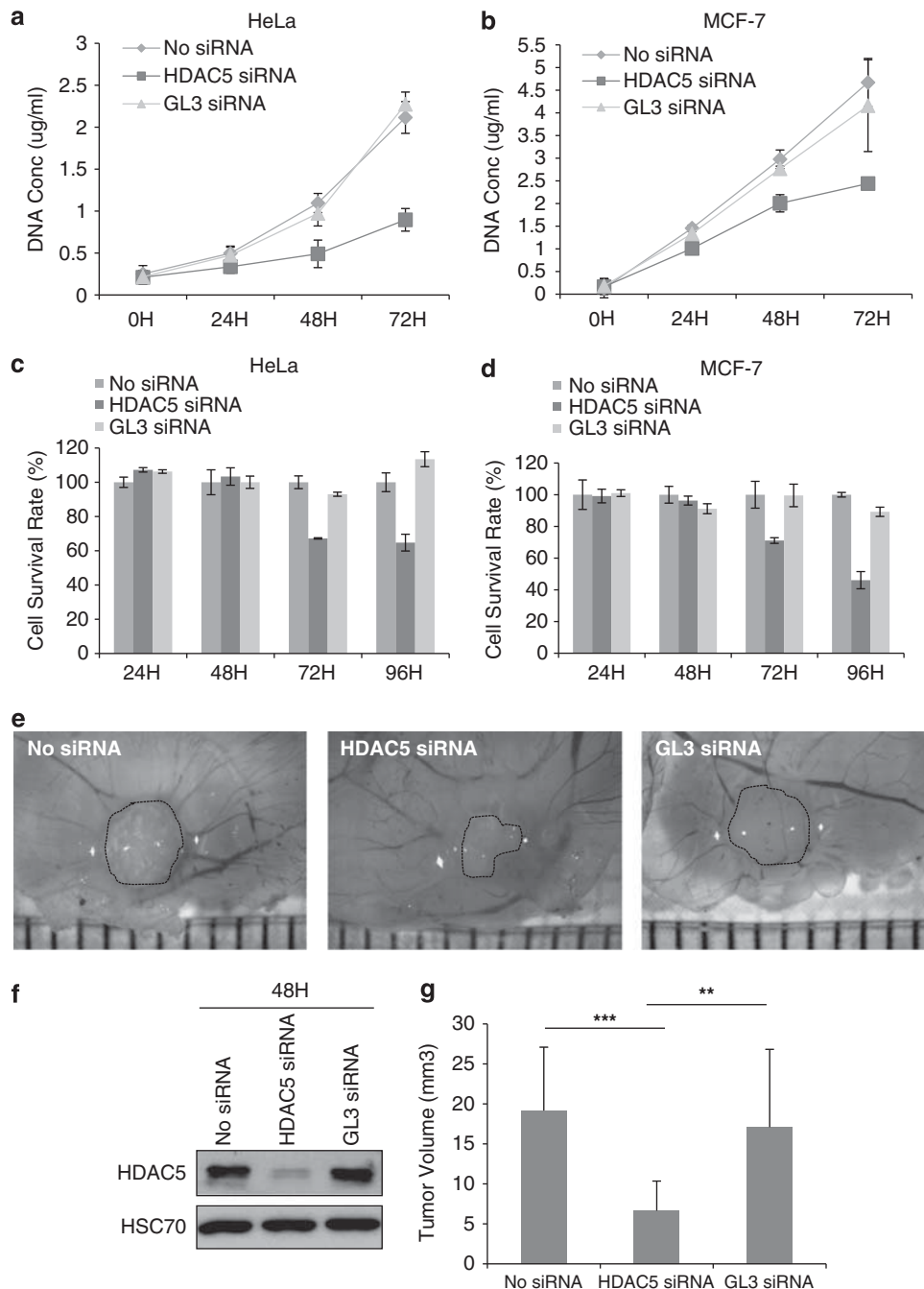
Figure 7 HDAC5 depletion blocks cancer cell proliferation, decreases cell survival, and inhibits tumor growth *in vivo*. HeLa (**a**) or MCF-7 cells (**b**) were mock-transfected (No siRNA) or transfected with a siRNA directed against either HDAC5 or GL3 for 24–48 and 72 h. Time-course analysis of DNA content was performed by fluorimetric DNA titration. The values are the mean ± S.D. of three replicates and are representative of three separate experiments. Both HeLa (**c**) and MCF-7 (**d**) cells were mock-transfected (No siRNA) or transfected with a siRNA directed against either HDAC5 or GL3 for 24–48–72 and 96 h. WST-1 cell survival assay was performed as described under Materials and Methods. The values are the mean ± S.D. of three replicates and are representative of three separate experiments. (**e**) MCF-7 cells were mock-transfected (No siRNA) or transfected with an HDAC5 or a GL3 siRNA, implanted on CAM 16 h later, and inoculated 7 days. A representative photograph of a 'No siRNA' tumor, an 'HDAC5 siRNA' tumor, and a 'siRNA GL3' tumor. The dotted lines indicate tumor boundaries at the end of the experiment. (**f**) In parallel, a fraction of transfected MCF-7 cells was plated and maintained in culture during the 48 h period. Total protein extracts were prepared from those cells and processed for western blotting using anti-HDAC5 antibodies. HSC70 was used as a loading control. (**g**) Volume of tumors resected 7 days after inoculation was calculated. The values are the mean ± S.D. of at least six tumors in each group and are representative of two separate experiments. Statistical analysis was performed by one-way ANOVA with a 95% interval of confidence followed by Bonferroni's post-test. $**P < 0.01$, $***P < 0.001$

silenced so that cell-cycle progression is allowed to resume. In HDAC5-depleted HeLa cells, we noticed resumption of normal cell-cycle progression after transient cell-cycle

blocking as demonstrated by biphasic modulation of cell-cycle inhibitors such as p21$^{WAF1/Cip1}$, p27^{kip1}, or P-pRb, which occurs in conjunction with release from cell-cycle blocking.
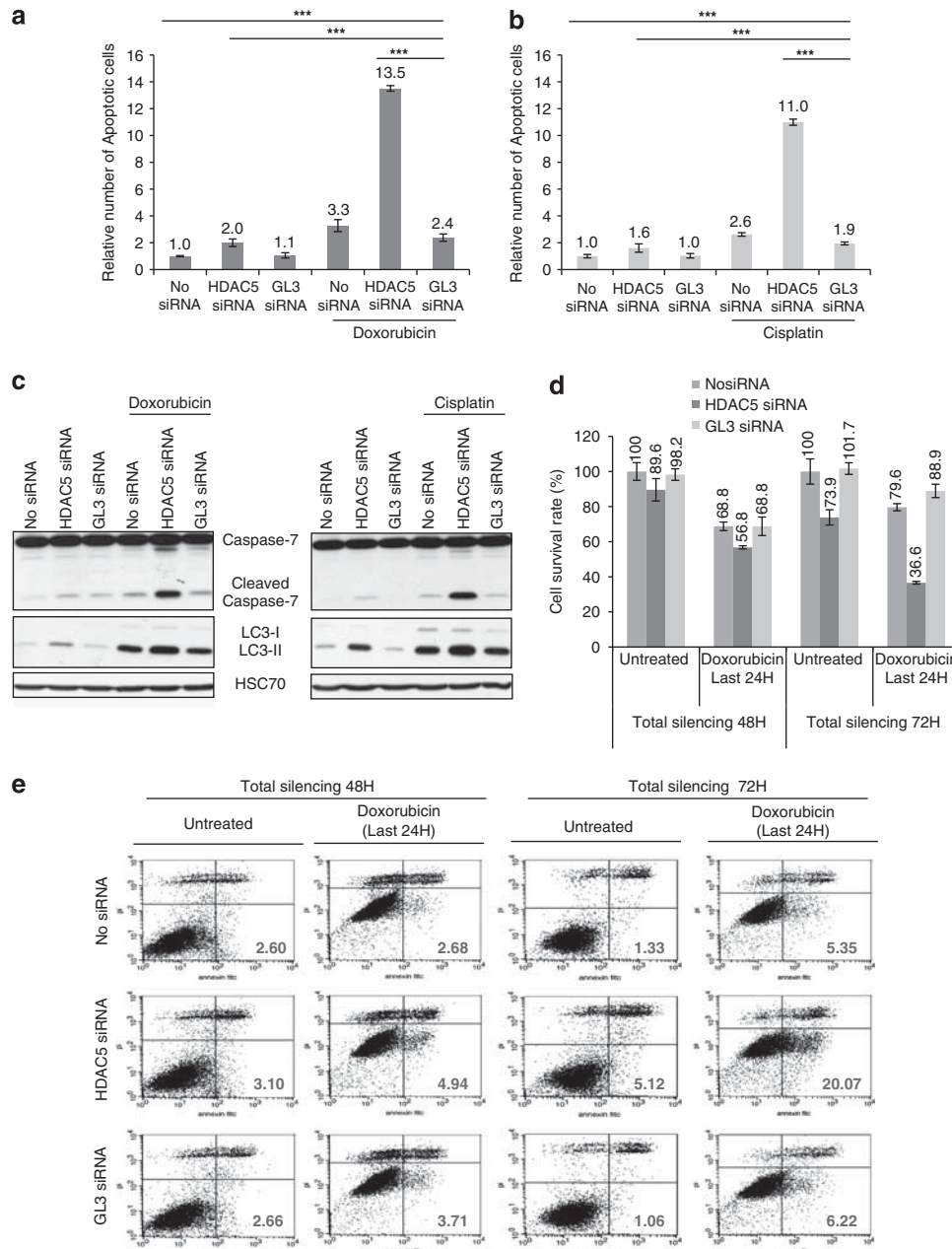
Figure 8 HDAC5 depletion sensitizes both HeLa and MCF-7 cells to chemotherapeutic agents. (**a** and **b**) HeLa cells were mock-transfected (No siRNA) or transfected with a siRNA directed against either HDAC5 or GL3 for 24 h and then treated either with doxorubicin (2 μM) (**a**) or cisplatin (7 μM) (**b**) for an additional 24 h. Apoptotic cells were quantified by Annexin V staining as described under Materials and Methods. ***$P < 0.001$. (**c**) HeLa cells were transfected as in panels **a** and **b**. Both floating and adherent cells were collected and lysed. Western blotting was performed using anti-caspase-7 and anti-LC-3 antibodies. HSC70 was used as a loading control. (**d**) MCF-7 cells were mock-transfected (No siRNA) or transfected with a siRNA directed against either HDAC5 or GL3 for 24 or 48 h, and then treated with doxorubicin (2 μM) for an additional 24 h. WST-1 cell survival assay was performed as described under Materials and Methods. (**e**) MCF-7 cells were transfected as in panel **d**. Apoptotic cells were quantified by Annexin V staining. For each condition, representative FACS dot plots are presented with number of cells in Annexin V$^+$/PI$^-$ quadrant

This transient cell-cycle arrest suggests that either checkpoint recovery (fulfillment of the requirement) or checkpoint adaptation occurs in HDAC5-depleted HeLa cells. In the light of an yeast two-hybrid screen showing interaction between HDAC5 and Mus81 (methyl methanesulfonate and ultraviolet-sensitive gene clone 81), we are actually investigating the role of this endonuclease Mus81 on cell-cycle resumption. Preliminary experiments demonstrated the possible

implication of Mus81 in the checkpoint recovery/adaptation of cells from HDAC5 depletion stress, allowing them to survive and proliferate with apparently intact chromosomes or at the cost of tolerating mutation. As defective DNA-damage repairs with Mus81 mutations are often observed in breast cancer patients,[33] we hypothesized that MCF-7 cells harbor mutations in gene encoding Mus81 and/or other DNA repair/checkpoint proteins that impair checkpoint recovery/adaptation,

leading to excessive unrepaired chromatin defects and consequently apoptosis.

After an initial attempt to recover or adapt, prolonged HDAC5 inhibition in HeLa cells overwhelms the cells and results in apoptosis, suggesting that either chromatin defects are too severe or recovery/adaptation mechanisms are followed by excessive genome instability, leading to cell death in subsequent cell cycles for a subpopulation of cells. In addition to activation of the apoptotic program, we noted that autophagy is still induced at late time point in the time course of HDAC5 depletion. Despite its initial role as a survival pathway, progressive autophagy can result in cell death if allowed to proceed to completion under persistent stress and therefore, both processes would cooperate to lead to cell death.

The role of HDAC5 in heterochromatin assembly and maturation also has an impact in DNA alteration-based cancer strategies. Consistent with others studies,[34,35] we reported here that HDAC5 depletion potentiates the effect of chemotherapeutic agents that target DNA by inducing heterochromatin de-condensation, thereby facilitating access of drugs to DNA. Despite a more accessible chromatin in both cell types, we found that a different sequencing and scheduling of the combination of HDAC5 silencing with DNA-damaging drugs is required for each cancer cell types. Why did HDAC5-depleted MCF-7 cells show a delayed death response to DNA-damaging drugs compared with HeLa cells? In MCF-7 cells, several factors such as caspase-3 deficiency, levels and activity of the Bax (Bcl-2-associated X)/Bcl-2 (B-cell lymphoma 2) proteins, or activation of phosphoinositide-3-kinase (PI3K)/Akt (protein kinase B) kinases can contribute to refractory to apoptosis induced by DNA-damaging drugs. Autophagy also represents a mechanism of resistance to modalities, which affect DNA. Because induction of autophagy delays apoptosis in the absence of HDAC5 only, we are currently focusing our research to further understand the impact of autophagy in the death response of HDAC5-depleted cells treated with chemotherapeutic agents.

Altogether, our findings revealed that HDAC5 is a regulator of pericentric heterochromatin assembly, and demonstrated that its inhibition alone or in combination with chemotherapeutic agents might represent a promising strategy in cancer therapy.

Materials and Methods

Cell culture, synchronization, and treatment. HeLa cells were maintained in Dulbecco's modified Eagle's medium (DMEM) with 10% heat-inactivated fetal bovine serum (FBS). MCF-7 cells were maintained in α-Modified Eagle's Medium (αMEM) supplemented with 10% heat-inactivated FBS. Synchronization was achieved by treating cells with 2 mM hydroxyurea (Sigma) and 200 μg/ml nocodazole (Sigma, St. Louis, MO, USA). TSA, cisplatin and doxorubicin were purchased from Sigma.

Antibodies. Anti-FLAG and anti-BrdU (clone BU-33) antibodies were purchased from Sigma. Anti-BrdU (clone BU1/75), anti-ORC1, anti-ORC3, and anti-ORC4 antibodies were from AbDSerotec (Kidlington, UK). Anti-HDAC5, anti-p16INK4A, anti-MCM2, anti-MEK2 (MAPK/ERK kinase 2), anti-ORC2, anti-Chk1, anti-phosphoSer317 Chk1, anti-Chk2, anti-phosphoThr68 Chk2, and anti-caspase-3/7 antibodies were purchased from Cell Signaling (Carlsbad, CA, USA). Anti-HDAC5, anti-histone H2AX, anti-phosphoSer139 histone H2AX and anti-phosphoSer10 histone H3 antibodies were from Millipore (Bedford, MA, USA). Anti-BrdU (clone B44), anti-MCM4, anti-MCM5, anti-MCM6, anti-p27,

anti-pRb, anti-cyclin E, and anti-cyclin A antibodies were purchased from BD Biosciences (Erembodegem, Belgium). Anti-p53 antibodies were from Upstate Biotechnology (Lake Placid, NY, USA). Anti-p21[WAF1/Cip1], anti-E2F1, anti-MCM3, anti-Cdc6, anti-PCNA (clone PC10), anti-HP-1, anti-HDAC5, and anti-HSC70 (heat-shock cognate 70-kDa protein) were purchased from Santa Cruz Biotechnology (Santa Cruz, CA, USA). Anti-LC3 antibodies were purchased from Abgent (San Diego, CA, USA).

siRNA transfection. siRNAs were synthesized either by Eurogentec (Liège, Belgium) or Dharmacon (Lafayette, CO, USA). Calcium phosphate-mediated transfections were performed as described previously.[36]

Immunocytochemistry. After fixation and permeabilization, cells were incubated with primary antibodies and with corresponding Alexa dye-conjugated secondary antibodies (Molecular Probes, Eugene, OR, USA) and mounted onto microscope slides. For nuclear counterstaining, cells were incubated with TOPRO-3 (Molecular Probes). For γ-H2AX and BrdU co-staining, cells were fixed and permeabilized. To denature DNA, fixed cells were resuspended in 4 N HCl and incubated for 30 min at 37 °C. After washing with borate buffer and phosphate-buffered saline (PBS) to remove any acid traces, cells were simultaneously incubated with a mouse anti-BrdU antibody and a rabbit anti-γ-H2AX antibody. Primary antibodies were detected with a secondary Alexa 546-conjugated goat, anti-mouse antibody and a secondary Alexa 488-conjugated goat, anti-rabbit antibody. Images were obtained with either a Leica TCS SP5 laser-scanning confocal microscope (Leica, Wetzlar, Germany) or with a FluoView Olympus laser-scanning confocal microscope (Olympus, Tokyo, Japan). Images were transferred to Adobe Photoshop CS4 (Adobe Systems) for assembly.

Transmission electron microscopy. Immunolabeling was performed on formaldehyde-fixed and Lowicryl-K4M-embedded cells as described previously.[37] For ultrastructure, samples were washed in Sörensen's buffer and fixed for 1 h at 4 °C with 2.5% glutaraldehyde in Sörensen's 0.1 M phosphate buffer (pH 7.4), and post-fixed for 30 min with 1% osmium tetroxide. After dehydration in graded ethanol, samples were embedded in Epon. Ultrathin sections obtained with a Reichert Ultracut S ultramicrotome were contrasted with uranyl acetate and lead citrate. Observations were made with a Jeol 100 CX II transmission electron microscope at 60 kV.

MNaseI sensitivity assay. MCF-7 cells (1×10^6) were Dounce-homogenized in RSB buffer (10 mmol/l Tris-HCl (pH 7.4), 10 mM NaCl, 3 mM MgCl$_2$, 0.5% NP-40) containing 10 μg/ml aprotinin and leupeptin, 1 mM phenylmethylsulfonyl fluoride, 1 mM Na$_3$VO$_4$, and 1 mM dithiothreitol (DTT), and incubated on ice for 15 min. Samples were centrifuged at 4 °C for 5 min at 1400 × g, the medium was removed, samples were washed twice with RSB buffer, and digested with 0.25 to 2.5 U of micrococcal nuclease in digestion buffer (15 mM Tris-HCl (pH 7.5), 60 mM KCl, 15 mM NaCl, 1 mM CaCl$_2$, 3 mM MgCl$_2$, 20% glycerol, 15 mM β-mercaptoethanol) for 5 min. Digestion was stopped by adding 1 volume of stop solution (50 mM Tris (pH 7.5), 150 mM NaCl, 50 mM EDTA, 0.3% sodium dodecyl sulfate (SDS)). DNA was extracted using 1 volume of phenol/chloroform/isoamyl alcohol (25 : 24 : 1) followed by 1 volume chloroform/isoamyl alcohol (24 : 1) and precipitated with 100% ethanol. DNA was washed once with 70% ethanol, resuspended in H$_2$O, and 1.5 μg of DNA was separated using 1.2% agarose gel.

Chromatin isolation. Chromatin fractionation was performed as described previously.[38] Three different fractions were collected: cytoplasmic fraction (S2), nuclear soluble proteins (S3), and chromatin-enriched fraction (P3).

Western blot analysis. Adherent (and floating depending on the experiment) cells were lysed into an SDS buffer (SDS 1%, Tris-HCl 40 mM (pH 7.5), EDTA 1 mM, protease inhibitor mixture) unless otherwise stated. Equal amounts of proteins were resolved by SDS-PAGE. Membranes were probed with primary antibodies, followed by horseradish peroxidase (HRP)-conjugated secondary antibodies, and developed by chemiluminescence detection.

WST-1 cell viability. Cell survival was determined by WST-1 (2-(4-iodophenyl)-3-(4-nitrophenyl)-5-(2,4-disulfophenyl)-2H-tetrazolium, monosodium salt) cell viability assay according to the manufacturer's instructions (Roche, Basel, Switzerland).

Cell-cycle analysis. The relative percentage of cells in each stage of the cell cycle was analyzed according to the procedure of labeling nuclei with propidium iodide (PI) followed by flow cytometric analysis using FACSCalibur II and the ModFit LT program.

In vitro DNA content measurement. Fluorimetric DNA titration was performed as described previously.[39]

In vivo DNA replication assay. Cells were labeled with 33 μM BrdU for 30 min, resuspended in PBS + 10% FBS, and then fixed with 70% cold ethanol. DNA was denatured with 4 N HCl + 0.5% Triton X-100 for 30 min at 37 °C. After washing cells with PBS, the pellet was resuspended in PBS + 10% FBS. An anti-BrdU antibody (clone BU-33; Sigma) was added and cells were incubated for 1 h at room temperature. After washing, an Alexa 488-conjugated goat, anti-mouse secondary antibody (Molecular Probes) was added for 1 h at room temperature in dark. After washing, cells were collected, resuspended in PI solution (EDTA 3 mM (pH 8.0), Tween 20 0.05%, PI 50 μg/ml, RNAse A 50 μg/ml in PBS), and analyzed using a FACSCalibur II and the CellQuest software (BD Biosciences).

DNA fiber assay. Cells were doubly labeled by incubating with 50 μM iododeoxyuridine (IdU) for 20 min followed by incubation with 50 μM chlorodeoxyuridine (CldU) for 30 min. A 2-μl volume of cells, resuspended in ice-cold PBS at 10^6 cells/ml, was spotted onto a silane-coated microscope slide (Sigma) and then overlaid with 10 μl of spreading buffer (SDS 0.5%, Tris-HCl 200 mM (pH 7.4), EDTA 50 mM). After 6 min, the slides were tilted by 15 degrees to allow lysates to slowly move down the slide. The DNA spreads were air-dried, fixed in a 3 : 1 mixture of methanol/acetic acid for 15 min at −20 °C, and stored in pre-chilled 70% ethanol at 4 °C overnight. The slides were then treated with 4 M HCl for 10 min at room temperature followed by 30 min at 37 °C in a water bath, washed three times in PBS, and incubated in blocking buffer (2% BSA in PBS) for 1 h at room temperature followed by 1 h at 37 °C with a rat anti-BrdU antibody (to detect CldU) (clone BU1/75; AbDSerotec) plus a mouse anti-BrdU (to detect IdU) (clone B44; BD Biosciences). After rinsing three times with stringency buffer (Tris-HCl 10 mM (pH 7.5), NaCl 400 mM, Tween 20 0.1%, NP-40 0.1%) the slides were incubated for 1 h with Alexa Fluor 488-conjugated rabbit, anti-mouse antibodies and Alexa Fluor 546-conjugated goat, anti-rat antibodies (Molecular Probes). Slides were rinsed three times with PBS, once with H_2O, and mounted in Mowiol medium. Microscopy was performed using a FluoView Olympus laser-scanning confocal microscope using the sequential scanning mode. A single-blind evaluation was performed to measure the lengths of continuously double-stained tracks using the ImageJ software (NCI/NIH, Bethesda, MD, USA) and the collected images were processed using the Adobe Photoshop CS4 software (Adobe Systems). Pictures were taken on the entire slide and on multiple slides, reducing the chance of over- or under-representing certain origins or genomes of individual cells. Micrometer values were converted into kilobase using the conversion factor 1 μm = 2.59 kb. Measurements were recorded from fibers in well-spread (untangled) areas of the slides to prevent the possibility of recording labeled patches from bundles of fibers.

Isolation of nascent-strand DNA. Isolation of nascent-strand DNA was performed as described previously.[40] The primers and PCR conditions are described by Rampakakis et al.[40]

Annexin V staining. Apoptotic cells were determined by Annexin V–FITC (fluorescein isothiocyanate) and non-vital dye PI staining using an FITC–Annexin V apoptosis detection kit I (BD Biosciences) according to the manufacturer's instructions. Flow cytometry was performed using a FACSCanto and samples were analyzed using the CellQuest software (BD Biosciences). Both Annexin V$^+$/PI$^-$ cells representing early-apoptotic cells and Annexin V$^+$/PI$^+$ mostly representing late-apoptotic/necrotic cells were considered as apoptotic cells.

CAM tumor model. A window was opened in the eggshell of a 3-day-old embryo using scissors after puncturing the air chamber. The window was sealed with tape and the eggs were incubated at 37 °C and 80% humidity until cell grafting. Eight days later, a Matrigel/cell mixture (1 : 1) was grafted within a plastic ring on the CAM surface. The window was sealed and eggs were incubated under the same conditions for 7 days. On day 18, tumors were dissected and diameters were measured with a caliper. Tumor volume was calculated using an ellipsoid formula: Volume $(mm^3) = (4 \times \pi \times Z_1 \times Z_2 \times Z_3)/3$, where Z_{1-3} are the main radii of the tumor.

Statistical analyses. Results were reported as means with their S.D. or S.E.M. as reported in the figure legends. Statistical analysis was performed by one-way ANOVA or two-way ANOVA regarding the number of grouping factors. Group means were compared by Bonferroni's post-test. Homoscedasticity was assayed by Levene's test. Normality was assayed by the D'Agostino and Pearson test. All tests were performed with a 95% interval of confidence.

Conflict of Interest

The authors declare no conflict of interest.

1. de Ruijter AJ, van Gennip AH, Caron HN, Kemp S, van Kuilenburg AB. Histone deacetylases (HDACs): characterization of the classical HDAC family. *Biochem J* 2003; **370** (Part 3): 737–749.
2. Bertrand P. Inside HDAC with HDAC inhibitors. *Eur J Med Chem* (2010); **45**: 2095–2116.
3. Duvic M, Vu J. Vorinostat: a new oral histone deacetylase inhibitor approved for cutaneous T-cell lymphoma. *Expert Opin Investig Drugs* 2007; **16**: 1111–1120.
4. Mottet D, Pirotte S, Lamour V, Hagedorn M, Javerzat S, Bikfalvi A et al. HDAC4 represses p21(WAF1/Cip1) expression in human cancer cells through a Sp1-dependent, p53-independent mechanism. *Oncogene* 2009; **28**: 243–256.
5. Wilson AJ, Byun DS, Nasser S, Murray L, Ayyanar K, Arango D et al. HDAC4 promotes growth of colon cancer cells via repression of p21. *Mol Biol Cell* 2008; **19**: 4062–4075.
6. Zhu C, Chen Q, Xie Z, Ai J, Tong L, Ding J et al. The role of histone deacetylase 7 (HDAC7) in cancer cell proliferation: regulation on c-Myc. *J Mol Med* 2011; **89**: 279–289.
7. Kitamura Y, Shimizu K, Tanaka S, Ito K, Emi M. Allelotyping of anaplastic thyroid carcinoma: frequent allelic losses on 1q, 9p, 11, 17, 19p, and 22q. *Genes Chromosomes Cancer* 2000; **27**: 244–251.
8. Scanlan MJ, Welt S, Gordon CM, Chen YT, Gure AO, Stockert E et al. Cancer-related serological recognition of human colon cancer: identification of potential diagnostic and immunotherapeutic targets. *Cancer Res* 2002; **62**: 4041–4047.
9. Ozdag H, Teschendorff AE, Ahmed AA, Hyland SJ, Blenkiron C, Bobrow L et al. Differential expression of selected histone modifier genes in human solid cancers. *BMC Genomics* 2006; **7**: 90.
10. Bradbury CA, Khanim FL, Hayden R, Bunce CM, White DA, Drayson MT et al. Histone deacetylases in acute myeloid leukaemia show a distinctive pattern of expression that changes selectively in response to deacetylase inhibitors. *Leukemia* 2005; **19**: 1751–1759.
11. Osada H, Tatematsu Y, Saito H, Yatabe Y, Mitsudomi T, Takahashi T. Reduced expression of class II histone deacetylase genes is associated with poor prognosis in lung cancer patients. *Int J Cancer* 2004; **112**: 26–32.
12. Milde T, Oehme I, Korshunov A, Kopp-Schneider A, Remke M, Northcott P et al. HDAC5 and HDAC9 in medulloblastoma: novel markers for risk stratification and role in tumor cell growth. *Clin Cancer Res* 2010; **16**: 3240–3252.
13. Van Hooser A, Goodrich DW, Allis CD, Brinkley BR, Mancini MA. Histone H3 phosphorylation is required for the initiation, but not maintenance, of mammalian chromosome condensation. *J Cell Sci* 1998; **111** (Part 23): 3497–3506.
14. Singer JD, Gurian-West M, Clurman B, Roberts JM. Cullin-3 targets cyclin E for ubiquitination and controls S phase in mammalian cells. *Genes Dev* 1999; **13**: 2375–2387.
15. Ahn JY, Schwarz JK, Piwnica-Worms H, Canman CE. Threonine 68 phosphorylation by ataxia telangiectasia mutated is required for efficient activation of Chk2 in response to ionizing radiation. *Cancer Res* 2000; **60**: 5934–5936.
16. Feijoo C, Hall-Jackson C, Wu R, Jenkins D, Leitch J, Gilbert DM et al. Activation of mammalian Chk1 during DNA replication arrest: a role for Chk1 in the intra-S phase checkpoint monitoring replication origin firing. *J Cell Biol* 2001; **154**: 913–923.
17. Falk M, Lukasova E, Kozubek S. Higher-order chromatin structure in DSB induction, repair and misrepair. *Mutat Res* 2010; **704**: 88–100.
18. Kim MS, Blake M, Baek JH, Kohlhagen G, Pommier Y, Carrier F. Inhibition of histone deacetylase increases cytotoxicity to anticancer drugs targeting DNA. *Cancer Res* 2003; **63**: 7291–7300.
19. Ahringer J. NuRD and SIN3 histone deacetylase complexes in development. *Trends Genet* 2000; **16**: 351–356.
20. Sims JK, Wade PA. Mi-2/NuRD complex function is required for normal S phase progression and assembly of pericentric heterochromatin. *Mol Biol Cell* 2011; **22**: 3094–3102.

21. David G, Turner GM, Yao Y, Protopopov A, DePinho RA. mSin3-associated protein, mSds3, is essential for pericentric heterochromatin formation and chromosome segregation in mammalian cells. *Genes Dev* 2003; **17**: 2396–2405.

22. Rountree MR, Bachman KE, Baylin SB. DNMT1 binds HDAC2 and a new co-repressor, DMAP1, to form a complex at replication foci. *Nat Genet* 2000; **25**: 269–277.

23. Bhaskara S, Chyla BJ, Amann JM, Knutson SK, Cortez D, Sun ZW *et al.* Deletion of histone deacetylase 3 reveals critical roles in S phase progression and DNA damage control. *Mol Cell* 2008; **30**: 61–72.

24. Conti C, Leo E, Eichler GS, Sordet O, Martin MM, Fan A *et al.* Inhibition of histone deacetylase in cancer cells slows down replication forks, activates dormant origins, and induces DNA damage. *Cancer Res* 2010; **70**: 4470–4480.

25. Bierne H, Tham TN, Batsche E, Dumay A, Leguillou M, Kerneis-Golsteyn S *et al.* Human BAHD1 promotes heterochromatic gene silencing. *Proc Natl Acad Sci USA* 2009; **106**: 13826–13831.

26. Heo K, Kim B, Kim K, Choi J, Kim H, Zhan Y *et al.* Isolation and characterization of proteins associated with histone H3 tails *in vivo. J Biol Chem* 2007; **282**: 15476–15483.

27. Lemercier C, Brocard MP, Puvion-Dutilleul F, Kao HY, Albagli O, Khochbin S. Class II histone deacetylases are directly recruited by BCL6 transcriptional repressor. *J Biol Chem* 2002; **277**: 22045–22052.

28. Zhang CL, McKinsey TA, Olson EN. Association of class II histone deacetylases with heterochromatin protein 1: potential role for histone methylation in control of muscle differentiation. *Mol Cell Biol* 2002; **22**: 7302–7312.

29. Seiler JA, Conti C, Syed A, Aladjem MI, Pommier Y. The intra-S-phase checkpoint affects both DNA replication initiation and elongation: single-cell and -DNA fiber analyses. *Mol Cell Biol* 2007; **27**: 5806–5818.

30. Willis N, Rhind N. Regulation of DNA replication by the S-phase DNA damage checkpoint. *Cell Div* 2009; **4**: 13.

31. Lee H, Larner JM, Hamlin JL. A p53-independent damage-sensing mechanism that functions as a checkpoint at the G_1/S transition in Chinese hamster ovary cells. *Proc Natl Acad Sci USA* 1997; **94**: 526–531.

32. Mathew R, Kongara S, Beaudoin B, Karp CM, Bray K, Degenhardt K *et al.* Autophagy suppresses tumor progression by limiting chromosomal instability. *Genes Dev* 2007; **21**: 1367–1381.

33. McPherson JP, Lemmers B, Chahwan R, Pamidi A, Migon E, Matysiak-Zablocki E *et al.* Involvement of mammalian Mus81 in genome integrity and tumor suppression. *Science* 2004; **304**: 1822–1826.

34. Marchion DC, Bicaku E, Turner JG, Schmitt ML, Morelli DR, Munster PN. HDAC2 regulates chromatin plasticity and enhances DNA vulnerability. *Mol Cancer Ther* 2009; **8**: 794–801.

35. Marchion DC, Bicaku E, Daud AI, Sullivan DM, Munster PN. Valproic acid alters chromatin structure by regulation of chromatin modulation proteins. *Cancer Res* 2005; **65**: 3815–3822.

36. Waltregny D, Glenisson W, Tran SL, North BJ, Verdin E, Colige A *et al.* Histone deacetylase HDAC8 associates with smooth muscle alpha-actin and is essential for smooth muscle cell contractility. *FASEB J* 2005; **19**: 966–968.

37. Vandelaer M, Thiry M. The phosphoprotein pp135 is an essential constituent of the fibrillar components of nucleoli and of coiled bodies. *Histochem Cell Biol* 1998; **110**: 169–177.

38. Mendez J, Stillman B. Chromatin association of human origin recognition complex, cdc6, and minichromosome maintenance proteins during the cell cycle: assembly of prereplication complexes in late mitosis. *Mol Cell Biol* 2000; **20**: 8602–8612.

39. Labarca C, Paigen K. A simple, rapid, and sensitive DNA assay procedure. *Anal Biochem* 1980; **102**: 344–352.

40. Rampakakis E, Di Paola D, Zannis-Hadjopoulos M. Ku is involved in cell growth, DNA replication and G_1–S transition. *J Cell Sci* 2008; **121** (Part 5): 590–600.

Supplementary Information accompanies the paper on Cell Death and Differentiation website (http://www.nature.com/cdd)

Revealing the anti-tumoral effect of Algerian Glaucium flavum roots against human cancer cells.

Bournine, L. Bensalem, S. Peixoto, P. Gonzalez, A. Maiza-Benabdesselam, F. Bedjou, F. Wauters, J. Tits, M. Frédérich, M. Castronovo, V. and Bellahcène, A.

Phytomedicine, 2013: p. 1211-8.

ANNEXE 3

Revealing the anti-tumoral effect of Algerian *Glaucium flavum* roots against human cancer cells

Lamine Bournine [a,b,c], Sihem Bensalem [a], Paul Peixoto [b], Arnaud Gonzalez [b],
Fadila Maiza-Benabdesselam [a], Fatiha Bedjou [a], Jean-Noël Wauters [c], Monique Tits [c],
Michel Frédérich [c], Vincent Castronovo [b], Akeila Bellahcène [b,*]

[a] *Laboratory of Plant Biotechnology and Ethnobotany, Faculty of Natural Sciences and Life, University of Bejaia, Bejaia, Algeria*
[b] *Metastasis Research Laboratory, GIGA-Cancer, University of Liege, Liege, Belgium*
[c] *Laboratory of Pharmacognosy, CIRM, University of Liege, Liege, Belgium*

ARTICLE INFO

ABSTRACT

Glaucium flavum (*G. flavum*) is a plant from the Papaveraceae family native to Algeria where it is used in local traditional medicine to treat warts. *G. flavum* root crude alkaloid extract inhibited breast cancer cell proliferation and induced G2/M phase cycle arrest and apoptosis without affecting normal cells, which is a highly awaited feature of potential anti-cancer agents. *G. flavum* significantly reduced growth and vascularization of human glioma tumors on chicken chorioallantoic membrane (CAM) *in vivo*. The chromatographic profile of the dichloromethane extract of *G. flavum* root showed the presence of different constituents including the isoquinoline alkaloid protopine, as the major compound. We report for the first time that *G. flavum* extract may represent a new promising agent for cancer chemotherapy.

© 2013 Elsevier GmbH. All rights reserved.

Introduction

Breast cancer is one of the most prevalent malignancies in women in many countries worldwide (Jemal et al. 2011; Youlden et al. 2012). After the rapid expansion of the use of monoclonal antibodies and various synthetic inhibitors directed against matrix metalloproteases or protein kinases, natural products are regaining attention in the oncology field. Due to their wide range of biological activities and low toxicity in animal models, natural products have been used as alternative treatments for cancers including breast cancer. An analysis of new and approved drugs for cancer by the United States Food and Drug Administration (FDA) over the period 1981–2010 showed that more than half of cancer drugs were of natural origin (Newman and Cragg 2012).

Cell cycle deregulation resulting in uncontrolled cell proliferation is one of the most frequent alterations that occur during tumor development. For this reason, blockade of the cell cycle is regarded as an effective strategy for eliminating cancer (Lapenna and Giordano 2009; Williams and Stoeber 2012). Key regulator proteins are cyclin-dependent kinases which activity is specifically controlled by cyclins and cyclin-dependent kinase inhibitor (CDKI)

at specific points of the cell cycle (Besson et al. 2008). The G2/M checkpoint is the most conspicuous target for many anticancer drugs. P21, a member of the CDKI family and cyclin B1 are the central players of G2/M phase transition (Vermeulen et al. 2003). There is a tight relationship between the control of cell cycle checkpoints and the progression to apoptosis, a mechanism responsible for maintaining tissue homeostasis by mediating the equilibrium between cell proliferation and death. Defective apoptosis represents a major causative factor in the development and progression of cancer (Cotter 2009; Ricci and Zong 2006). In cancer therapy, induction of apoptosis cells is one of the strategies for anticancer drug development (Alam 2003; Fischer and Schulze-Osthoff 2005; Ocker and Hopfner 2012).

Several drugs currently used in chemotherapy were isolated from plant species. The best known are the Vinca alkaloids, vinblastine and vincristine, isolated from *Catharanthus roseus*, etoposide and teniposide, which are semi-synthetic derivatives of the natural product epipodophyllotoxin, Paclitaxel isolated from the bark of *Taxus brevifolia*, the semi-synthetic derivatives of camptothecin, irinotecan and topotecan, isolated from *Camptotheca acuminata*, among several others (Cragg et al. 1993).

G. flavum belongs to the family of Papaveraceae. The aerial part of this plant is very rich in isoquinoline alkaloids, especially in aporphine bases namely, didehydroglaucine, 6',7-dehydroglaucine,(+)-glaucine, (+)-isocorydine, (+)-corydine, (+)-cataline, 1,2,9,10-tetramethoxyoxoaporphine, α-allocryptopine, corunnine, and isoboldine (Israilov et al. 1979; Daskalova et al.

* Corresponding author at: Metastasis Research Laboratory, GIGA-Cancer, University of Liege, 4000 Liege, Belgium. Tel.: +32 04 366 25 57;
fax: +32 04 366 29 75.
E-mail address: a.bellahcene@ulg.ac.be (A. Bellahcène).

1988). The latter are known for exhibiting promising pharmacological activities including anti-inflammatory, analgesic and antipyretic (Pinto et al. 1998), hypoglycemic (Cabo et al. 2006) and antioxidant activity (Tawaha et al. 2007).

Interestingly, a recent study demonstrated that Sardinian *G. flavum* contained a homogeneous alkaloid pattern of aporphine type, significantly different from those reported for populations from other parts of Europe (Petitto et al. 2010). In this study, we used *G. flavum* collected in Algeria where the root is widely used in local traditional medicine to treat warts and inflammatory diseases. To our knowledge, the potential anticancer activities of *G. flavum* have never been investigated. We decided to evaluate the effects of its alkaloid extract on human normal and malignant cells.

We explored the potential inhibitory growth effect of the dichloromethane extract of *G. flavum* root on 3 human breast cancer cell lines: MDA-MB-435, MDA-MB-231 and Hs578T and non malignant human cells. Interestingly, *G. flavum* induced cell cycle arrest and apoptotic cell death in all breast cancer cells tested but not in MCF10A normal mammary epithelial cells. Based on our results *in vitro*, we decided to explore further the anti-tumoral effect of *G. flavum* extract using the *in vivo* tumor chorioallantoic membrane (CAM) model. We demonstrated that *G. flavum* extract treatment induced a significant decrease in tumor growth and affected tumor associated angiogenesis *in vivo*. The chemical characterization of the dichloromethane extract was evaluated using HPLC analysis, which showed the presence of protopine as the major alkaloid.

Materials and methods

Plant material extraction

The root of flowering plant *G. flavum* was collected in littoral area and far from any contact with pollution in Tichy, province of Bejaia (Algeria) according to botanists (University of Bejaia) previous identification. The alkaloids were extracted as described by Suau et al. (Suau et al. 2004). Briefly, the extraction was undertaken with (10 g) of powdered plant material and (100 ml) of methanol in a Soxhlet apparatus. The methanol was evaporated using a rotavapor and the residue was taken up in 2% hydrochloric acid (50 ml), neutral components being removed by filtration. The filtrate was adjusted to pH 8 with aqueous ammonia and extracted with dichloromethane (3×25 ml). The resulting extracts were dried with $MgSO_4$ and the solvent evaporated to obtain the crude alkaloid extract. The solid extract was reconstituted in DMSO solvent (50 mg/ml stock solution) and then filtered using 0.22 μm filters before storage at $-20\,°C$. During all experiments, DMSO dilutions of *G. flavum* extract were adjusted in the culture media to achieve the indicated final concentrations and control cells were treated at the maximum concentration used in the experiment, 0.1%.

High performance liquid chromatography (HPLC) profiling

The HPLC of dichloromethane root extract of *G. flavum* (stock solution 20 mg/50 ml) was carried out for identification. The extract was dissolved in methanol and filtered through Acrodisc PSF GXF/GHP 0.45 nm filter. An injection of 10 μl of this filtered extract was chromatographed with an Agilent 1100 HPLC with DAD (diode-array detector) detection. The working wavelength was 290 nm. The column was a Polaris amide C-18 column (5 μm, 250 mm × 4.6 mm) operated at 25 °C. The mobile phase was composed of solution A (trifluoroacetic acid 0.05% in water) and solution B (acetonitrile) with the following gradient: equilibration time 15 min at 100% A and linear gradient elution: 0 min 100% A; 1 min 97% A; 45 min 60% A; 55 min 40% A; 65 min 40% A and 66 min 100%

A. The flow rate was 1 ml/min. The structure of protopine was elucidated using NMR spectroscopy (^{1}H, ^{13}C, COSY, HMBC, HSQC), mass spectrometry (MS), and UV spectroscopy.

Cell culture

MCF10A cells (CRL-10317, ATCC) were cultured in DMEM/HAM'S F-12 medium supplemented with 0.01 mg/ml of human insulin, 2.5 μM L-glutamine, 20 ng/ml of epidermal growth factor, 0.5 mg/ml of hydrocortisone, 5% horse serum, and 100 ng/ml of cholera toxin. HUVEC (Human Umbilical Vein Endothelial) and skin fibroblast were isolated and maintained in culture as described previously (Jaffe et al. 1973; Rittié and Fisher 2005). MDA-MB-231 (HTB-26, ATCC), MDA-MB-435 (HTB-129, ATCC) cells were grown in Dulbecco's modified Eagle's medium (DMEM), supplemented with 10% of fetal bovine serum and 1% L-glutamine. Hs578T cells (HTB-126, ATCC) were cultured in DMEM supplemented with 10 μg/ml of bovine insulin, 1 mM sodium pyruvate and 10% of fetal bovine serum. Human glioma cells U87-MG (89081402, ATCC) were maintained in Minimum Essential Medium with 10% FBS, 2 mM L-glutamine, 1% non essential amino acid, and 1 mM sodium pyruvate. All the cells were cultured at 37 °C in a humidified atmosphere and 5% CO_2.

Viability assay

Cell viability was determined using the cell proliferation reagent WST-1 assay according to the manufacturer's instructions (Roche, Basel, Switzerland). All analyzed cells were seeded to obtain 50% of confluence after 24 h of incubation in 96-well plates then treated with serial dilutions of the plant extract (0–40 μg/ml). Cells were incubated with the WST-1 reagent for 4 h. After this incubation period, the formazan dye formed is quantified with a scanning multi-well spectrophotometer at 450 nm. The measured absorbance directly correlates to the number of viable cells. Percentages of cell survival were calculated as follows: % cell survival = (absorbance of treated cells/absorbance of cells with vehicle solvent) × 100. The half inhibitory concentration (IC_{50}) was calculated from the dose-response curve obtained by plotting the percentage of cell survival *versus* the concentration of plant extract used.

Cell cycle analysis

Cells were seeded and incubated overnight to attach, and exposed to DMSO (control) or desired concentrations of *G. flavum* for specified time periods. Both floating and adherent cells were collected, washed with phosphate buffered saline (PBS), and fixed in 70% ethanol. The cells were then treated with 50 μg/ml RNase A and 50 μg/ml propidium iodide for 30 min and analyzed using a FACSCalibur II and the Cell ProQuest program.

Antibodies

Anti-p21 and anti-cyclin B1 antibodies were purchased from Santa Cruz Biotechnology (Santa Cruz, CA, USA). Anti-beta actin from Sigma (Saint Louis, Missouri, USA).

Immunoblotting analysis

Desired cell line was seeded in 6 well plates, allowed to attach overnight and treated according to their respective IC_{50} with *G. flavum* extract. Both floating and attached cells were collected and lysed into an SDS buffer (SDS 1%, Tris–HCl 40 mM (pH 7.5), EDTA 1 mM, protease inhibitor mixture). Protein concentration was determined using a BCA kit according to manufacturer's
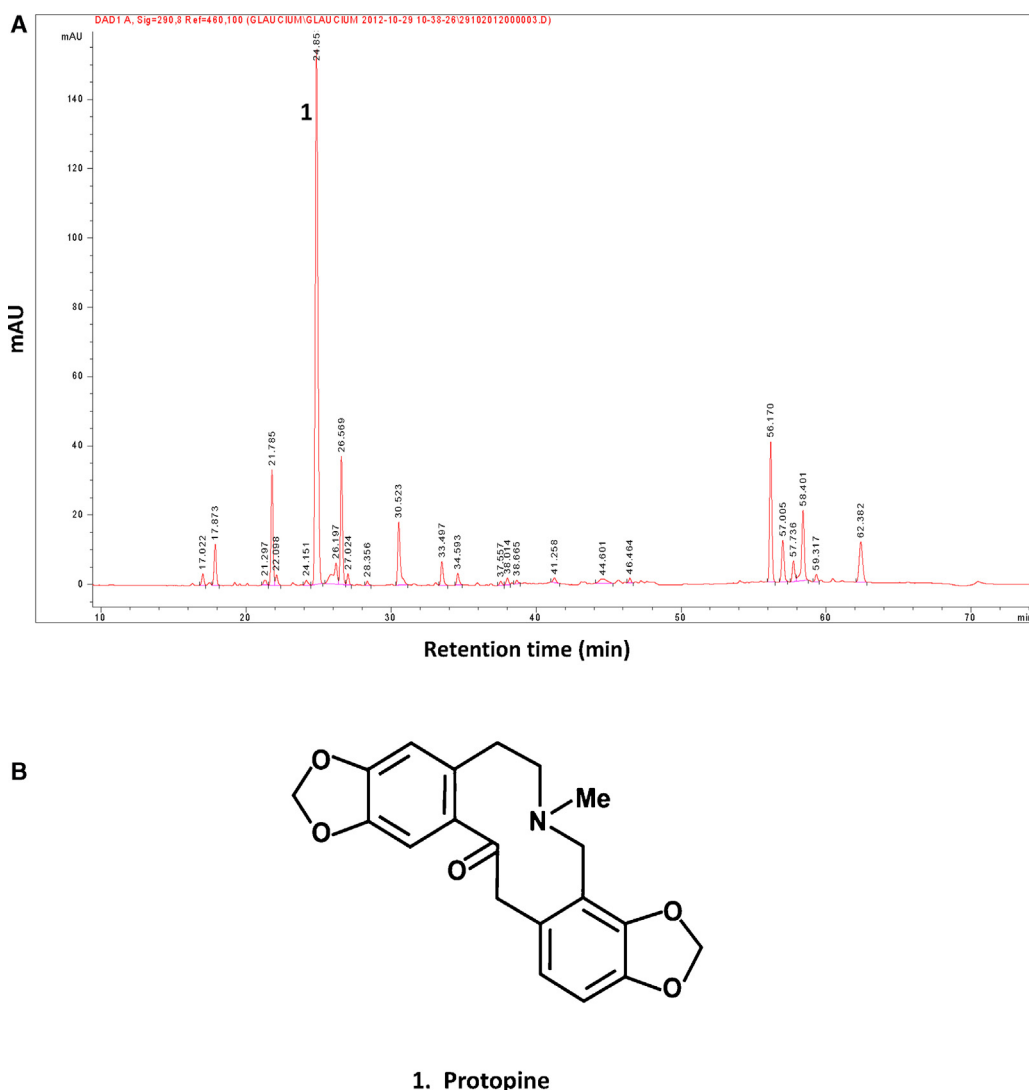
Fig. 1. High-performance liquid chromatography profile of *G. flavum* extract at OD 290 nm and major compound identification: (A) HPLC chromatogram of *G. flavum*, the major peak corresponding to protopine (retention time = 24.85 min, peak 1) was isolated and identified as described in "Materials and methods" section and (B) molecular structure of protopine.

instructions (Pierce, Rockford, IL). Equal amounts of proteins were resolved by sodium dodecyl sulfate-polyacrylamide gel electrophoresis and transferred to nitrocellulose or PVDF membrane (Invitrogen). Membranes were probed with primary antibodies, followed by horseradish peroxidase (HRP)-conjugated secondary antibodies, and developed by chemiluminescence detection. Blots were stripped and re-probed with anti-actin to normalize. Scanned bands were quantified using ImageJ software Version 1.43 (National Institutes of Health, http://rsb.info.nih.gov/ij/).

DAPI staining

DAPI staining method was used to observe apoptotic morphological changes (chromatin condensation and nuclear fragmentation) in treated cells. Cancer cells were treated with *G. flavum* extract at their respective IC_{50} values and MCF10A breast cells was treated at the highest IC_{50} observed for cancer cells (15 μg/ml) during 24 h. Briefly, the cells were seeded in 6 well plates and treated with *G. flavum* or with nocodazole (3 μM) used as a positive control of apoptosis inducer. Cells were fixed with paraformaldehyde 3% and incubated in Vectashield solution (Vector Laboratories) for
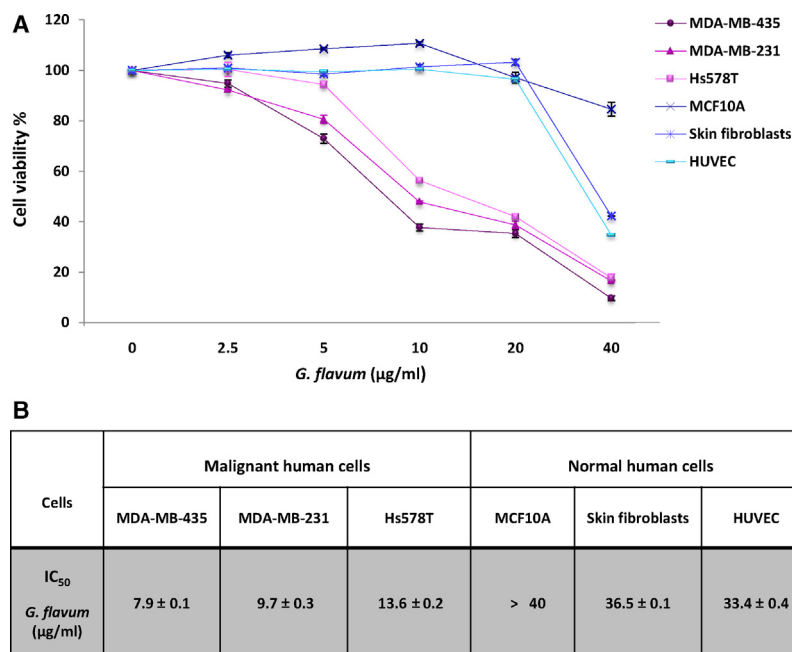
30 min in the dark. Cells were then examined and photographed using a fluorescence microscope (EVOS, AMG).

Quantitation of apoptosis by flow cytometry

Apoptotic cells were determined by Annexin V-FITC (fluorescein isothiocyanate) and non-vital dye PI staining using an FITC-Annexin V apoptosis detection kit I (BD Biosciences) according to the manufacturer's instructions. Flow cytometry was performed using a FACS Caliber II and samples were analyzed using the CellQuest software (BD Biosciences).

Tumor CAM assay

The implantation of human glioblastoma U87-MG cells on the chorio-allantoic membrane (CAM) of embryonic chicken was performed as we described previously (Lamour et al. 2010). On day 13, size-matched tumors were divided into control and treatment groups. *G. flavum* extract was deposited locally at 100 μg/ml per egg per day. Digital pictures were taken under a stereomicroscope (Leica). On day 17, tumor size was calculated based on tumor volume formula: $V = (d_1/2) * (d_2/2) * (d_3/2) * 3.14 * 4/3$, with

A

B

Cells	Malignant human cells			Normal human cells		
	MDA-MB-435	MDA-MB-231	Hs578T	MCF10A	Skin fibroblasts	HUVEC
IC_{50} G. flavum (µg/ml)	7.9 ± 0.1	9.7 ± 0.3	13.6 ± 0.2	> 40	36.5 ± 0.1	33.4 ± 0.4

Fig. 2. *G. flavum* extract inhibited the viability of malignant human breast cancer cells (MDA-MB-435, MDA-MB-231, Hs578T) in a dose-dependent manner without affecting normal human cells (MCF10A human normal mammary cells, human skin fibroblasts and HUVEC): (A) cells were treated with DMSO vehicle or the indicated concentrations of *G. flavum* extract for 24 h. Cell viability was determined using Wst1 assay and expressed as means ± SD of at least two separate experiments and (B) IC_{50} values of *G. flavum* extract were determined based on the dose-response curves shown in (A) (means ± SD of at least two separate experiments).

d_1, d_2, d_3 corresponding three measures taken on the experimental tumors. Quantification of drug effects on tumor cell growth were determined in ten representative tumors per group. For histological studies, U87-MG experimental tumors were embedded in paraffin and cut into 5 µm sections. Tissue sections were stained with hematoxylin and eosin (H&E). Vessels were stained using fluorescein-coupled *Sambucus nigra* lectin SNA-1 (FL-1301; Vector Laboratories). Statistical comparison between the two groups was performed by using the Student's *t* test. A value of $p < 0.05$ was considered significant.

Results

Phytochemical profile of G. flavum extract

The HPLC chromatogram of *G. flavum* root extract (Fig. 1A) revealed several peaks with a significant peak eluting at 24.85 min (peak 1) which is the major compound of dichloromethane extract and was identified as protopine. Fig. 1B shows the structure of protopine.

G. flavum extract treatment specifically decreased the viability of human breast cancer cells

We first investigated the effects of *G. flavum* extract on MDA-MB-231, MDA-MB-435 and Hs578T human breast cancer cell lines. WST1 viability assay was used for the determination of *G. flavum* extract IC_{50} values in these cells thus establishing the starting point for the next experiments. Cells were treated during 24 h at the following concentrations: 0, 2.5, 5, 10, 20 and 40 µg/ml (Fig. 2A). The treatment significantly affected the viability of all cancer cell lines tested and displayed low IC_{50} values (<15 µg/ml) after 24 h of treatment (Fig. 2B). Following the standard National Cancer Institute (NCI) criteria, an IC_{50} less than 30 µg/ml of crude extract is considered as an active compound against cancer cells (Suffness and Pezzuto 1990). Next, we tested the effect of *G. flavum* extract on non malignant human cells such as spontaneously

immortalized breast epithelial cells (MCF10A), human umbilical vein endothelial cells (HUVEC) and skin fibroblasts (Fig. 2A). For these cells, the calculated IC_{50} values were higher than 30 µg/ml indicating that *G. flavum* extract mainly inhibited breast cancer cell viability without affecting normal cells (Fig. 2B).

G. flavum extract treatment caused G2/M phase cell cycle arrest in human breast cancer cells

Next, we tested whether inhibitory effect of *G. flavum* on breast cancer cell viability was due to perturbations in cell cycle progression. Fig. 3 depicts flow cytometry histograms for cell cycle distribution in *G. flavum*-treated MDA-MB-231, Hs578T and MCF10A cells. After 24 h, *G. flavum* treatment (IC_{50}) resulted in statistically significant enrichment of G2/M phase cell population in MDA-MB-231 cells as compared with DMSO-treated control cells (44.4% and 19.5%, respectively). In these cells, *G. flavum* mediated G2/M phase cell cycle arrest accompanied by a significant decrease in G0/G1 (from 62.8% to 26.5%) and S phase cells (from 16.5% to 12.7%). With time, a major increase from 0.6% to 16.2% in subG1 population was observed and corresponded to cells that have lost some of their DNA in late stages of the apoptotic process following endonucleases activity (Fig. 3). Notably, *G. flavum*-treated Hs578T cells presented with similar cell cycle pattern (Fig. 3). Consistent with the cell viability experiment, *G. flavum* extract used at the highest cancer cells IC_{50} value (15 µg/ml) did not affect cell cycle distribution of MCF10A cells and stability was generally observed in all cell cycle subpopulations after 12 and 24 h of treatment (Fig. 3).

G. flavum extract treatment altered the expression level of proteins involved in the regulation of G2/M transition in MDA-MB-231 cells

To gain insight into the mechanism of G2/M phase cell cycle arrest, we determined the effect of *G. flavum* treatment on the expression of proteins known to be involved in the regulation of G2/M transition. The level of p21 protein was increased after 12 h
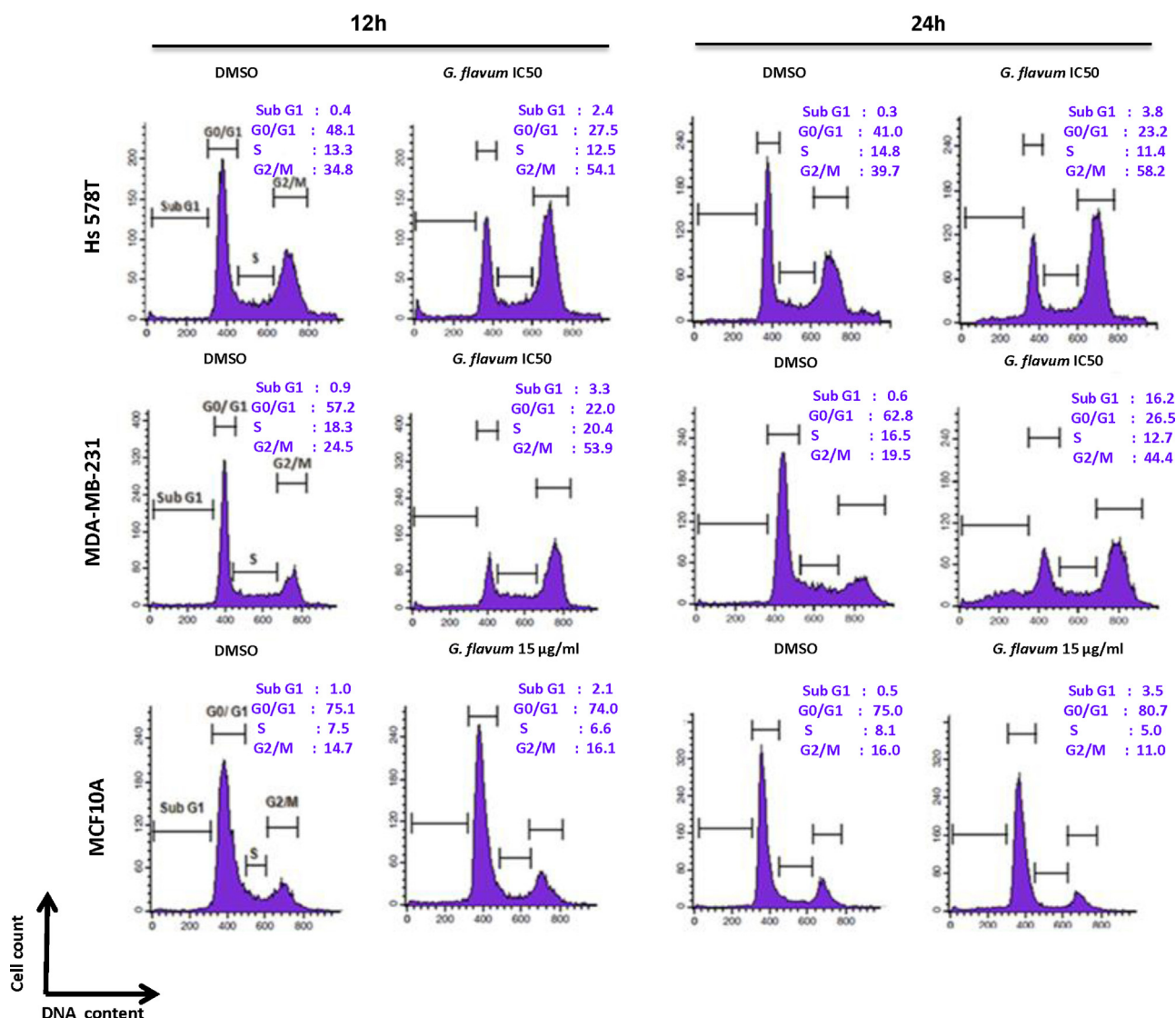
Fig. 3. *G. flavum* extract treatment caused G2/M phase cell cycle arrest in MDA-MB-231 and Hs578T cells. Representative histograms depicting cell cycle distribution in Hs578T, MDA-MB-231 and MCF10A cultures following 12 h and 24 h treatment with DMSO vehicle or the indicated concentrations of *G. flavum* extract corresponding to IC$_{50}$ for Hs578T, MDA-MB-231 and to the highest cancer cells IC$_{50}$ (15 μg/ml) for MCF10A. The experiment was performed three times.

of treatment with *G. flavum* extract and was still high after 48 h. Interestingly, *G. flavum* treatment caused an early increase in the level of cyclin B1 that was sustained after 24 h and showed a slight decrease at 48 h (Fig. 4).

G. flavum extract treatment induces apoptosis in breast cancer cells in vitro

Staining of cells with DAPI showed morphological features characteristic of apoptotic cells such as DNA fragmentation and condensation of chromatin in breast cancer cells treated with *G. flavum* extract (IC$_{50}$, 24 h) that were comparable to nocodazole treated cells used as control (Fig. 5A). Untreated breast cancer cells and MCF10A cells treated with *G. flavum* extract exhibited a normal nuclear morphology characterized by large nuclei with distinguishable nucleoli and diffused chromatin structure (Fig. 5A). The quantification of apoptosis was next evaluated by annexin-V/propidium iodide (PI) staining. Dual staining with annexin-V and PI allowed clear discrimination between unaffected cells (annexin-V negative and PI negative), early apoptotic cells (annexin-V positive and PI negative) and late apoptotic cells (annexin-V
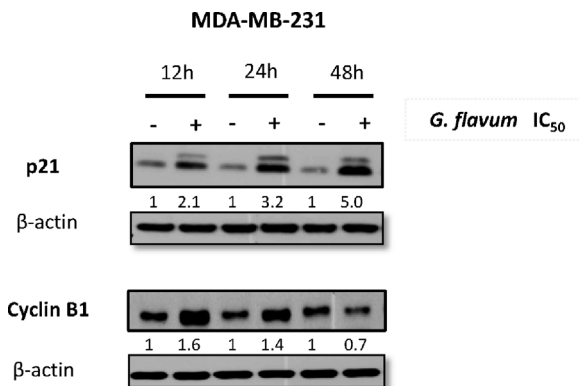
Fig. 4. *G. flavum* extract induced p21 protein expression and an accumulation of cyclin B1 in breast cancer cells. Immunoblotting for p21, cyclin B1 using lysates from MDA-MB-231 cells treated with DMSO (−) or IC$_{50}$ of *G. flavum* extract (+) for 12 h, 24 h and 48 h. Changes in protein levels as determined by densitometric analysis of the immunoreactive bands and corrected for actin are shown. Immunoblotting for each protein was performed at least three times using independently prepared lysates.
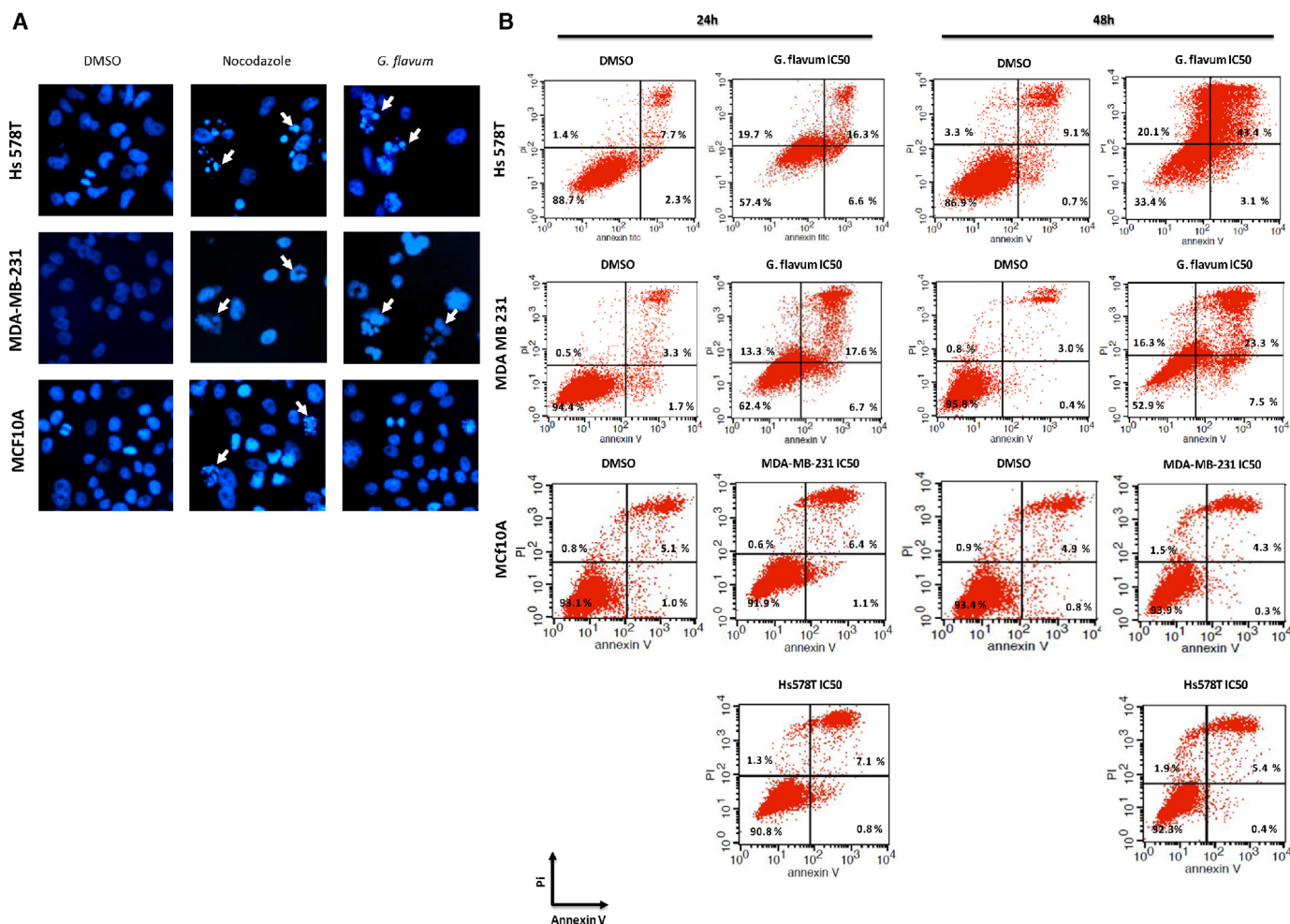
Fig. 5. *G. flavum* extract induced apoptotic cell death in human breast cancer (MDA-MB-231 and Hs578T) but not in normal mammary epithelial cell (MCF10A): (A) morphological apoptosis evaluated by nuclear staining with DAPI and visualized by fluorescence microscopy in breast cancer cells after treatment with IC$_{50}$ of *G. flavum* extract for 24 h or nocodazole used as positive control (magnification 400×). Arrows point to typical chromatin condensation and nuclear fragmentation and (B) flow cytometry-based annexin V/Pi labeling of apoptotic cells. Cancer cells were treated for 24 h and 48 h with DMSO (control) or with their respective *G. flavum* IC$_{50}$. MCF10A cell line was treated with MDA-MB-231 and Hs578T IC$_{50}$ for 24 h and 48 h. Living cells (AnnV$^-$/Pi$^-$ left lower), early apoptotic (AnnV$^+$/Pi$^-$ right lower) cells, necrotic cells (AnnV$^-$/Pi$^+$ left upper) and late apoptotic (AnnV$^+$/Pi$^+$ right upper) are delineated.

positive and PI positive). As shown in Fig. 5B, *G. flavum* extract induced the apparition of an apoptotic sub population in MDA-MB-231 and Hs578T cell lines (24.3% compared to 5% in the control at 24 h and 30.8% compared to 3.4% in the control at 48 h for MDA-MB-231). In accordance with DAPI staining, only minimal cell death was observed with MCF10A cells, even after 48 h of treatment, thus confirming the specific effect of *G. flavum* on cancer cell viability.

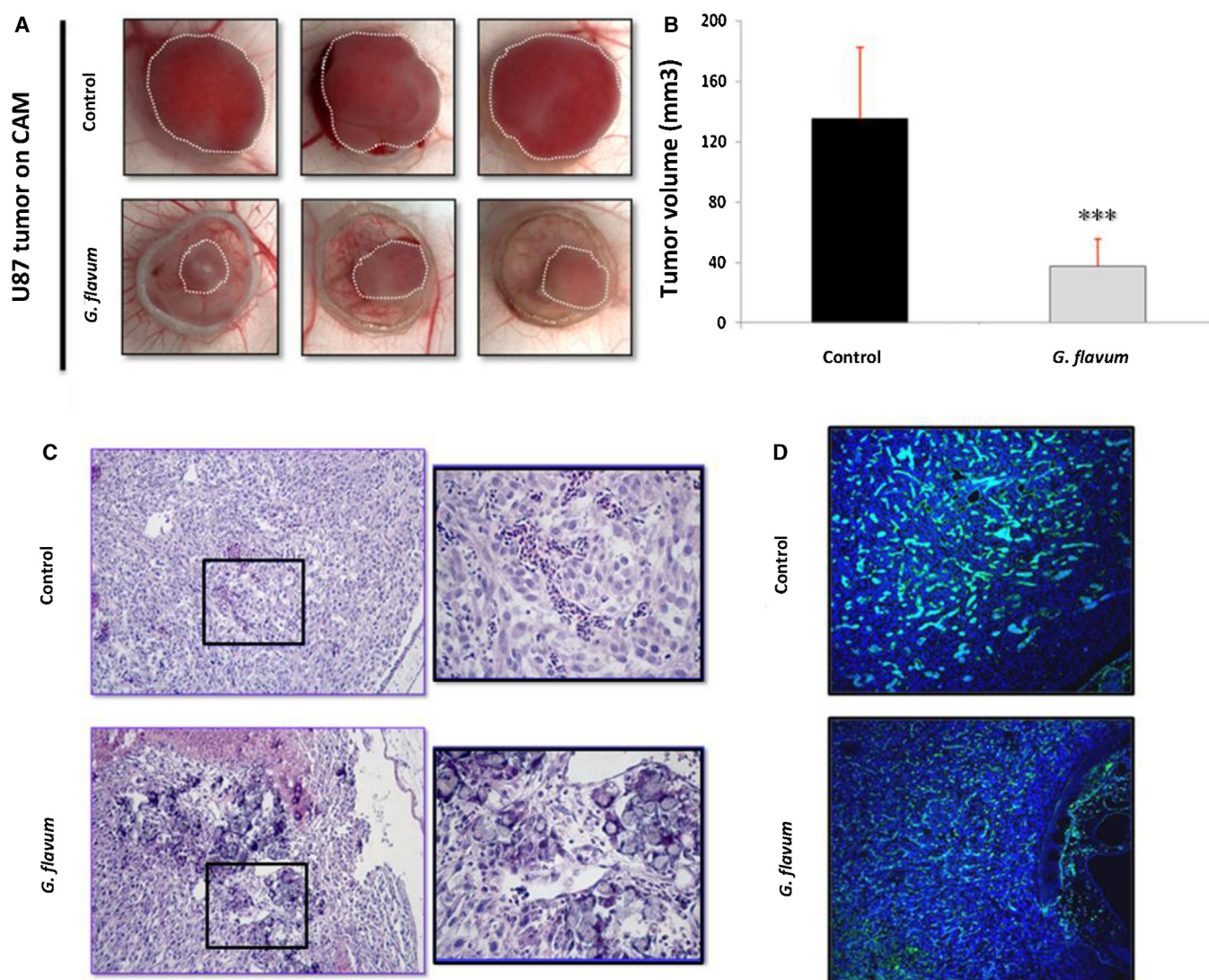### G. flavum extract decreases glioma tumor growth in vivo

To further confirm the anti-tumoral effect of *G. flavum* extract *in vivo*, we used a robust and highly reproducible glioma progression model where U87-MG human glioma cells that are grafted onto the vascularized chicken CAM develop into a tumor within a short period of time (Hagedorn et al. 2005). Tumors were treated daily by a local deposition of *G. flavum* extract (100 μg/ml) or vehicle from the second to the seventh day post-implantation. At the end of the experiment, treated tumors appeared clearly smaller and visibly less vascularized than the control tumors (Fig. 6A). Indeed, the volume of treated experimental glioma was reduced up to 70% when compared to control tumors (Fig. 6B). The hematoxylin and eosin staining of histological sections generally showed a massive necrosis and infiltration of immune cells in *G. flavum* treated

tumors (Fig. 6C, see inserts). Finally, the selective lectin staining of tumoral vasculature demonstrated noticeable differences between treated and non-treated tumors. Treated tumors consistently showed smaller vessels presenting with reduced lumen when compared with vessels in untreated tumor (Fig. 6D).

Discussion

Medicinal herbs and plants continue to play a significant role in drug discovery and development, particularly in cancer research. Previous phytochemical analysis of *G. flavum* has shown that it is rich in several aporphine alkaloids: glaucine, isocorydine, protopine and isoboldine (Yakhontova et al. 1973). More recent studies reported the presence of other minor alkaloids such as adihydrochelirubine, dihydrosanguinarine, norsanguinarine and dihydrochelerythrine. Several other plants of the genus Papaveraceae are nowadays used to treat human tumors including *Chelidonium majus*, *Sanguinaria canadensis L.* and *Macleaya cordata* (Ahmad et al. 2000; Chmura et al. 2000). To date no study has reported anti-neoplasic activity for *G. flavum*.

In this study, we present the first evidence that *G. flavum* alkaloid root extract exerts a tumor cell growth inhibitory activity by using *in vitro* and *in vivo* experimental models. We show that *G. flavum*

Fig. 6. *G. flavum* extract inhibits glioma tumor growth *in vivo* using CAM model: (A) representative pictures of 3 control (DMSO) and 3 *G. flavum* treated (100 μg/ml) experimental glioma tumors grown on CAM (dotted line), (B) tumor volume was calculated as described in "Material and methods" section. *G. flavum* extract induced a significant decrease of tumor volume compared with the controls. Results are expressed as the mean ± SD of 10 replicates of a representative experiment ($n = 3$). ***$p < 0.001$, (C) H&E staining of glioma tumor sections shows massive necrosis with infiltration of immune cells in *G. flavum* treated tumors that were not generally observed in control tumors, (D) specific FITC-lectin staining was used for vizualisation of blood vessels in the tumors shown in panel A. Tumor-associated vasculature was visibly less developed in treated tumors when compared to control tumors. Nuclei appeared blue after TOPRO-3 staining (magnification 100x).

extract decreased the viability of all breast cancer cell lines analyzed in this study in a dose specific manner, while it did not affect human normal cells including mammary epithelial cells, fibroblasts and endothelial cells. A previous study demonstrated that at low concentrations, sanguinarine strongly inhibited the growth of all tested tumor and normal cell lines. With normal human fibroblasts showing a similar sensitivity to that of cancer cells, and no differential cytotoxicity could be observed (Debiton et al. 2003). In contrast, *G. flavum* extract exhibited a selective effect on cancer cells suggesting that this effect could be attributed to the major alkaloids of this plant (aporphine alkaloids) rather than to the minor quaternary benzo[c]phenanthridine alkaloids (*e.g.* sanguinarine). Interestingly, the HPLC profile revealed that the main compound of the root of *G. flavum* is protopine. It has been recently reported that protopine exhibited an anti-proliferative effect by induction of tubulin polymerization and mitotic arrest on human hormone refractory prostate cancer cells (Chen et al. 2012). This evidence indicates that protopine might be responsible for the anticancer activity of *G. flavum* dichloromethane extract reported in this study.

Disturbance of the cancer cell cycle is one of the therapeutic targets for development of new anticancer drugs (Carnero 2002). We showed that *G. flavum* extract induces G2/M arrest on breast cancer cells without affecting the cell cycle distribution in MCF10A cells. We further demonstrated that the anti-proliferative effects of *G. flavum* extract are linked, at least in part, with the specific induction of p21 expression in breast cancer cells. Cyclin B1 plays an important role in the regulation of G2/M transition. Flow cytometry studies performed on cycling cells reported that the level of cyclin B1 protein accumulates substantially during G2 phase and before cells enter mitosis, peaks during metaphase, and declines rapidly as the cells proceed through anaphase (King et al. 1994; Widrow et al. 1997). We observed an accumulation of cyclin B1 after 12 h while its expression level tended to slightly decrease after 48 h of treatment. As such, cyclin B1 accumulation is a marker of cells stopped in G2 and/or M cell cycle phases.

The process of programmed cell death, or apoptosis is an important homeostatic mechanism that balances cell division and cell death to maintain appropriate cell number in tissues (Elmore 2007).

Disturbance of apoptosis pathways is a common feature of cancer cells and thus represents one of the strategies for anticancer drug development. Our findings demonstrate that *G. flavum* extract significantly inhibited cell viability through the specific induction of apoptosis in breast cancer cells. An interesting finding in the present study is that alkaloid extract of *G. flavum* committed cells to apoptosis at a concentration that was below the concentration ranges reported for other plant extracts (Cheng et al. 2005). Altogether our results indicate that *G. flavum* treated MDA-MB-231 show an increased p21 expression, are arrested in G2/M and driven to apoptotic death. Further experiments are needed to dissect cell cycle events and all molecular players associated with *G. flavum* treatment.

Our *in vitro* findings urged us to test whether *G. flavum* extract has anti-tumoral effects *in vivo*. For this purpose, we used a CAM tumor glioma cell model which allows the evaluation of both tumor growth and tumor associated-angiogenesis *in vivo*. Interestingly, we observed a significant impact of *G. flavum* treatment on both processes. Treated experimental tumors were significantly smaller and less vascularized, as they appeared whiter than fully vascularized control tumors. These observations suggest for the first time that *G. flavum* extract possesses not only an anti-proliferative effect on cancer cells but may also affect endothelial cells and impede angiogenesis. Hematoxylin and eosin staining exhibited large zones of necrosis that could be associated with less vascularized regions in treated tumor sections when compared to untreated tumors. In light of these data, it is tempting to speculate that inhibition of tumor growth *in vivo* by *G. flavum* is associated with induction of apoptotic processes and/or limited neovessel formation inside the tumor. Ongoing and further studies will help define the potential anti-angiogenic activity of *G. flavum.*

Conclusion

In summary, we demonstrate for the first time that *G. flavum* root extract inhibits the growth of breast cancer cells by causing specific cell cycle arrest in G2/M phase and leading to apoptosis, without affecting normal breast cells. These anticancer effects of *G. flavum* extract could be attributed to the alkaloid protopine, which is the major compound of the root. This hypothesis remains nevertheless to be confirmed. Besides, additional studies are necessary to identify the possible correlation between the anticancer activity and the major alkaloids present in *G. flavum* extract to ensure the proper medicinal use of this natural wealth, which could lead to the potential development of an effective cancer chemotherapy agent.

Acknowledgments

References

Ahmad, N., Gupta, S., Husain, M.M., Heiskanen, K.M., Mukhtar, H., 2000. Differential antiproliferative and apoptotic response of sanguinarine for cancer cells versus normal cells. Clinical Cancer Research 6, 1524–1528.

Alam, J.J., 2003. Apoptosis: target for novel drugs. Trends in Biotechnology 21, 479–483.

Besson, A., Dowdy, S.F., Roberts, J.M., 2008. CDK inhibitors: cell cycle regulators and beyond. Developmental Cell 14, 159–169.

Cabo, J., Cabo, P., Jimenez, J., Zarzuelo, A., 2006. *Glaucium flavum* Crantz. Part V: hypoglycemic activity of the aqueous extract. Phytotherapy Research 2, 198–200.

Carnero, A., 2002. Targeting the cell cycle for cancer therapy. British Journal of Cancer 87, 129–133.

Chen, C.H., Liao, C.H., Chang, Y.L., Guh, J.H., Pan, S.L., Teng, C.M., 2012. Protopine, a novel microtubule-stabilizing agent, causes mitotic arrest and apoptotic cell death in human hormone-refractory prostate cancer cell lines. Cancer Letters 315, 1–11.

Cheng, Y.L., Lee, S.C., Lin, S.Z., Chang, W.L., Chen, Y.L., Tsai, N.M., Liu, Y.C., Tzao, C., Yu, D.S., Harn, H.J., 2005. Anti-proliferative activity of *Bupleurum scrozonerifolium* in A549 human lung cancer cells in vitro and in vivo. Cancer Letters 222, 183–193.

Chmura, S.J., Dolan, M.E., Cha, A., Mauceri, H.J., Kufe, D.W., Weichselbaum, R.R., 2000. In vitro and in vivo activity of protein kinase C inhibitor growth delay in vivo chelerythrine chloride induces tumor cell toxicity and growth delay in vivo. Clinical Cancer Research 6, 737–742.

Cotter, T.G., 2009. Apoptosis and cancer: the genesis of a research field. Nature Reviews. Cancer 9, 501–507.

Cragg, G.M., Schepartz, S.A., Suffness, M., Grever, M.R., 1993. The taxol supply crisis. New NCI policies for handling the largescale production of novel natural product anticancer and antiHIV agents. Journal of Natural Products 56, 1657–1668.

Daskalova, E., Iskrenova, E., Kiryakov, H.G., Evstatieva, L., 1988. Minor alkaloids of *Glaucium flavum*. Phytochemistry 27, 953–955.

Debiton, E., Madelmont, J.C., Legault, J., Barthomeuf, C., 2003. Sanguinarine-induced apoptosis is associated with an early and severe cellular glutathione depletion. Cancer Chemotherapy and Pharmacology 51, 474–482.

Elmore, S., 2007. Apoptosis: a review of programmed cell death. Toxicologic Pathology 35, 495–516.

Fischer, U., Schulze-Osthoff, K., 2005. Apoptosis-based therapies and drug targets. Cell Death & Differentiation 12 (Suppl. 1), 942–961.

Hagedorn, M., Javerzat, S., Gilges, D., Meyre, A., de Lafarge, B., Eichmann, A., Bikfalvi, A., 2005. Accessing key steps of human tumor progression in vivo by using an avian embryo model. Proceedings of the National Academy of Sciences of the United States of America 102, 1643–1648.

Israilov, I.A., Karimova, S.U., Yunusov, M.S., 1979. Glaucium alkaloids. Chemistry of Natural Compounds 15, 103–113.

Jaffe, E.A., Nachman, R.L., Becker, C.G., Minick, C.R., 1973. Culture of human endothelial cells derived from umbilical veins identification by morphologic and immunologic criteria. The Journal of Clinical Investigation 52, 2745–2756.

Jemal, A., Bray, F., Center, M.M., Ferlay, J., Ward, E., Forman, D., 2011. Global cancer statistics. CA: A Cancer Journal for Clinicians 61, 69–90.

King, R.W., Jackson, P.K., Kirschner, M.W., 1994. Mitosis in transition. Cell 79, 563–571.

Lamour, V., Le Mercier, M., Lefranc, F., Hagedorn, M., Javerzat, S., Bikfalvi, A., Kiss, R., Castronovo, V., Bellahcene, A., 2010. Selective osteopontin knockdown exerts anti-tumoral activity in a human glioblastoma model. International Journal of Cancer 126, 1797–1805.

Lapenna, S., Giordano, A., 2009. Cell cycle kinases as therapeutic targets for cancer. Nature Reviews. Drug Discovery 8, 547–566.

Newman, D.J., Cragg, G.M., 2012. Natural products as sources of new drugs over the 30 years from 1981 to 2010. Journal of Natural Products 75, 311–335.

Ocker, M., Hopfner, M., 2012. Apoptosis-modulating drugs for improved cancer therapy, European surgical research. Europaische chirurgische Forschung Recherches chirurgicales europeennes 48, 111–120.

Petitto, V., Serafini, M., Gallo, F.R., Multari, G., Nicoletti, M., 2010. Alkaloids from *Glaucium flavum* from Sardinia. Natural Product Research 24, 1033–1035.

Pinto, L., Borrelli, F., Bombardelli, E., Cristoni, A., Capasso, F., 1998. Anti-inflammatory, analgesic and antipyretic effects of glaucine in rats and mice. Pharmacy and Pharmacology Communications 4, 502–505.

Ricci, M.S., Zong, W.-X., 2006. Chemotherapeutic approaches for targeting cell death pathways. The Oncologist 11, 342–357.

Rittié, L., Fisher, G.J., 2005. Isolation and culture of skin fibroblasts. Methods in Molecular Medicine 117, 83–98.

Suau, R., Cabezudo, B., Rico, R., Nájera, F., López-Romero, J.M., Cuevas, A., 2004. Phytochemical variations within populations of *Platycapnos saxicola* Willk. Biochemical Systematics and Ecology 32, 565–572.

Suffness, M., Pezzuto, J.M., 1990. Assays related to cancer drug discovery. In: Hostettmann, K. (Ed.), Methods in Plant Biochemistry: Assays for Bioactivity. Academic Press, London, pp. 71–133.

Tawaha, K., Alali, F., Gharaibeh, M., Mohammad, M., Elelimat, T., 2007. Antioxidant activity and total phenolic content of selected Jordanian plant species. Food Chemistry 104, 1372–1378.

Vermeulen, K., Bockstaele, D.R.V., Berneman, Z.N., 2003. The cell cycle: a review of regulation, deregulation and therapeutic targets in cancer. Cell Proliferation 36, 131–149.

Widrow, R.J., Rabinovitch, P.S., Cho, K., Laird, C.D., 1997. Separation of cells at different times within G2 and mitosis by cyclin B1 flow cytometry. Cytometry 27, 250–254.

Williams, G.H., Stoeber, K., 2012. The cell cycle and cancer. The Journal of Pathology 226, 352–364.

Yakhontova, L.D., Sheichenko, V.I., Tolkachev, O.N., 1973. A study of the alkaloids of *Glaucium flavum* the structure of glauvine. Union Scientific: Research Institute of Medicinal Plants 2, 214–218.

Youlden, D.R., Cramb, S.M., Dunn, N.A., Muller, J.M., Pyke, C.M., Baade, P.D., 2012. The descriptive epidemiology of female breast cancer: an international comparison of screening, incidence, survival and mortality. Cancer Epidemiology 36, 237–248.